BLM LIBRARY
88081619

LANDSAT ENHANCEMENT PROJECT

FINAL REPORT

PREPARED BY:

GENERAL ELECTRIC COMPANY
SPACE DIVISION

PREPARED FOR:

U.S. DEPARTMENT OF THE INTERIOR
BUREAU OF LAND MANAGEMENT

AUGUST 1979

space division

ENERAL ELECTRIC

TL
798
.S3
G46
1979

#8484915

ID:88081619

~~CALIFORNIA STATE OFFICE~~
~~CENTRAL LIBRARY COPY~~

TL
798
.S3
G46
1979

LANDSAT ENHANCEMENT PROJECT

FINAL REPORT

PREPARED BY:

THE GENERAL ELECTRIC COMPANY
SPACE DIVISION

PREPARED FOR:

U.S. DEPARTMENT OF THE INTERIOR
BUREAU OF LAND MANAGEMENT

AUGUST 1979

BLM Library
Denver Federal Center
Bldg. 85, OC-521
P.O. Box 25047
Denver, CO 80225

TABLE OF CONTENTS

SECTION PAGE

1 INTRODUCTION 1-1

1.1 Project Objectives and Background 1-1
1.2 Geographic Location of the Three Project Areas . . 1-3

2 TECHNICAL APPROACH 2-1

2.1 Digital Image Processing and Enhancement (Phase One) 2-3
2.1.1 Contrast Stretch Enhancement Product Preparation 2-3
2.1.2 Ratio-Stretch Enhancement Product Preparation 2-4
2.2 Lineament Interpretation Techniques (Phase Two) . . 2-5
2.2.1 Lineament Interpretation Techniques 2-5
2.2.2 "Levels of Agreement" (Confidence) Lineament Overlay (Phase Three) 2-6
2.3 Mapping of Tonal Anomalies (Inferred Hydrothermal Alteration Areas) (Phase Four) 2-7
2.4 Correlation Between Lineament Patterns and Tonal Anomalies (Phase Five) 2-8
2.5 Statistical Interpretation: Relative Potential Evaluation (Phase Six) 2-15
2.5.1 Grid System 2-27
2.6 Preparation of "Areas Having Mineral Potential" Overlay (Phase Seven) 2-28
2.7 Preparation of Bibliography (Phase Eight) 2-30

3 RESULTS 3-1

3.1 "Levels of Agreement" (Confidence) Lineament Overlays (Overlays 1A, 2A, and 3A) 3-2
3.1.1 Area 1 Correlations 3-6
3.1.2 Area 2 Correlations 3-7
3.1.3 Area 3 Correlations 3-8
3.2 Major Lineament Trends 3-10
3.3 Detection of Tonal Anomalies (Inferred Hydrothermal Alteration Areas) (Overlays 1B, 2B, 3B) 3-14
3.3.1 Tonal Anomalies in Area 1 3-14
3.3.2 Tonal Anomalies in Area 2 3-17
3.3.3 Tonal Anomalies in Area 3 3-21

TABLE OF CONTENTS

SECTION PAGE

3.4 Correlation Between Lineaments and Tonal Anomalies 3-27
3.4.1 Area 1 Lineament/Tonal Anomaly Correlation 3-28
3.4.2 Area 2 Lineament/Tonal Anomaly Correlation 3-37
3.4.3 Area 3 Lineament/Tonal Anomaly Correlation 3-46
3.4.4 Summary of Correlation Results 3-54
3.5 Relative Potential Evaluation (Overlays 1C, 2C, 3C) 3-56
3.5.1 Area 1 3-57
3.5.2 Area 2 3-62
3.5.3 Area 3 3-66
3.6 Areas Having Mineral Potential (Overlays 1D, 2D, and 3D) 3-72
3.6.1 Mineral Potential Areas in Project Area 1 3-72
3.6.2 Mineral Potential Areas in Project Area 2 3-73
3.6.3 Mineral Potential Areas in Project Area 3 3-74

4 SUMMARY AND CONCLUSIONS 4-1

5 RECOMMENDATIONS 5-1

APPENDIX A: DIGITAL IMAGE ANALYSIS LABORATORY A-1

APPENDIX B: BIBLIOGRAPHY .B-1

APPENDIX C: ROSE DIAGRAMS C-1

APPENDIX D: CORRELATION #1 DATA SHEETS D-1

APPENDIX E: CORRELATION #2 DATA SHEETS E-1

APPENDIX F: CORRELATION #3 DATA SHEETS F-1

APPENDIX G: REFERENCES G-1

APPENDIX H: DELIVERABLES .H-1

SECTION 1

INTRODUCTION

1.1 PROJECT OBJECTIVES AND BACKGROUND

The Landsat Enhancement Project was conducted for the Bureau of Land Management's Riverside, California office by the General Electric Company, Space Division, located in Beltsville, Maryland. This report describes the results of this project.

The Landsat Enhancement Project consisted of the analysis of published and remotely sensed data covering three 80 x 80 kilometer (km) project areas within the California Desert Conservation Area (CDCA) for the purpose of mapping potential hydrothermal alteration areas, lineament patterns, and potential mineralized areas.

In order to satisfy these objectives, a variety of available (published) information and remotely sensed data were collected and interpreted. For mapping lineament features, digitally enhanced Landsat images and available Skylab and aerial photography were interpreted. Lineament information was also extracted from published maps showing known faults and geophysical lineaments.

In order to identify potential hydrothermally altered areas, digitally ratioed-stretched Landsat images were prepared to enhance subtle terrain characteristics that are suggestive of hydrothermal alteration. Previous work conducted by U.S. Geological Survey geologists in a Nevada test site (Rowan, et. al., 1975) indicates the potential of this technique in detecting some known alteration areas.

In order to identify metallic mineralization areas, two basic approaches were developed. The first approach - the Relative Potential Evaluation - consisted of a subjective geostatistical analysis technique that considered the relative importance of multiple geologic factors available for the project areas. For this project, four factors were considered and assessed: lineament density, lithology, known metallic mineralization, and inferred hydrothermal alteration. Since these four factors were available for the entire project area, it was possible to evaluate the relative significance of each factor within a given area. The greater the significance for each of the four factors, the higher the metallic mineralization potential. To identify the relative potential for the different areas, each project area was subdivided into 2 x 2 km grid cells; relative potential was evaluated for each factor within each grid cell. This evaluation resulted in a score for each grid cell. A level of potential for mineralization was assigned based on the total score for a grid cell relative to all other grid cells in the project area, based on a percentage ranking.

The second approach to identification of potential metallic mineralization areas considered the possibility that alteration areas were located on lineaments, or lineament intersections, having a particular azimuth(s). To accomplish this, the relationships between each potential hydrothermal alteration area and nearby lineaments were measured and recorded. Histograms and other graphs utilizing these data were developed for the interpretation of these relationships.

The primary products of this project consist of overlays and enhanced images at 1:100,000 scale. The four overlays provided for each project area are:

(1) Levels of Agreement (Confidence) Lineaments; (2) Inferred Hydrothermal Alteration Areas (Tonal Anomalies); (3) Relative Potential Evaluation; and (4) Areas Having Potential for Mineral Resources.

1.2 GEOGRAPHIC LOCATION OF THE THREE PROJECT AREAS

Figure 1-1 shows the approximate locations of the three project areas evaluated in the Landsat Enhancement Project.

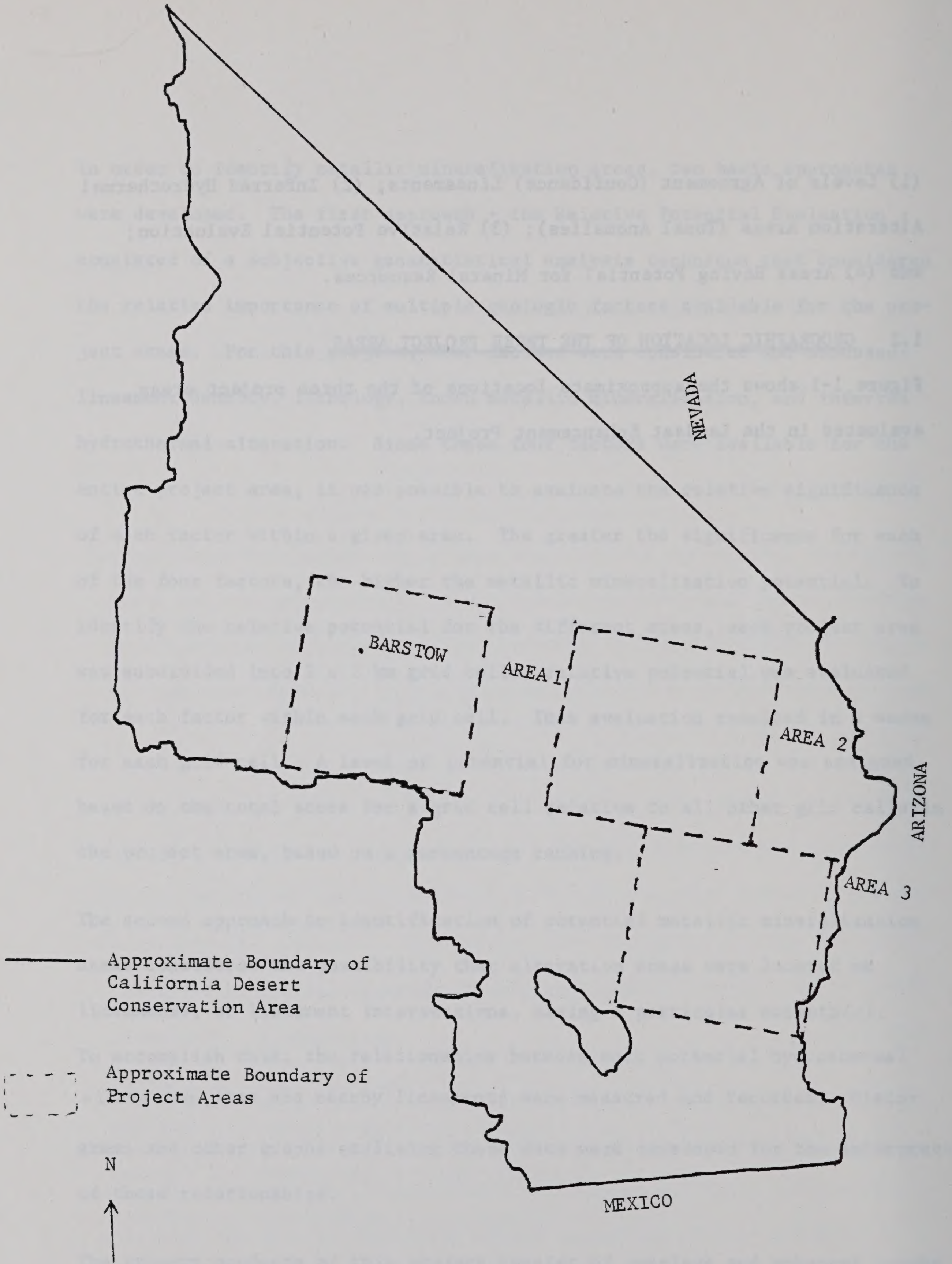
NEVADA
BARSTOW
AREA 1
AREA 2
ARIZONA
AREA 3
MEXICO
Approximate Boundary of California Desert Conservation Area
Approximate Boundary of Project Areas
N

Figure 1-1. Location of the Three Project Areas

SECTION 2

TECHNICAL APPROACH

In order to satisfy the project objectives, several specific methodologies (phases) were defined to ensure optimum utilization of the remotely sensed data and existing published information.

Phase One of the project consisted of the digital processing and enhancement of BLM-provided Landsat tapes (CCTs) covering the three project areas. Digital processing and enhancement resulted in the preparation of two different types of enhanced products. The first type of product prepared were black and white and color geometrically corrected, de-striped, edge enhanced and contrast stretched Landsat images for each project area. The black and white enhancements consisted of Landsat MSS bands 5 and 7 only; the color enhancements consisted of MSS bands 4 (blue), 5 (green), and 7 (red). The second type of products prepared consisted of digitally ratioed-stretched Landsat images. For each project area, three color enhancements and one black and white (4/5) ratioed-stretched enhancements were prepared.

Phase Two of the project consisted of the photogeologic interpretation of the digital enhancements, Skylab and aerial photography for lineament features. Overlays were generated for each of the above product types at a scale of 1:100,000 and then combined with overlays showing known fault and geophysical (aeromagnetic and gravity) lineaments for development of a "Levels of Agreement (Confidence)" composite lineament overlay. Areas of commonality between lineaments were identified.

Phase Three of the project consisted of the photogeologic interpretation of the ratioed-stretched enhancements for identification of tonal anomalies that are inferred to be potential hydrothermal alteration areas.

Phase Four of the project consisted of correlating the lineaments and tonal anomalies in order to determine whether any spatial relationship existed between these two features. The rationale for conducting this correlation has been based in part on investigations recently conducted by Rowan (1975) and Raines (1978) of the U.S. Geological Survey. Results of their work indicate that: (1) some hydrothermal alteration areas can be detected on ratioed-stretched Landsat images (Rowan, 1975); and (2) that, for at least one area, hydrothermal alteration is apparently related to the intersection of a certain set of intersecting Landsat lineaments (Raines, 1978).

Phase Five consisted of the synthesis of the above data and the preparation of overlays showing the relative metallic mineralization potential of the three areas. This task consisted of the evaluation of four geologic factors (lineament desnity, lithology, known minerals, and tonal anomalies) using a subjective geostatistical procedure based on a grid cell format.

Phase Six consisted of the synthesis of the relative potential overlays, lineament overlays and tonal anomalies overlays for identification of areas having potential for mineral resources.

Phase Seven consisted of the preparation of a bibliography listing relevant literature pertaining to each of the three project areas.

A more detailed description of selected facets of these phases is provided in the following sections.

2.1 DIGITAL IMAGE PROCESSING AND ENHANCEMENT (PHASE ONE)

2.1.1 CONTRAST STRETCH ENHANCEMENT PRODUCT PREPARATION

The objective of the digital processing phase was to prepare enhanced, high resolution black and white and color Landsat products covering each project area. The following methodologies were used to produce the contrast enhanced, corrected Landsat images.

2.1.1.1 Geometric Correction

Geometric correction of Landsat data eliminates inconsistencies introduced by the collection platform (satellite) and the spacecraft sensor (Multispectral Scanner). The correction was performed automatically from information provided on the Landsat tape header with special geographic inputs provided by the operator. Cartographic ground control points (GCPs) were matched with Landsat GCPs to geometrically correct the Landsat data to an approximate Universal Transverse Mercator (UTM) map projection (at 1:250,000 scale).

2.1.1.2 Destriping

Several system components in the Landsat imaging and preprocessing systems can create objectionable effects that can be corrected by digital processing. Sensitivity and calibration differences between sensors can produce these effects, commonly called "banding." Any significant miscalibration of this type was removed by applying a correction factor to the gray scale (brightness) value of each sensor.

2.1.1.3 Edge Enhancement

The edge enhancement process compares each Landsat picture element (pixel) gray value with the gray values of the surrounding 48 pixels. The gray value of elements determined to be on an edge was then increased or decreased accordingly.

2.1.1.4 Contrast Enhancement

This technique improves the contrast of a selected Landsat band by modifying the scene's dynamic range (brightness). Since the distribution of gray values of a given Landsat image will generally occupy only part of the possible gray scale, the enhancement procedure modifies the distribution of the brightness values over a range that improves image detail.

2.1.2 RATIO-STRETCH ENHANCEMENT PRODUCT PREPARATION

Interactive digital image analysis using IMAGE 100 (see Appendix A) was conducted to review, analyze and select the optimum combination of ratioed-stretched enhancements for each test site. The six possible Landsat ratios of the MSS Bands (4/5, 5/6, 6/7, 4/6, 4/7, 5/7) were prepared and stored on a "working" product tape. Different ratio combinations were then contrast stretched interactively and compiled into color composites using different combinations of the six ratio channels. General Electric geologists evaluated the various combinations in order to select the three "best" (for each project area) for product generation. The selected ratioed-stretched combinations were then processed on a digital-to-film recording system for preparation of color and black and white transparencies.

The ratioed-stretched transparencies and the contrast stretch-edge enhanced transparencies were then photographically enlarged to 1:100,000 scale for photointerpretation purposes.

2.2 LINEAMENT INTERPRETATION TECHNIQUES (PHASE TWO)

A major part of this project consisted of the visual photointerpretation of several types of remotely sensed data for the purpose of mapping lineament features within each of the three test sites. Available high-altitude aerial photography, Skylab photography, digitally enhanced Landsat images, and existing geophysical lineament information compiled in a previous BLM project (Landsat Lineament Study, 1978) constituted the specific data sources interpreted. Lineament data were plotted onto overlays at 1:100,000 scale.

2.2.1 LINEAMENT INTERPRETATION TECHNIQUES

2.2.1.1 LANDSAT LINEAMENTS

GE geologists utilized conventional photointerpretation techniques for interpretation of lineament features evident on the digitally enhanced black and white and color Landsat images. Data were interpreted at various scales (1:500,000, 1:250,000 and 1:100,000) and plotted on overlays at 1:100,000 scale.

Regarding the relative utility of each of the Landsat image types utilized for lineament mapping, color images are generally more useful then the black and white images for interpretation. The greater color contrast subtle differences in terrain. The variety of colors, hues, and brightness characteristics of the color enhancements, in particular, improves the detectability of lineaments.

2.2.1.2 SKYLAB LINEAMENTS

Skylab photographs were also analyzed for mapping lineament features. The methodology employed to interpret the Skylab data was similar to that used for the interpretation of Landsat images.

2.2.1.3 AERIAL PHOTOGRAPHY

Conventional photointerpretation techniques were also employed to interpret lineament features on the high and medium altitude (60,000' and 40,000') aerial photographs made available during this project. The identification of regional lineaments on these data is relatively difficult due to their field of view characteristics. Regional lineament patterns are more evident on the synoptic Landsat images.

2.2.1.4 PLOTTING GEOPHYSICAL LINEAMENTS

Geophysical lineament overlays produced in the earlier BLM-CDCA project were used as input for this project. Lineaments were manually transferred to overlays at a scale of 1:100,000 from the original 1:250,000 scale overlays.

2.2.1.5 PLOTTING KNOWN FAULTS

Known faults as shown on the published California Division of Mines and Geology (CDMG) 1:250,000 scale geologic maps were also plotted onto overlays. This task was accomplished by photographically enlarging each map to a scale of 1:100,000 and tracing the fault data directly onto a mylar overlay.

2.2.2 "LEVELS OF AGREEMENT" (CONFIDENCE) LINEAMENT OVERLAY (PHASE THREE)

This task consisted of the integration of all lineament data onto a single composite overlay. The synthesis task was accomplished by combining all lineaments on a single composite overlay at 1:100,000 scale on which each lineament type was identified by a different color. Based on this working composite, five "levels of agreement" were assigned to these lineaments:

Level 1 - Previously known faults that were also detected on at least one of the remote sensing sources (i.e., Landsat, Skylab, aerial, gravity, aeromagnetic).

Level 2 - Previously known faults not detected on any remote sensing sources.

Level 3 - Agreement between any three remote sensor sources (i.e., Landsat, Skylab, aerial, gravity, aeromagnetic).

Level 4 - Agreement between any two of the above five sources.

Level 5 - Detected on only one of the five sources.

2.3 MAPPING OF TONAL ANOMALIES (INFERRED HYDROTHERMAL ALTERATION AREAS) (PHASE FOUR)

The term hydrothermal alteration is not used in this report because it would suggest that field or previously published information has been utilized. Since this has not been the case at the time of report preparation, the term "tonal anomaly" is used in describing anomalous tonal patterns that represent inferred hydrothermal alteration areas.

Identification of tonal anomalies for the three project areas was accomplished by interpreting the ratioed-stretched images and correlating any anomalies detected with the published geologic maps, aerial and Skylab photos, and contrast enhanced Landsat images.

The effort to identify tonal anomalies consisted first of the identification of the mapped rock units that could be correlated with color tonal patterns evident on the ratioed-stretched data. It was then possible to locate the remaining questionable areas in which correlations were either ambigious or nonexistent. These areas were identified as tonal anomalies. Both the black and white MSS ratio (4/5) and color ratio composites were interpreted. In general, because of greater color variations, the color ratioed-stretched images are more valuable than black and white images for mapping tonal anomalies. Tonal anomalies were plotted onto overlays at 1:100,000 scale.

2.4 CORRELATION BETWEEN LINEAMENT PATTERNS AND TONAL ANOMALIES (PHASE FIVE)

One of the objectives of this project was to identify a lineament trend (or trends), sets of lineaments, or a common angle(s) between intersecting lineaments that had good spatial correlations with tonal anomalies mapped from the ratioed-stretched Landsat data. The premise on which this task was undertaken was that the location of inferred hydrothermal alteration (tonal anomalies) existing in the project areas may be due largely to certain structural relationships that could be detected best from remote sensing data.

The three aspects of this problem were: (1) Was there a repetitive lineament trend along which many tonal anomalies were located?; (2) Was there a repetitive correlation between certain sets of intersecting lineaments, based on their trend, and tonal anomalies?; and (3) Did tonal anomalies repeatedly occur at the intersection of two (or more) lineaments having a certain angular difference?

Specifically, three different types of correlations between lineaments and tonal anomalies were considered in this project. Each correlation methodology was assigned a different number (i.e., #1, #2, #3) for discussion purposes. Each correlation type provides a somewhat different interpretation aspect to the major spatial relationships. Figure 2-1 shows a schematic diagram of these three correlation categories.

The five major types of lineament data considered in this correlation were:

- Landsat lineaments (all)
- Landsat lineaments (major) (20 km in length or greater)
- Skylab lineaments

CORRELATION # 1 (LINEAMENTS)

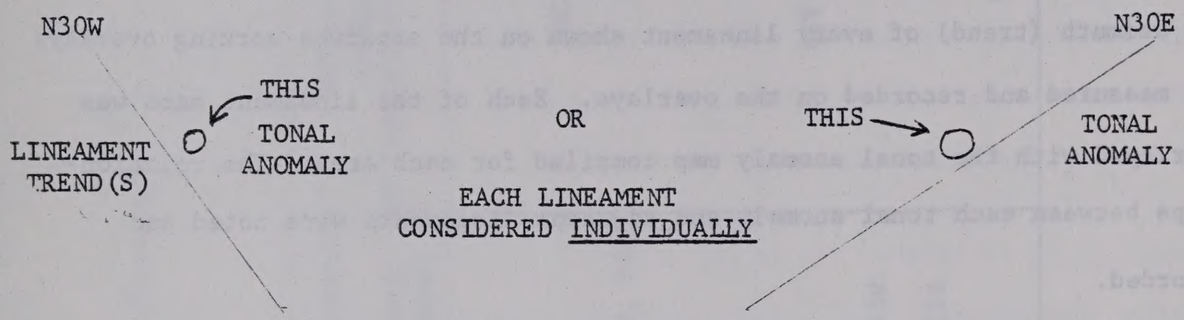
N30W
THIS TONAL ANOMALY
LINEAMENT TREND(S)
OR
EACH LINEAMENT CONSIDERED INDIVIDUALLY
THIS
N30E
TONAL ANOMALY

CORRELATION # 2 (ANGLES)

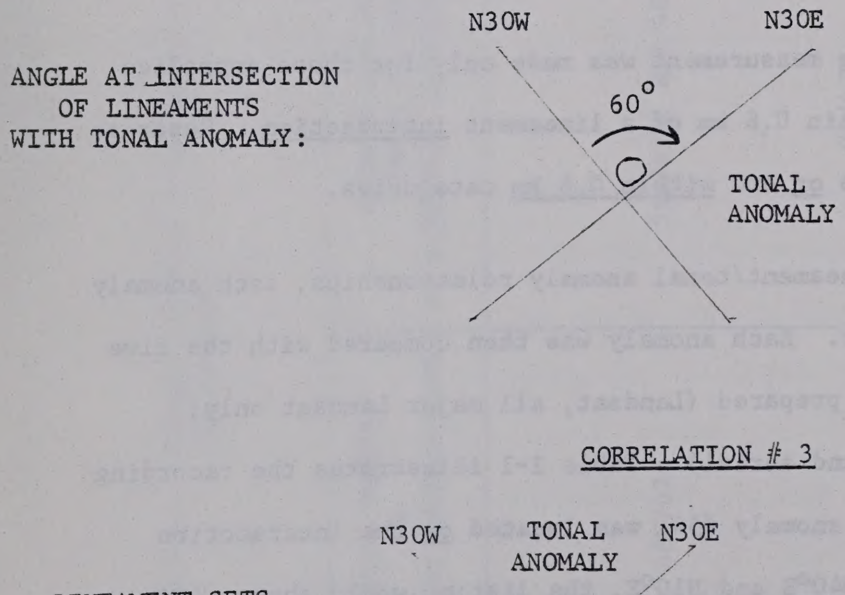
ANGLE AT INTERSECTION OF LINEAMENTS WITH TONAL ANOMALY:
N30W
N30E
60°
TONAL ANOMALY

CORRELATION # 3 (LINEAMENT SETS)

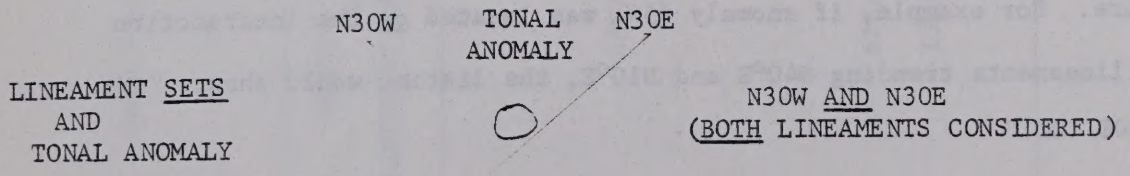
N30W
TONAL ANOMALY
N30E
LINEAMENT SETS AND TONAL ANOMALY
N30W AND N30E
(BOTH LINEAMENTS CONSIDERED)

Figure 2-1. Types of Lineaments/Tonal Anomaly Correlations

- Level 1, 2, 3 lineaments (from composite lineament overlay)
- Aerial photo lineaments

The azimuth (trend) of every lineament shown on the separate working overlays was measured and recorded on the overlays. Each of the lineament maps was overlayed with the tonal anomaly map compiled for each area. The relationships between each tonal anomaly and adjacent lineaments were noted and recorded.

Two types of measurements were recorded. The first recording was for those tonal anomalies that were located on or within 0.6 km of a lineament, (whether at a single lineament or at intersection of several lineaments). Separate readings were made for both the on and within 0.6 km categories.

A second more discriminating measurement was made only for those anomalies that were located on or within 0.6 km of a lineament intersection. Separate recordings were made for the on and within 0.6 km categories.

In order to record these lineament/tonal anomaly relationships, each anomaly was assigned a unique number. Each anomaly was then compared with the five types of lineament overlays prepared (Landsat, all major Landsat only, Skylab, Levels 1, 2 and 3, and aerial). Table 2-1 illustrates the recording procedure. For example, if anomaly #54A was located on the intersection of two lineaments trending N40°E and N10°E, the listing would show: "ON; #54A; 40E/10E."

From these recorded data, the different types of correlations could be made. Correlation #1 considered the possibility that tonal anomalies are located

Table 2-1. Example of Data Recording Sheet/Tonal Anomaly Correlation (by Anomaly)

TONAL ANOMALY NUMBER	ANOMALY LOCATED ON LINEAMENT INTERSECTION	ANOMALY LOCATED WITHIN 0.6 KM OF LINEAMENT INTERSECTION	ANOMALY LOCATED ON LINEAMENT(S) (ONE OR MORE)	ANOMALY LOCATED WITHIN 0.6 KM OF LINEAMENT(S) INTERSECTION
65A			90	
B				30E, 46W
C	48W/62E	55W/62E, 85E/48W	85E, 48W, 62E	55W
66A			1E	
B			0	
C		90/47W	90	47W, 48W
D	62E/45W		62E, 45W	0
E	13W/62F		13W, 62E	
F		65E/13W	13W	65E

along lineaments having a particular trend or trends (azimuths). To determine this, a tabulated sheet was prepared, divided into one degree units from 0-90 degrees west to 0-90 degrees east (see example in Table 2-2). For each category where a correlation appeared, a "1" (called an "alarm") was placed in the appropriate block. Based on the resulting data, histograms and other correlations could be made.

Correlation #2 considered the angle between intersecting lineaments having a spatial relationship with a tonal anomaly. The angles between these particular lineaments were recorded on another sheet (Table 2-3) that was divided into increments ranging from 0-180 degrees. For example, if anomaly #54A was located on intersecting lineaments having azimuths of N10°E and N40°E, an angle difference of 30 degrees was recorded. This correlation allowed the subsequent preparation of histograms and bar charts for more in-depth analysis.

In this correlation it was necessary to record complex lineament intersections/ tonal anomaly relationships where it was not readily evident whether the anomaly was related to the acute or the obtuse angle. For example, in Figure 2-2, the tonal anomaly correlates with both the 50 degree (the acute) as well as with the 120 degree (the obtuse) angle; both angles were recorded since it was not possible to objectively eliminate either one.

Correlation #3 considered the possibility that tonal anomalies have a correlation with certain sets of intersecting lineaments having particular azimuths. For example, anomalies might occur repeatedly at the intersection of lineaments having a N10°E trend and N50°E trend. In order to consider

Table 2-2. Example of Data Recording Sheets for Lineament/Tonal Anomaly Correlations (by Lineament Trend) Correlation #1

NW	On	Within 0.6 km	NW	On	Within 0.6 km	NW NE	On	Within 0.6 km	NE	On	Within 0.6 km	NE	On	Within 0.6 km
0	~~1111~~ 11	11	37			74			21			58	1	
1	1	1	38			75			22			59		
2			39			76			23			60		
3			40			77			24			61	1	
4			41			78			25	1	11	62	~~1111~~	
5			42	1		79			26			63		
6			43			80			27			64	1	
7			44			81			28			65	1	1
8			45	111	~~1111~~	82			29			66		11
9			46	1	11	83			30	11	1	67	11	
10		1	47	1	11	84			31	1111	1	68	1	
11			48	~~1111~~ 11	1	85			32	11	111	69		
12			49			86			33			70	1	1
13	~~1111~~ 11	111	50			87			34			71		
14			51			88			35	1111		72		
15			52	1		89			36			73		1
16			53			90	~~1111~~ 111	~~1111~~	37			74		
17	1	1	54	11		1	111		38			75	11	11
18			55	1	1	2			39	1		76		
19	11	11	56			3			40		11	77	11	111
20			57			4			41			78		
21			58		1	5			42	11	11	79		
22	1		59			6			43			80		
23	1	1	60			7			44			81		
24	111	11	61	11	1	8			45	~~1111~~	1	82		
25	11	1	62			9			46	1	1	83	111	1
26			63			10			47			84		
27			64			11			48	1111	1111	85	1111	11
28			65			12			49			86		
29			66			13			50			87		
30			67			14			51			88		
31			68			15	1	1	52			89		
32			69			16			53					
33			70			17			54					
34	1		71			18			55	111				
35	111	11	72			19			56	1				
36			73			20			57					

Table 2-3. Example of Data Recording Sheet for Lineament Angle/Tonal Anomaly Correlations (By Lineament Intersection Angle) Correlation #2

DEG.	On	Within 0.6 km	DEG.	On	Within 0.6 km	DEG.	On	Within 0.6 km	DEG.	On	Within 0.6 km	DEG.	On	Within 0.6 km
0			37			74			111			148		1
1			38		1	75	11	1	112	1		149		
2			39	1		76			113			150	1	
3			40			77	11	1	114			151	1	
4			41			78		1	115			152		
5			42	1		79			116			153		
6			43			80			117		1	154		
7	1		44			81			118			155	1	1
8			45	1		82			119		1	156		
9			46			83		1	120	1	1	157		1
10			47		1	84		1	121			158		
11			48		1	85			122			159	1	
12		1	49			86	1	11	123			160		1
13		1	50			87		1	124			161		
14		1	51			88			125	1		162	1	
15			52	1		89		1	126		1	163		
16			53	1		90		11	127	1		164		
17			54			91	1		128			165		
18			55	1		92		1	129	1		166		
19			56	1		93			130	1		167		1
20			57			94		11	131			168		
21			58			95			132	11		169		
22			59			96	1		133			170		
23			60			97		1	134		1	171		
24			61		1	98			135	1	1	172		
25			62			99			136			173		
26			63			100		1	137		1	174		
27		1	64			101			138		1	175		
28			65			102	1	1	139			176	1	
29			66			103	1		140			177		
30			67			104		1	141	1		178		
31			68			105	1		142			179		
32			69			106			143			180		
33			70			107			144					
34			71			108			145	1				
35	1		72			109	1		146					
36			73			110	11	1	147					

this particular correlation, the primary data listings developed in Correlation #2 were used to develop a matrix (Figure 2-3). Figure 2-3, for example, shows that anomaly #54B occurs at the intersection of lineaments trending N30°E and N30°W.

Histograms were then developed for some of these correlations to graphically describe the resulting relationships. Major lineament trends, lineament intersections, and angles between lineaments were then identified. Figure 2-4, for example, is a histogram showing the correlation between individual lineaments and tonal anomalies.

Statistical recordings were not made for either aerial or geophysical lineaments. These lineament data were too generalized to be of use in detailed analysis.

2.5 STATISTICAL INTERPRETATION: RELATIVE POTENTIAL EVALUATION (PHASE SIX)

A review of the available geologic data pertinent to this study indicated that the data are not as complete or detailed as would be desired. Although a variety of published or unpublished data were available in the project, they generally contained inconsistencies in information quality and geographic coverage. Additional data required to fill the gaps may be unavailable or different in format and detail.

With this in mind, the development of a method was required to evaluate and quantify in some manner the diverse data inputs frequently encountered in a remote sensor based survey, particularly one where evaluation of the metallic mineral potential was the prime objective.

The method developed to fill this need is based on the fact that individual sources of information are generally incomplete by themselves; it is the

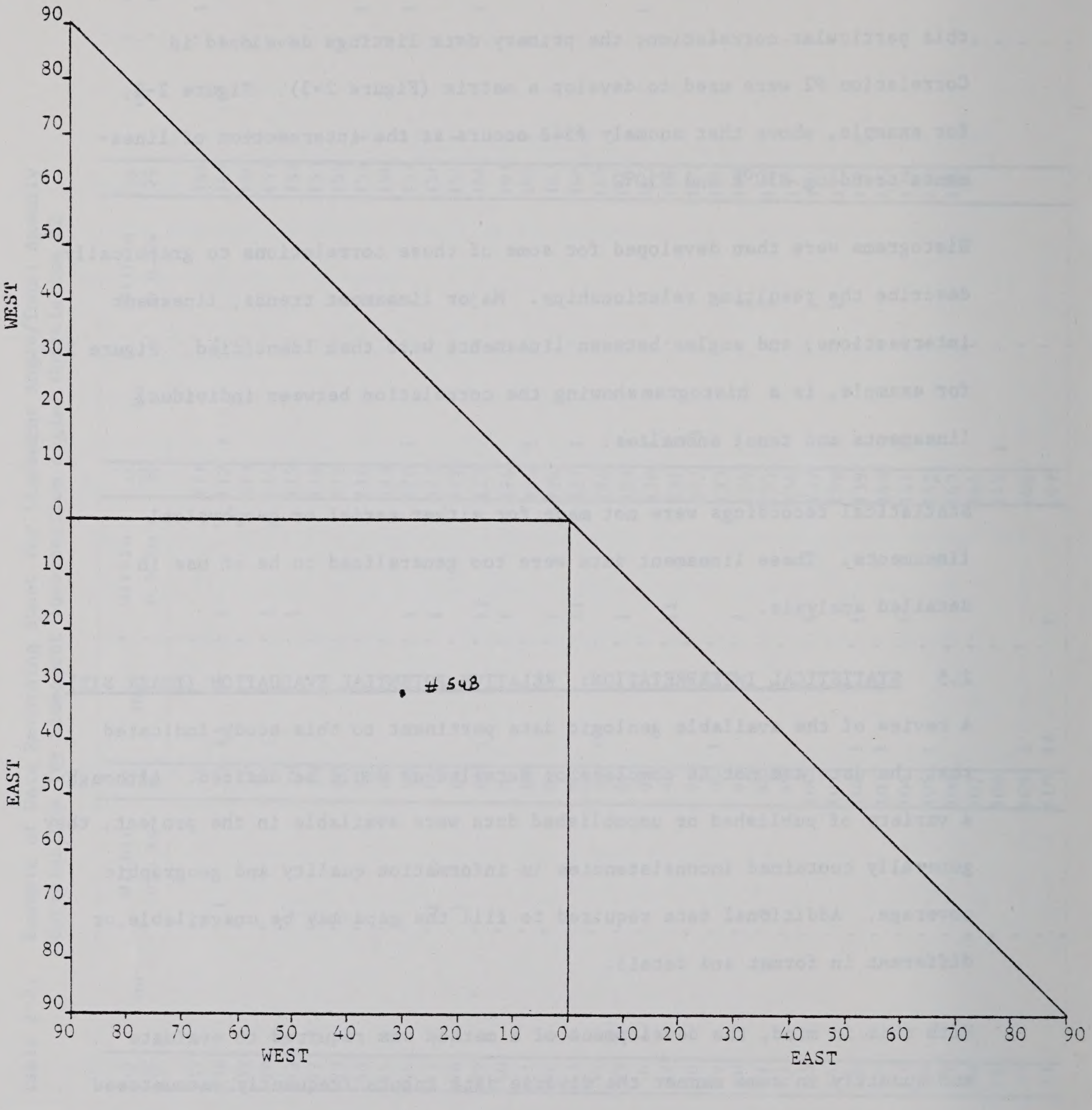

Figure 2-3. Matrix Developed to Record Lineament Set/Tonal Anomaly Correlations

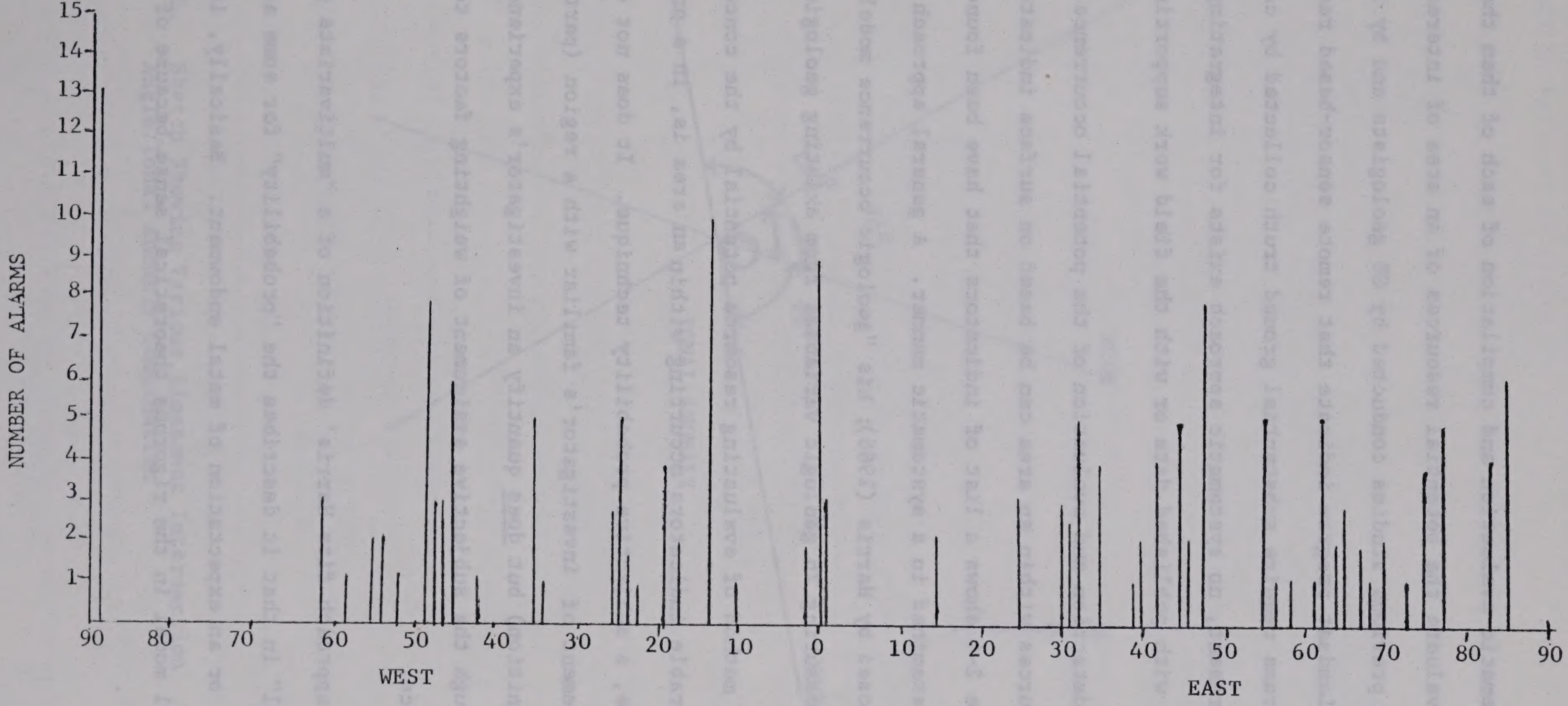

Figure 2-4. Histogram Showing Correlation Between Alarms and Lineament Trends

systematic evaluation and compilation of each of them that provides a way to evaluate the potential resources of an area of interest. Experience from previous studies conducted by GE geologists and by investigators in the Landsat program indicate that remote sensor-based resources exploration programs require substantial ground truth collected by conventional methods. At present, no systematic approach exists for integrating the remote sensor data with published data or with the field work supporting it.

The detection and evaluation of the potential occurrence of selected resources within an area can be based on surface indicators of these deposits. Table 2-4 shows a list of indicators that have been found useful when they are examined in a systematic manner. A general approach of this type was proposed by Harris (1966); his "geologic occurrence model" was generated by measuring 26 geologic variables from existing geologic maps.

This method of evaluating resource potential by the concentration of favorable indicators occurring within an area is, in a practical sense, a subjective probability technique. It does not quantify the judgement of investigator's familiar with a region (part of Harris' 1966 definition) but does quantify an investigator's experience and knowledge through the subjective assignment of weighting factors to each information source.

The approach fits Harris' definition of a "multivariate geostatistical model" in that it describes the "probability" for some aspect of endowment .... or an expectation of metal endowment. Basically, it is not a statistical model in the rigorous theoretical sense because of the uncertain

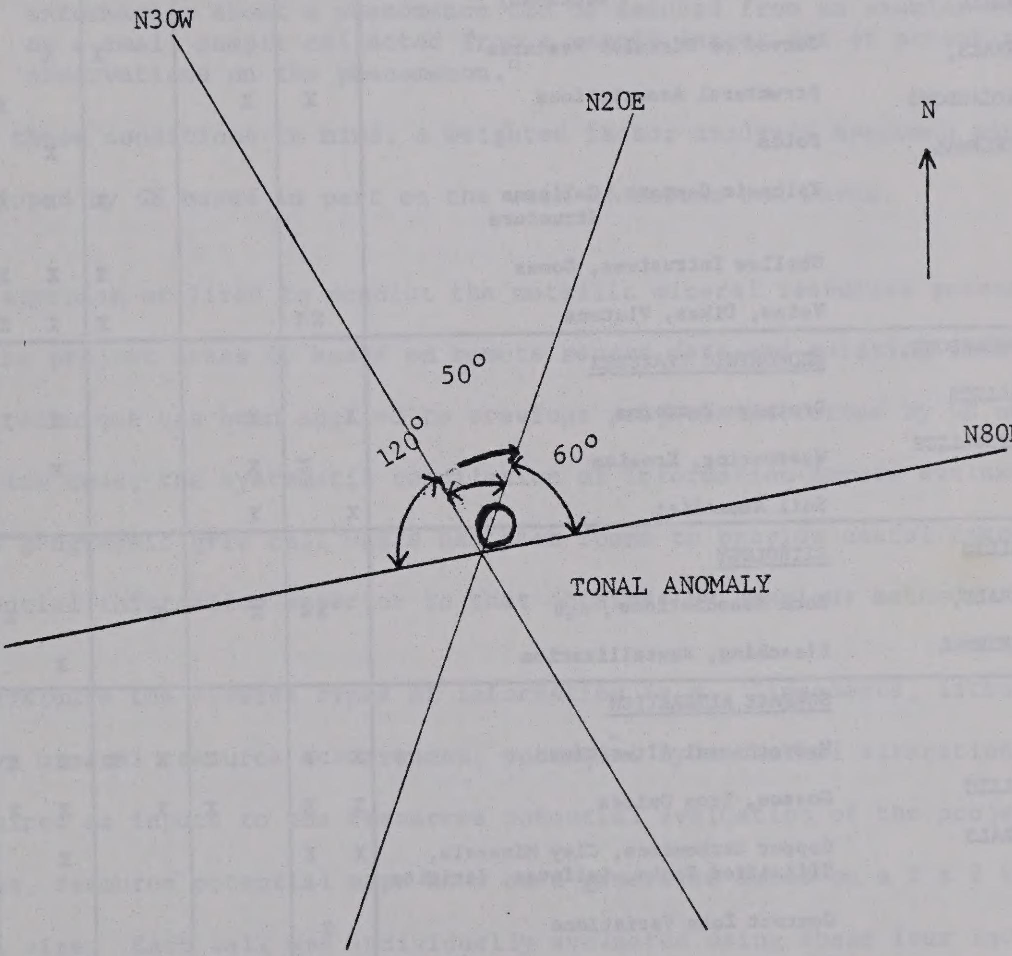
N30W
N20E
N
50°
120°
60°
N80E
TONAL ANOMALY

Figure 2-2. Sketch Showing Various Lineament Intersection Angle/Tonal Anomaly Combination

Table 2-4. Geologic Indicators of G-E-M Resources as Reported in the Literature

PRIMARY G-E-M RESOURCES INDICATED	GEOLOGIC INDICATOR	HAWKES & WEBB (1962) HARRIS (1966) Nat.Ac.Sci (69)	BECASSIO (1972)	SHORT (1973, 1974)	JENSEN (1974)	KIEPPER (1974)	LIGGETT *et al* (1974)	BAKER (1975 , 1976b)	NASA (1975) Table 3.5	ROWAN (1975)	HALBOUTY (1976)	SHORT & STEWART (1976)
	GEOLOGIC STRUCTURE											
METALLIC MINERALS, HYDROCARBONS GEOTHERMAL	Linear Features (Density Intersections)	XX		X	X	X	X	X		X	X	X
	Curved or Circular Features					X	X				X	X
	Structural Associations	X	X					X			X	
	Folds						X					
	Volcanic Centers, Collapse Structure					X	X	X				
	Shallow Intrusives, Domes					X	X	X				
	Veins, Dikes, Plutons	XX				X	X	X				
HYDROCARBONS, METALLICS NONMETALLICS	GEOMORPHIC FEATURES											
	Drainage Patterns	X	X				X	X				
	Weathering, Erosion	X	X				X					
	Soil Anomalies	X	X									
METALLIC MINERALS, GEOTHERMAL	LITHOLOGY											
	Rock Associations , Age	XX	X		X			X			X	
	Bleaching, Rextallization						X					
METALLIC MINERALS	SURFACE ALTERATION											
	Hydrothermal Alterations	X X		X	X	X	X	X	X	X		X
	Gossan, Iron Oxides	X X		X	X		X	X	X	X		X
	Copper Carbonates, Clay Minerals, Silicified Rocks, Sulfates, Sericite	X X					X					X
	Contact Zone Variations	X										X
	Mineralization	X			X	X	X	X				
HYDROCARBONS METALLICS GEOTHERMAL	VEGETATION											
	Enhancement or Stress	X	X					X	X			X
NONMETALLICS	SOIL MOISTURE		X									
RARE EARTHS, NONMETALLICS	THERMAL ANOMALIES											
	Radiogenic	X	X					X				
	Exothermal		X					X				
	Thermal Inertia	X	X							X		
METALLIC MINERALS HYDROCARBONS	AEROMAGNETIC SURVEYS	X										
	BOUGER GRAVITY SURVEYS											

nature of the body of geologic knowledge involved; rather, it falls within the realm of the "quasi" or "protostatistics" of Davis (1973):

> "All of the techniques of quantitative geology we will discuss can be regarded as statistical procedures, or perhaps quasistatistical or protostatistical procedures. Few, perhaps none, are sufficiently developed to be used in rigorous tests of statistical hypotheses. Neither is there an adequate body of general theory about the nature of geologic populations. However, like statistical tests, geomathematical techniques are based on the premise that information about a phenomenon can be deduced from an examination of a small sample collected from a vastly larger set of potential observations on the phenomenon."

With these conditions in mind, a weighted factor analysis approach was developed by GE based in part on the work of Harris and Davis.

The approach utilized to predict the metallic mineral resources potential of the project areas is based on remote sensor data and existing information. The technique has been applied to previous projects performed by GE analysts. In each case, the systematic compilation of information inputs evaluated on a geographic grid cell basis has been found to provide useful resource potential information superior to that obtained by previous methods.

To evaluate the diverse types of information (e.g., lineaments, lithology, known mineral resource occurrences, potential hydrothermal alteration) required as inputs to the resources potential evaluation of the project areas, resource potential maps have been generated based on a 2 x 2 km grid cell size. Each cell was individually evaluated using these four indicators. These indicators were weighted subjectively in two ways. The first considered the significance of the indicator as a guide to resource prediction; this was established by factors such as data quality, completeness of coverage, value as a resource indicator, previous in-house experience, and results of similar investigations published in the literature. The second factor considered the significance of the indicator within the context of all available information sources. The total "pool" of information (resource indicators) available for the given resource evaluation was assigned an arbitrary value of 100. Each individual resource indicator within this pool was given a value based on its relative significance; the sum of the resource indicators was set equal to 100. The pool of information available for evaluating the metallic mineral potential of the three project areas consisted of four information sources:

1. Lineaments as detected from remote sensor data and ancillary published data;
2. Known mineral occurrences within each project area as shown on maps compiled by the U.S. Bureau of Mines (Mineral Industry Location System - MILS);
3. Lithology as provided by the California Geologic Atlas and compiled by the California Division of Mines and Geology (CDMG); and
4. Tonal anomalies as identified on the ratioed-stretched Landsat images.

It was subjectively decided that the lineaments data and the known mineral occurrences were slightly more significant indicators of potential additional metallic mineral deposits than the information provided by the ratioed-stretched Landsat images or by existing geologic (lithologic) maps of the study area. Thus, the individual information sources (indicators) were weighted in the following manner:

Lineaments	30 Points
Known metallic mineral occurrences	30 "
Lithology	20 "
Tonal anomalies	20 "
Total	100

The weighting of information sources is subjective, but this subjectivity can be minimized by considering the characteristics of the data and the correlation of the geology of the project areas.

After weighting these information categories and assigning each a maximum point value, it was necessary to develop criteria within each category to determine the actual points (within the range assigned) to be assigned to a cell based on the features present within it. The evaluation weighting criteria developed for each geology resource category are shown in Table 2-5.

The sum of the evaluation scores for each information source represents the total resource evaluation score for the unit cell. The distribution of these scores for each project area was plotted on a histogram and resource potential categories determined. The relative potential categories represented a percentage of the total resource potential evaluation score as compared to the total scores of all other grid cells. In this project, the following percentage figures were developed to define each relative potential category:

Category (A) (Upper 5% of total scores) = highest potential (relative to other cells)
(B) (Next 5% of total scores) = moderately high potential
(C) (Between 10-20%) = good potential
(D) (Between 20-30%) = some potential
(E) (less than 30%) = little potential based on data analyzed.

The following example illustrates the technique employed: Hypothetical grid cell "c" was evaluated for metallic mineral potential using the factor weighting categories previously described. Grid cell "c" had the following evaluation:

Table 2-5. Geologic Factor Weightings for
Metallic Mineralization Evaluation

Points	Lineaments (30 Points)	# Sources Recognized
0-1-2	None, Single	
3-4-5	Single	
6-7-8	Multiple Lineament	
9-10-11	Multiple Lineament	
12-13-14-15	Single Intersection	
16-17-18	Single Intersection	
19-24	Multiple Intersections	
25-30	Multiple Intersections	
	Known Metallic Mineral Occurrences (30 Points)	
0 - 3	No mining activity or apparent interest in cell and no deposits within 10 km (0). Some mining activity in region (1, 2), but more than 10 km away, notable mining activity in region, but more than 15 km away (3).	
4 - 8	Known mineral localities occur within 6-10 km	
9 - 16	Known mineral localities occur within 4-6 km	
17 - 24	Known mineral localities occur within 2-4 km	
25 - 30	Known mineral localities occur within 0-2 km	
	Lithology (From Existing Data) (20 Points)	
0 - 2	Widespread alluvium, unconsolidated surficial material	
3 - 8	Widespread sedimentary strata	
9 - 14	Widespread igneous/or intrusive or extrusive volcanics, or mixed cell	
15 - 20	Favorable lithologic indicators or combinations of favorable indicators, such as: • carbonate rocks near igneous contacts • sedimentary or volcanic rocks invaded by igneous intrusions • ultramafic rocks	
	Tonal Anomalies (20)	
0 - 5	Grid cell contains no tonal anomalies or contains tonal anomalies having no apparent correlation with faults or known mineralization	
6 - 10	Grid cell contains tonal anomalies having spatial correlation with known faults	
11 - 15	Grid cell contains tonal anomalies having spatial correlation with known metallic mineralization	
16 - 20	Spatial correlation between tonal anomalies, known metallic mineralization and known faults	

Lineaments = 19 (i.e., multiple intersections occur within cell)

Known Occurrences = 19 (i.e., cell adjacent to known mineralization)

Lithology = 18 (i.e., favorable lithologic indicators occur within cell (e.g., carbonate rocks near igneous contacts)

Anomalies = 15 (tonal anomaly has spatial relationship to known faults and known mineral deposits).

Adding the individual scores resulted in:

Total Score = 19 + 19 + 18 + 15 = 71

The score of 71 for cell c will place it in category "A" if, based on the histogram, it occurs within the upper 5% of the cells analyzed based on the histogram showing these results (Figure 2-5). Note that this evaluation is relative to the scores calculated for each of the other cells within the CDCA. The calculation technique was repeated for each cell within each project area, and a resource potential map overlay was generated at 1:100,000 scale for each project area.

This approach has been developed to provide a logical, methodical technique for evaluating regional areas of interest and specific areas within them that appear promising. As data from other sensors or ground truth become available, these inputs can be incorporated into the existing evaluation.

The rationale for the scoring within each of the four factors is as follows:

Lineament Density - This is based on the premise that mineralized fluids have a greater tendency to migrate along existing zones of weakness. Therefore, in general, the greater the intensity of fracturing in a given area, the greater the metallic mineralization potential.

Lithology - Certain rock types have a more favorable environment for metallic mineral resources than others. For example, an area characterized by igneous

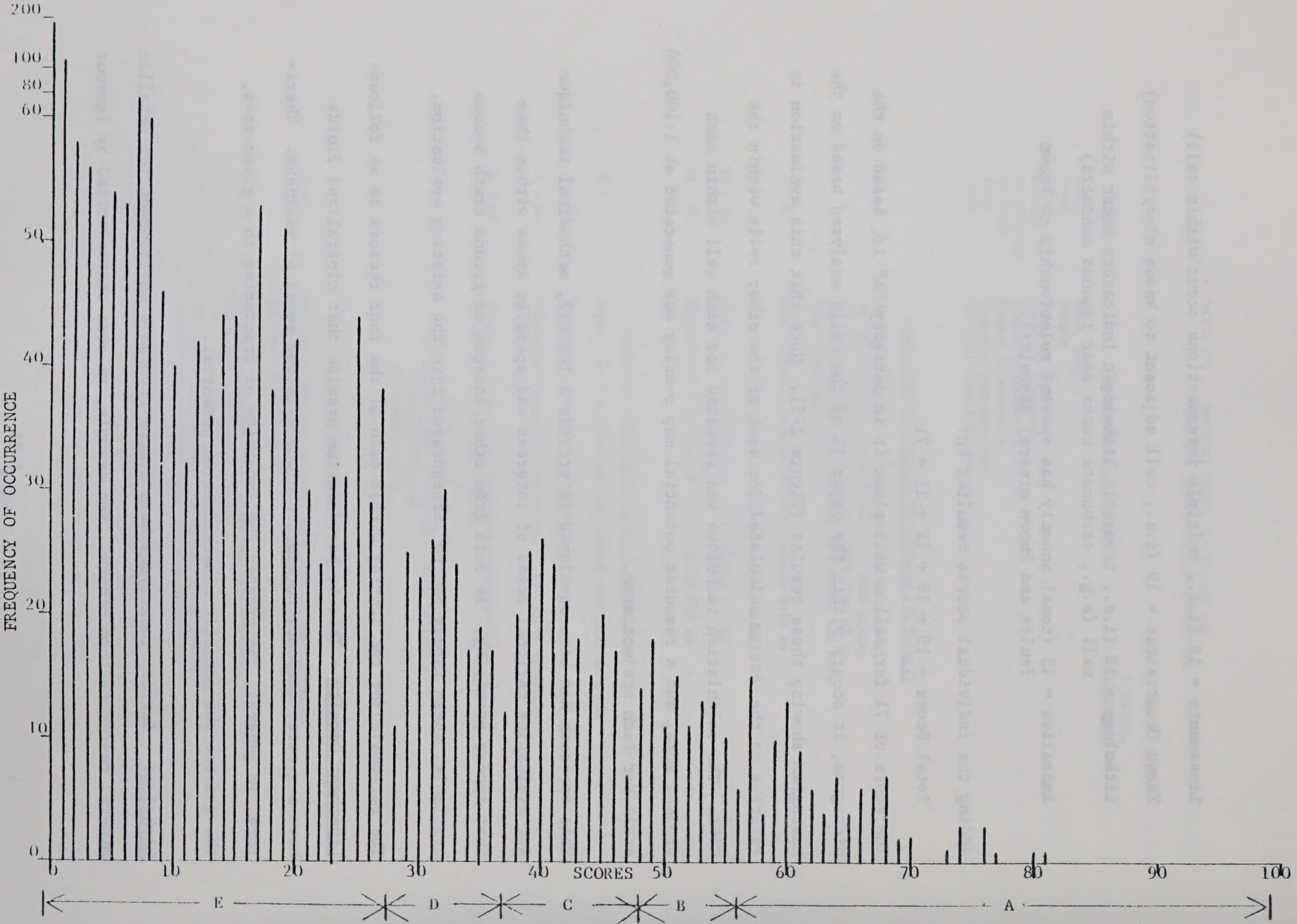

Figure 2-5. Example of Histogram Showing Range of Total Scores

or volcanic intrusives have higher potential for contact metamorphism (and possible metallic mineralization) than an area covered by a homogenous cover of alluvium or consolidated marine or continental sediments. Likewise, certain relationships, such as the contact between igneous rock and carbonates, are considered to have a high mineral potential. It should be noted that the lithology scoring procedure considered the percentage of the rock type contained within the grid cell. For example, a grid cell containing 70% alluvium and 30% granite did not receive as high a score as a grid cell containing 70% granite and 30% alluvium.

Known Metallic Mineralization - Areas containing known mineral deposits suggest a more favorable geologic environment than areas for which published maps indicate no mining activity has occurred. The highest scores in this category were assigned to those grid cells containing multiple known mineral deposits. The fewer the number of known deposits within the cell, and the greater the distance of the grid cell from mineralization (if no deposits occur), the lower the score.

Tonal Anomalies - No readily evident relationships could be established between tonal anomalies and any known geologic characteristic. Therefore, assignment of a score to a grid cell containing an anomaly had to be based on available data. In this project, the more favorable the spatial correlation between the anomaly and (1) known mineral deposits, and (2) known faults, the higher the assigned score.

2.5.1 GRID SYSTEM

Each 10 x 10 km UTM block within each of the project areas has been labeled on the horizontal and vertical numbering system, with block A1 starting at the upper left and increasing to the right (A, B, C, etc.) and downward (1, 2, 3, etc.)

In order to pinpoint more precisely the location of selected grid cells, each 2 x 2 km grid cell within each UTM block has been assigned a number from 1-25, as shown on the following sketch, for discussion purposes:

5	4	3	2	1
6	7	8	9	10
15	14	13	12	11
16	17	18	19	20
25	24	23	22	21

2.6 PREPARATION OF "AREAS HAVING MINERAL POTENTIAL" OVERLAY (PHASE SEVEN)

An overlay was also prepared to show the most favorable mineralization areas based on a somewhat different synthesis technique. Rationale for development of the "Areas Having Mineral Potential" overlay is as follows:

The category "A" on the Relative Potential overlay, as previously described in Section 2.5, indicates that the total score of that grid cell fell within the top 5% of all grid cell total scores, as represented on a histogram showing total score versus number of grid cells having a particular score. The total score represented the summation of individual factor scores for lineament density, lithology, known metallic minerals, and tonal anomalies.

The fact that an area contains known mineralization does not necessarily indicate that it possesses a higher relative mineral potential than other areas containing no known mineralization. Exclusion of the "known minerals" category in developing the total score statistics would indicate those areas that possess favorable geologic characteristics regardless of its previously documented mineralization. To identify these areas, the individual scores for the factors lineament density, lithology, and tonal anomalies were summed; the known minerals score was not included. The range of total scores versus frequency were plotted on a histogram (as previously described), and the top 5% scores were identified. The grid cells meeting there criteria were then identified. Those grid cells that represented the top 5% based on both total score and "partial" score were plotted onto a working overlay.

Major fracture (lineament) intersection areas were also plotted onto this overlay. These areas were based on the information displayed on the "Levels of Agreement" composite lineaments overlay; they were depicted as polygons.

In addition, tonal anomalies as shown on the "Tonal Anomalies" overlay were added to this working overlay. These areas were also shown as polygons.

The compositing of the above areas onto one overlay showed areas of overlap and areas where little or no correlation (overlays) were evident. Based on these data, the "Areas Having Mineral Potential" overlay was developed. Six "levels" - defined as potential mineral areas - were identified, as follows:

Level 1 - Overlap of top 5% grid cells based on both total score and "partial" score (also may include overlapping tonal anomalies and intersection area polygons).

Level 2 - Top 5% grid cells based on total score (no overlap) (also may include overlapping tonal anomalies and intersection area polygons).

Level 3 - Top 5% grid cells based on "partial" score (no overlap) (also may include overlapping tonal anomalies and intersection areas polygons).

Level 4 - Overlap between major lineament intersection areas and tonal anomalies.

Level 5 - Major lineament intersection areas only.

Level 6 - Tonal anomalies only

This particular approach identifies potential mineral areas that may or may not have been identified on the "Relative Potential" overlay.

2.7 PREPARATION OF BIBLIOGRAPHY (PHASE EIGHT)

Research was conducted at several libraries for the preparation of a comprehensive bibliography listing all relevant published and documented (but unpublished) literature pertaining to the three test sites. The sources listed in this bibliography have been grouped using the following subject groups: Author's Name; Lithology; Structure/Tectonics; Geophysics; Geothermal; Mineral Resources; Seismicity; and General Geology.

Sources researched for compilation of this bibliography include the following: USGS-Reston Library (card and map files, etc.); NASA-Goddard Space Flight Center Library, GEOREF (AGI), RECON (NASA); Economic Geology; GSA Bulletin; Journal of Geology; several sources listing Masters and PhD publications; the NASA/GSFC Landsat Investigation Support computer data base; California Division of Mines and Geology listings of publications; USGS publication catalog listing: 1879-1961, 1967-1972, 1973, 1974, 1975, 1976, and 1977; and the GSA Bulletin cumulative indices.

SECTION 3

RESULTS

This section presents the results of the mapping of tonal anomalies and lineaments, the correlation between these two features, and the evaluation of relative potential of the project areas based on a grid cell format.

Section 3.1 describes the relative agreement between the six types of lineament features mapped during the project. General results indicate relatively good correlation between some lineament categories and relatively poor correlation for others.

Section 3.2 describes the major lineament trends (azimuths) recognized in the three project areas as determined from rose diagrams generated for each lineament type.

Section 3.3 describes the tonal anomalies recognized in the Landsat ratioed-stretched enhancements, their tonal characteristics, their location, and their relationship to the lithology with which they appear related.

Section 3.4 correlates the spatial relationship between the tonal anomalies and the lineament features as identified on the six lineament sources. The purpose of this correlation was to determine whether tonal anomalies mapped in the project areas are structurally related to lineament features or to intersections of lineaments.

Section 3.5 documents the results of the relative potential evaluation task. Areas of potential metallic mineralization are prioritized based on their total score relative to the total scores for all other grid cells evaluated for each project area. Five levels of priority have been assigned.

Section 3.6 describes the results of the synthesis of the several types of data generated in the Landsat Enhancement Project. Specifically, the individual correlations between lineament intersection areas, tonal anomalies, and high potential grid cells (based on two different scoring formats) were combined to identify areas favorable for metallic mineralization.

3.1 "LEVELS OF AGREEMENT" (CONFIDENCE) LINEAMENT OVERLAYS (OVERLAYS 1A, 2A, and 3A

The results of the synthesis of the six lineament data sources are graphically shown in Overlays 1A (Area 1), 2A (Area 2) and 3A (Area 3) and summarized in Tables 3-1, 3-2 and 3-3. These tables indicate the approximate total number of lineaments mapped from each source and, in a matrix format, indicate the approximate number of lineaments that were in agreement with one another for each possible combination. These tables should be considered subjective in that they attempt only to provide a medium on which discussion can center. They provide only a general reflection of the relative agreement between lineament sources. Due to the multitude and complexity of lineament data compiled in this study, and the many variations of possible correlations and analyses, it has been necessary to discuss only the most important and salient aspects of this synthesis.

An initial observation is the lack of correlation of geophysical lineaments with any other lineament source. This low correlation is due to the generalized geophysical lineament information available for this project.

The tables also indicate that Landsat and Skylab lineament data have relatively good correlation with one another. The primary reason for this favorable agreement is due in part to the synoptic view that is characteristics of each. Resolution differences between the two types of data affect, to some extent, the detection of certain lineaments having local, rather than regional extent.

Table 3-1. Correlation Between Lineaments in Area 1

	# Lineaments Mapped	K 200	L 149	S 81	A 0	G 9	Amg 0
Known Faults (K)	200	--	15	15	0	1	0
Landsat Lineaments (L)	149		--	23	0	1	0
Skylab Lineaments (S)	81			--	0	0	0
Aerial Lineaments (A) (Not Plotted)	0				--	0	0
Gravity Lineaments (G)	9					--	0
Aeromagnetic Lineaments (Amg)	0						--

Explanation: 200 Known Faults Shown on Published Maps; portions of 15 of the 149 Landsat lineaments were in agreement (detected) with the Known Fault data.

Table 3-2. Correlation Between Lineaments in Area 2

	# Lineaments Mapped	K 80	L 145	S 88	A 100	G 10	Amg 18
Known Faults (K)	100	--	16	10	10	0	0
Landsat Lineaments (L)	145		--	25	18	0	1
Skylab Lineaments (S)	88			--	12	0	0
Aerial Lineaments (A)	100				--	0	0
Gravity Lineaments (G)	10					--	0
Aeromagnetic Lineaments (Amg)	18						--

Table 3-3. Correlation Between Lineaments in Area 3

	# Lineaments Mapped	K 160	L 149	S 90	A 110	G 15	Amg 10
Known Faults (K)	160	--	22	5	15	1	1
Landsat Lineaments (L)	149		--	25	30	0	1
Skylab Lineaments (S)	90			--	21	0	0
Aerial Lineaments (A)	110				--	0	1
Gravity Lineaments (G)	15					--	1
Aeromagnetic Lineaments (Amg)	10						--

The relative agreement between high altitude aerial lineaments and Skylab, and between Landsat lineaments and known faults, is relatively low. Again, the very high resolution and field-of-view characteristics of the aerial photos preclude to some extent the detection of regional lineament features.

The following sections discuss the salient observations regarding the relative correlation between the lineament data for each project area.

3.1.1 AREA 1 CORRELATIONS

3.1.1.1 Known Faults/Landsat Lineaments

Many of the major known faults in Area 1 are evident on the Landsat data. In particular, the ratioed-stretched color enhancements are especially useful for mapping some of the known faults. For example, the Helendale, Calico, Camp Rock and Lenwood faults are well expressed in the ratioed image. Based on this enhancement, a possible fault, also trending NW-SE, is evident between the Calico and Camp Rock faults. The E-W trending Cady fault is not well expressed on the Landsat data due to the surficial patterns in the area. Since many of the known faults were identified in the field based on subtle terrain characteristics not detectable from remote sensing platforms, a relatively poor correlation could have been anticipated.

3.1.1.2 Known Faults/Skylab Lineaments

A relatively good correlation exists between known faults and Skylab lineaments. All or portions of the major faults have been detected on the Skylab data. The number of lineaments on the Skylab data exceeds the number of known faults shown on the published maps. A NE-SW trending Skylab lineament in the Newberry Mountains area appears to be an unmapped fault; it is especially evident on the color ratioed-stretched Landsat image.

3.1.1.3 Landsat/Skylab Lineaments

A relatively good correlation is evident between Landsat and Skylab lineaments. The greater number of lineaments detected on the Landsat data is due to several reasons, including the fact that more varieties of Landsat data were available for interpretation (i.e., bands 5 and 7, color, color ratio-stretches, etc.).

3.1.2 AREA 2 CORRELATIONS

3.1.2.1 Known Faults/Landsat Lineaments

The low correlation between known faults and Landsat lineaments is due to the relatively short length (i.e., less than 3 km) of most of the known faults as compared to the average longer length of the Landsat lineaments (approximately 6 km). The major NW-SE trending fault is evident on Landsat data. On the other hand, faulting shown in the Twenty-Nine Palms area, Clipper Mountains, Iron Mountains and Old Woman Mountains area is not evident.

3.1.2.2 Known Faults/Skylab Lineaments

In general, low correlation is evident between known faults and Skylab data. Areas of favorable correlation include: (1) Twenty-Nine Palms; (2) Lead Mountains; (3) Bristol Mountains; and (4) Calumit Mountains. Areas of known faulting not evident on Skylab images include the Piute, Old Woman, Iron and Providence Mountains.

3.1.2.3 Known Faults/Aerial Lineaments

As with the above comparison, the areas having the best fault/aerial lineament correlations are in the Twenty-Nine Palms area, Lead Mountains, and the Bristol Mountains. Areas of low correlation include the Iron, Old Woman, Piute, and Providence Mountains.

3.1.2.4 Landsat/Skylab Lineaments

A good correlation is evident between Skylab and Landsat lineaments for Area 2. Correlations are best in the Twenty-Nine Palms area, Old Dad/Bristol Mountains, Granite Mountains, and Calumit Mountains, and lowest in the Iron, Old Woman, Piute, and Clipper Mountains.

3.1.2.5 Landsat/Aerial Lineaments

A relatively good correlation exists between Landsat and aerial lineaments in most of Area 2, except in the Old Woman and Piute Mountain area. Comparison of the two overlays prepared during interpretation indicates that in some instances aerial photography contains lineament information that has no correlation with Landsat lineament information in the same locality.

3.1.2.6 Skylab/Aerial Lineaments

Correlation of these two lineament types is moderate to low for Area 2. In the Twenty-Nine Palms area more Skylab lineaments were identified than aerial lineaments. Correlations were generally low in the Old Woman, Piute, Clipper, and Providence Mountains area, and higher in the Bristol and Calumit Mountain area.

3.1.3 AREA 3 CORRELATIONS

3.1.3.1 Known Faults/Landsat Lineaments

The best correlation between these two types of lineament data occurs in the Chocolate, Eagle, and Chuckawalla Mountain area. Correlations are lowest in the Big Maria, Palen, Coxcomb and Granite Mountains. The NW-trending faults located in the Chocolate Mountains and numerous faults located in the Chuckawalla Mountains are readily evident in the Landsat data. There is little evidence on the Landsat data of thrust faults in the Big Maria Mountains.

3.1.3.2 Known Faults/Skylab Lineaments

Correlations are generally similar to the above discussion. The best correlation occurs in the Chocolate and the Chuckawalla Mountains, the lowest in the Big Maria, Little Maria, Granite, and Coxcomb Mountains. The N-S trending fault in the western flank of the Black Hills and the NE-SW trending fault in the Little Chuckawalla Mountains are evident on the Skylab data.

3.1.3.3 Known Faults/Aerial Lineament

This correlation is essentially the same as for the two subsections above. The best correlations occur in the Chuckawalla and Chocolate Mountains areas where the fault pattern is well expressed topographically. Otherwise, few correlations are evident.

3.1.3.4 Landsat/Skylab Lineament

Good correlations occur between Landsat and Skylab lineaments detected in Area 3. Although these lineaments may vary slightly in length and regional extent, lineament patterns evident on each source are quite similar.

3.1.3.5 Landsat/Aerial Lineaments

A relatively good correlation is evident between Landsat and aerial lineaments in Area 3. Agreement is best in the Chuckawalla and Coxcomb Mountains, moderate in the Big Maria Mountains (for the longer faults) and low in Palo Verde, Palen and Granite Mountains.

3.1.3.6 Skylab/Aerial Lineaments

Correlations are relatively good for these two lineament categories in Area 3. In some localities a better correlation is evident between Skylab and aerial lineaments than between the Landsat and aerial lineament data. Similarities in resolution may account in part for this better agreement.

3.2 MAJOR LINEAMENT TRENDS

The major trends of the lineaments mapped for each of the project areas are shown in Table 3-4 and in rose diagram format in Appendix C. The five lineament categories included in this discussion are:

- Landsat lineaments (all)
- Landsat lineaments (major: > 20 km in length)
- Skylab lineaments
- Level 1, 2, and 3 lineaments (from Levels of Agreement Overlay)
- Aerial lineaments.

Results range from moderate to good correlation among the five categories within each project area; results are random when comparing major trends for one area to the trends of another area. For example, the major NW-SE fault trend of the three areas (as shown on the published map) is reflected in the N40-50W trend for the Levels 1, 2, and 3 lineament category.

The variations in lineament trends as reflected in Table 3-4 and the related rose diagrams are due in part to the geologic variety of each project area as well as to the quantity and quality of remote sensing data available for this project. Two factors affecting lineament pattern mapping were the heterogeneity and complexity of the geologic patterns and the relatively large percentage of alluvial cover within each area.

Table 3-4 shows that the N40-50W trend is the primary trend for four of the five lineament categories identified in Area 1 (aerial data were not included). This trend is particularly evident in the color ratioed-stretched Landsat enhancement and the Skylab photos. A N60-70E trend represents the second most prevalent trend for Landsat lineaments in Area 1.

Table 3-4. Major Lineament Trends Defined in Areas 1, 2, & 3

	LINEAMENT TYPES	TOTAL # OF LINEAMENTS MAPPED	PRIMARY TREND(S)	SECONDARY TRENDS
AREA 1	Major Landsat Lineaments	43	N40-50W	--
	Landsat Lineaments (all)	149	N40-50W	N40-50E, N60-70E
	Skylab Lineaments	81	N40-50W	--
	Levels 1,2,4 (no Level 3) Lineaments	121	N40-50W	--
	Aerial	Not Mapped		
AREA 2	Major Landsat Lineaments	18	N 0-10W	N40-50E
	Landsat Lineaments (all)	145	N80-90E	N40-50E
	Skylab Lineaments	88	N70-80E N50-60W	N70-80W
	Levels 1,2,3	107	N40-50W	N30-40W
	Aerial	126	N80-90E N10-20E N50-60W	
AREA 3	Major Landsat Lineaments	9	N50-90E	
	Landsat Lineaments (all)	149	N30-40W	N50-60W
	Skylab Lineaments	90	N60-70E	
	Levels 1, 2, 3	182	N40-50W	N50-60W
	Aerial	107	N30-40W N50-60E	

Table 3-5. Tonal Anomalies in Area 1

AREA OF TONAL ANOMALIES	GRID CELL LOCATION Block/Cell(s)	LITHOLOGIC ASSOCIATION	TONAL ANOMALY COLOR (on 4/5,5/6,6/7 ratio)	# OF ANOMALIES	LITHOLOGY CONTACT
Silver Mts.	B7 12,18,22,23	Metavolcanics	Dark Blue	6	JTrv/gr^{a}
Stoddard Mts.	C7 1, 2, 8	Metavolcanics	Dark Blue	2	JTrv
Sidewinder Mts.	D7 23, 24	Metavolcanics	Dark Green	4	JTrv/gr^{a}
Stoddard Ridge	E7 3, 7	Metavolcanics	Blue	2	JTrv/gr^{a}
Ord Mountains	E7 13, 21	Intrusives	Blue	2	gr^{a}/bi/pЄg
	E7 21, 23	Intrusives	Dark Green	2	gr^{a}/bi/pЄg
Newberry Mts.(W.)	E5 21-23	Intrusives	Dark Blue	5	gr^{a}/JTrv
	E6 1				
Newberry Mts.	F5 20-23	Intrusives	Dark Green	4	gr^{a}/Ti^{a}/Mv^{a}
	G5 15,16,25	Intrusives	Dark Green	2	
Newberry Mts.(E.)	G5 19,21,23	Intrusives	Blue/Green	8	Ti^{r}/mv/JTrv
Newberry Mts.	G6 2,6,9,14,17	Intrusives	Blue/Green	5	Mv^{p}/Ti^{r}/gr^{a}
Rodman Mts.	G7 22,25	Metavolcanics	Blue	2	gr^{a}/JTrv
Rodman Mts	H7 13,22,25	Metavolcanics	Blue	4	gr^{a}/JTrv
Rodman Mts.	H8 3, 4,6	Metavolcanics	Blue	3	gr^{a}/JTrv
Rodman Mts.(E.)	I6 16,23,25	Volcanics	Green/Blue/Red	3	Mv^{a}
Rodman Mts.(E.)	I7 2,8,13,23	Volcanics	Green/Blue	4	Ti/gr
Rodman Mts.(E.)	I8 4, 5, 6	Volcanics	Blue	2	Ti

Table 3-5. Tonal Anomalies in Area 1 (Con't.)

AREA OF TONAL ANOMALIES	GRID CELL LOCATION Block/Cell(s)	LITHOLOGIC ASSOCIATION	TONAL ANOMALY COLOR	# OF ANOMALIES	LITHOLOGY CONTACT
Calico Mts.	F3 13,18,23,24,25	Intrusives	Blue Green	6	$Mv^a/Mv^p/Ti^r/Ti^a$
Calico Mts.	F4 1,3,5,6	Intrusives	Blue Green	4	$Mv^a/Mv^p/Ti^r/Ti^a$
Lane Mts.	E2 5,15,19	Intrusives	Lavender	4	Ti^r/gr
Black Mts.	E3 5,10,21	Intrusives	Lavender	3	Ti^r/gr
Opal Mts	D1 21, 23	Intrusives	Lavender	2	Ti^r/gr
Black Mts	C1 16, 24	Intrusives	Lavender	4	Ti^r/gr
Alvord Mts.	H 21	Volcanics	Blue	1	Mv^a/gr

Table 3-4 also shows that approximately the same relative number of lineaments were mapped for Landsat and Skylab data for each of the project areas. Also, the major Landsat lineaments evident in Area 1 suggest a regional fracture pattern, based on the number of lineaments detected. Few regional Landsat lineaments were detected in Areas 2 and 3.

3.3 DETECTION OF TONAL ANOMALIES (INFERRED HYDROTHERMAL ALTERATION AREAS) (OVERLAYS 1B, 2B, 3B)

Based on the interpretation of the ratioed-stretched Landsat enhancements, a number of tonal anomalies have been identified in each of the three project areas.

Tonal anomalies are defined as areas where distinct color (or tonal) patterns occur in exposed bedrock areas. They appear anomalous in that their color is unlike the surrounding bedrock, or have a color unlike rocks of similar lithology (based on published maps) in other regions.

In general, dark blue and green colors appear most frequently as anomalous color patterns in the three project areas. Other colors detected include medium blue and green, lavender, and yellow. The following sections provide a discussion of the tonal anomalies identified in the three project areas.

3.3.1 TONAL ANOMALIES IN AREA 1

Numerous tonal anomalies occur within Area 1, primarily in the southern half of the region south of the Mojave Valley and east of the Mojave River. North of the Mojave River widespread tonal anomalies occur only in the Calico Mountain region. On the 4/5, 5/6, 6/7 ratioed-stretched composite prepared for Area 1, tonal anomalies are represented primarily by dark blue, dark green and medium green colors. Surficial and alluvial cover areas possess an overall light to medium blue, light green, or dark red color (in agricultural fields). The primary color characteristics for the major bedrock areas within Area 1 are: Granite Mountains (greenish beige-brown); Silver Mountains (greenish brown); Stoddard Mountains (several shades of green); Stoddard Ridge (beige); Ord Mountains (rust/red); Newberry Mountains (a variety of colors); Rodman Mountains (white, beige, green); Cady Mountains (beige, yellowish green); and Calico Mountains (a variety of colors).

Table 3-5 lists the tonal anomalies mapped for Area 1. Colors described are those evident on the 4/5, 5/6, 6/7 ratio-stretched image. Beginning at the lower left portion of Area 1, several distinct blue tonal anomalies occur within the Silver Mountains, east of the Mojave River and west of Interstate 15, along a contact zone between Jurassic-Triassic metavolcanics (JTrv) and Mesozoic granite (gr). On the Skylab images this area has a distinctly reddish surface color.

The next significant area having distinct anomalous color patterns occurs within and on the western end of the Stoddard Ridge area, north of Turtle Valley and west of Stoddard Well. The entire portion of the isolated mountain area has a distinct blue color; the geologic map shows the area as a Jurassic-Triassic metavolcanic unit. On the Skylab image this area also has a distinctive reddish tone. Structurally, this anomaly is located on the western flank of the inferred portion of a known (concealed) fault shown on the published map.

The Newberry Mountains area contains by far the greatest number of tonal anomalies. In the extreme eastern tip of these mountains the most prevalent colors are dark and medium blues. Farther to the west, dark green is the most prevalent color. Still farther to the west, towards Daggett Ridge, dark blue tonal patterns reappear. The dark green colors can be correlated with the Mesozoic granite unit (gr); the dark blues color generally correlate with Miocene volcanics (Mv). The entire extreme eastern portion of the Newberry Mountains has a distinct dark blue or dark green color. Several lavender-colored areas also appear. In the Newberry Mountains, an east-west trending lineament clearly has had an apparent structural influence on the dark green anomaly (granite) outcrop pattern.

Widespread dark blue or dark green tonal anomalies appear in the Calico Mountain area, primarily in the southern region. Mapping of distinct anomalies in this region was complicated by the widespread color patterns.

The Tertiary intrusive (rhyolite) areas north of the Calico Mountains appear as a deep purple color anomaly on the 4/5, 5/6, 6/7 ratioed-stretched image.

Evidence of tonal anomalies within the Lane Mountains is limited to a few areas having a dark red or purple pattern.

Evidence of tonal anomalies east of the Calico Mountains is limited to one dark blue area east of Coyote Lake in the Alvord Mountains.

Evidence of tonal anomalies within the Cady Mountains is limited to several isolated yellow-green patterns shown as Miocene volcanics-andesite (Mv^a) or Teritary intrusives-andesite. However, this tonal pattern was too widespread to justify the classification of these areas as tonal anomalies.

3.3.1.1 Correlation Between Tonal Anomalies and Known Faults

A visual interpretation of the data indicates that little or no spatial correlation exists, except possibly in the highly faulted Calico Mountains. Several tonal anomalies occur along the Calico and Camp Rock faults in the Ord Mountain area, and several small faults do appear to be correlated with anomalies in the Silver Mountains. One possibly notable observation is that tonal anomalies, more often than not, occur between major known fault zones.

3.3.1.2 Correlation Between Tonal Anomalies and Known Metallic Mineralization

No significant correlation is apparent between metallic mineralization and tonal anomalies in Area 1.

3.3.2 TONAL ANOMALIES IN AREA 2

A large percentage of Area 2 is covered by Quaternary alluvium (Qal) or Quaternary lake deposits (Ql). Areas of exposed bedrock where potential alteration might be located are thus restricted to a relatively few number of mountains including: (1) the Old Woman Mountains; (2) Piute Mountains; (3) Bristol Mountains; (4) Granite Mountains; (5) Providence Mountains; (6) Iron Mountains, and (7) Twenty-Nine Palms.

Analysis of the ratioed-stretched Landsat enhancements provides some information regarding evidence of anomalous tonal patterns. The 4/5, 5/6, 6/7 enhancement is discussed in this section to describe colors and patterns of these anomalies. Table 3-6 lists these areas, their location, and their correlation with lithology as shown on the published maps.

Beginning at the extreme upper left of the project area, north of Devils Playground area, several blue tonal anomalies are evident in early

Table 3-6. Tonal Anomalies in Area 2

AREA OF ALTERATION	GRID CELL LOCATION Block/Cells(s)		LITHOLOGIC ASSOCIATION	TONAL ANOMALY COLOR (on 4/5,5/6,6/7 ratio)	# OF ANOMALIES	LITHOLOGY CONTACT
Twenty-Nine Palms	A7	8, 9	Volcanics	Blue	3	Mv^P
Twenty-Nine Palms	B8	5, 6	Intrusives	Green	3	gr
Bristol/Old Dad Mts.	B4	7,15,17,21	Volcanics	Blue	6	Mv^P/gr
Bristol/Old Dad Mts.	B3	22	Volcanics	Blue	1	Mv^P
Granite Mts.	C3	6	Metamorphics	Blue	1	m/gr^m
Old Dad Mts.	C4	6, 14	Volcanics	Blue	3	Mv^P
Marble Mts.	D5	1,2,3,9, 10	Granites	Blue Lavender	7	gr/Tv
Bristol Mts.(E.)	D6	4, 6	Granites	Green	3	gr/m
Providence Mts.	E1	20, 22	Metamorphics	Blue/Green	2	Tv/pЄc/Pm
Providence Mts.	E2	2, 13	Metamorphics	Green	3	Tv/pЄc/Pm
Providence Mts.	E3	15, 17	Granite	Blue	3	gr/JTrv?
Marble Mts.	E5	16, 23	Granites	Blue	6	gr/IP/ls/Є
Clipper Mts.	F4	2,8,9,11,12 14,15,17 19,20,24	Volcanics	Green,Blue Red	15	Tv^P
Ship Mts.	F6 G5	11, 21 15	Volcanics	Green	3	Tv^P/gr
Blind Hills	G3	7,14,25	Volcanics	Green	4	Tv^P

Table 3-6. Tonal Anomalies in Area 2 (Con't.)

AREA OF ALTERATION	GRID CELL LOCATION Block/Cell(s)		LITHOLOGIC ASSOCIATION	TONAL ANOMALY COLOR	# OF ANOMALIES	LITHOLOGY CONTACT
Piute Mts.	H4 I4	1,11,19 53	Granites	Blue	3	gr/Tv
Piute Mts.	I4 I5	19,22,23 5,6	Granites	Blue	3	gr/gr
Piute Mts.	J3	5,6,7,13,15	Granites	Blue	5	gr/p€gr, p€g
Old Woman Mts.	H5	8, 9, 19	Granites	Blue	5	gr/p€g
Old Woman Mts.	I5	10,11,15,21,22	Volcanics	Blue	9	Tv/p€gr
Old Woman Mts.	H6	9,11,19,21	Granites	Blue	5	gr/p€
Old Woman Mts.	H7	19,20,21	Metamorphics	Blue	4	p€gr

Precambrian metamorphic rocks (epЄ). This area is slightly outside of the project area, however.

Evidence of tonal anomalies in the Granite Mountains is subdued to the apparent heavy vegetation cover. Only one blue tonal anomaly appears sufficiently distinct to merit its plotting.

Tonal anomalies within the Providence Mountains area generally limited to the extreme southern end of the mountain range (Granite Pass area) or to the eastern flank of the mountain. Again, vegetation cover in this area subdues the reflectance variations. The blue tonal anomalies on this eastern flank are located within the Mesozoic granite (gr) units south of the fault at Foshay Pass. North of this area the tonal anomalies are associated with a Tertiary intrusive (Ti) contact with a Permian marine (Pm) unit, or within Precambrian igneous and metamorphic rocks (pЄc).

Widespread tonal anomalies appear in the contact zone separating Precambrian granite (pЄgr) rock and Tertiary volcanics (Tv) in the extreme northern portion of the project area (Whisky Spring area), to the east of the main Providence Mountains bedrock area. These dark blue anomalies are located just beyond the boundary line for Area 2.

Widespread tonal anomalies are evident within the Clipper Mountains. Dark and medium greens and blues, reds, and lavender colors are especially prevalent. The green color on the southeast flank appears to be related to a contact between Tertiary intrusives (Ti^{r}) and Tertiary volcanics (Tv).

Few distinctive tonal anomalies occur within the Old Woman Mountains. The widespread dark green colors are primarily due to desert varnish coating on

Quaternary deposits. The red color is thought to be due primarily to topographic characteristics (steep slopes). A few blue anomalies are evident toward the southern portion. A widespread blue anomaly occurs within the Little Piute Mountains on the northeast edge of the mountain along a contact of Tertiary volcanics (Tv) and Precambrian granites.

Evidence of tonal anomalies within the Piute Mountains occurs in the southern portion along a Mesozoic granite/Precambrian granite contact. In this area, blue tonal patterns are evident. Several green tonal anomalies are evident north of Interstate 40 on the eastern flank of these mountains in a contact zone between Mesozoic granite (gr) and Precambrian metamorphics (p€g).

3.3.2.1 Correlation Between Tonal Anomalies and Known Faults

Favorable correlations between these two types of data are evident in the Lead Mountains, Cadiz Mountain area (in the Marble Mountains), several areas in the Clipper Mountains, and in the Little Piute Mountains. Many tonal anomalies occur, however, in areas that do not contain any known faults as shown on the published data.

3.3.2.2 Correlation Between Tonal Anomalies and Known Metallic Mineralization

No significant correlation is apparent between known metallic mineralization and tonal anomalies in Area 2, based on a visual interpretation.

3.3.3 TONAL ANOMALIES IN AREA 3

Since a relatively large percentage of Area 3 consists of unconsolidated alluvial deposits, a large portion of the surface area could thus be ruled out as having any potential for hydrothermal alteration. Table 3-7 shows the potential alteration areas for Area 3.

Table 3-7. Tonal Anomalies in Area 3

AREA OF ALTERATION	GRID CELL LOCATION Block/Cell(s)	LITHOLOGIC ASSOCIATION	TONAL ANOMALY COLOR	NUMBER OF ANOMALIES	LITHOLOGIC CONTACTS
Chocolate Mts.	A8,A9,B9,B10 C9,C10,D9	Mesozoic granite(gr) Tertiary volcanic(Tv) Tertiary intrusive (Ti)	Dark Blue Dark Blue Dark Blue	Numerous Numerous Numerous	gr/pЄc
Chuckawalla Mts.	C7,D8	Precambrian Gneiss (pЄg)	Green	1	
		Precambrian igneous/ metamorphic	Green		
Little Chuckawalla Mts.	F9,G9	Tertiary volcanics (Tv)	Blue	5	gr/pЄg
		Precambrian granites (pЄg)	Green		gr/pЄc
Palo Verde Mts.	I10	Tertiary volcanics (Tv)	Dark Blue	4	Ti/Tv
		Tertiary intrusives (Ti)	Dark Blue		
Black Hills	A10	Tertiary volcanics (Tv)	Dark Blue	5	None
		Tertiary intrusives (Ti)	Green	1	
McCoy Mts.	H5	Mesozoic granites(gr)	Dark Blue	1	gr/ms
Palen Mts.	G5,G4	Pre-Cretaceous volcanics (mv)	Dark Blue	3	ms/mv
	F4	Pre-Cretaceous meta-sedimentary (ms)	Dark Green	1	ms/mv
		Mesozoic granite (gr)	Green	3	gr/IP/m

Table 3-7. Tonal Anomalies in Area 3 (Con't.)

AREA OF ALTERATION	GRID CELL LOCATION Block/Cell(s)	LITHOLOGIC ASSOCIATION	TONAL ANOMALY COLOR	NUMBER OF ANOMALIES	LITHOLOGIC CONTACTS
Little Maria Mts.	G4, H4	Mesozoic granite (gr)	Dark Blue	Several	-
		Mesozoic granite (gr)	Green	Several	gr/IP
Big Maria Mts.	I4,J4,J5	Pre-Cretaceous metamorphics (m)	Green	Widespread	-
Coxcomb Mts.	D5	Pre-Cretaceous metasedimentary (ms)	Lavender	1	mv/ms
Eagle Mts.	C4,B5,B6	Mesozoic granite (gr)	Light Blue Blue Green	Numerous	gr/ms

BLM Library
Denver Federal Center
Bldg. 85, OC-521
P.O. Box 25047
Denver, CO 80225

As noted for Areas 1 and 2, dark blues and dark and medium greens appear frequently in the bedrock areas. The Chocolate Mountains in the southwest corner of Area 3 contain the most widespread dark blue tonal anomaly. The dark blues correlate generally with Tvp (Tertiary pyroclastics), Mesozoic granite (gr), p€c (Precambrian igneous and metamorphic rocks), and Ti (Tertiary intrusive). Tonal anomalies in the Chocolate Mountains appear related to the primary NW fault trend characteristic of this area.

Most of the Mesozoic granites (gr) prevalent in the Chocolate Mountains area appear to contain significant anomalous tonal patterns. The dark blue anomaly patterns appear to be contained within lenses in the Mesozoic granite (gr) unit. These lenses could possibly be portions of the Precambrian complex (p€c) as suggested by the geologic map. There are at least two major dark blue anomalies, both of which are associated with a known fault (shown on the published map), that are definitely within the Mesozoic granite unit.

Few anomalous tonal patterns occur within the Chuckawalla Mountains area. The primary tonal patterns of the area include reddish-brown for the Precambrian gneiss (p€g) unit, and yellow-beige for the Mesozoic granite (gr) unit and the Precambrian (p€c) unit. The predominant medium to dark green anomalous tonal pattern in the Pilot Mountain area appears too widespread for correlation to any specific lithologic unit or locality. Two areas appear sufficiently distinct for mapping, one on the extreme north-western tip of the Chuckawalla Mountains, and the other on the extreme eastern end. Several anomalous tonal patterns are evident within the strip of Chuckawalla Mountains south and east of the Aztec mine area. These colors are associated with a Tertiary volcanic (Tv) unit.

Farther to the east in the Little Chuckawalla Mountains, several distinct northeast-trending dark blue and dark green areas are evident. The dark blue areas are associated with the Tertiary volcanic (Tv) unit, while the dark greens occur within a Precambrian granite (p€gr) unit.

Widespread evidence of anomalous tonal patterns occur in the Tertiary volcanics (Tv) comprising the Black Hills region. Although several distinct dark blue tones are evident in this area, the general bluish tint to the entire area raises doubts as to the validity of these observations.

A widespread bluish tint also appears in the Palo Verde Mountains to the east. Again, although several distinctly darker blue zones can be identified, the widespread blue color raises doubts as to the validity of these points. The Tertiary andesite intrusive (Ti^a) appears as a yellowish-red tonal pattern. Evidence of potential alteration within the McCoy Mountains to the north is restricted to one dark green anomaly evident at the extreme northwest-trending mountain. The anomaly appears to be related to a contact zone between Pre-Cretaceous metasedimentary unit (ms) and a Mesozoic granite (gr).

The most distinct tonal anomaly within Area 3 occurs immediately to the west in the Palen Mountains area. In this area the primary dark blue tonal anomaly appears related to a contact between Pre-Cretaceous metavolcanics (mv) and Pre-cretaceous metasedimentary units (ms). A similar tonal anomaly occurs directly to the north along a similar contact zone. A suggestion of alteration is also evident by the dark green tonal anomaly located at a complex intersection of lithologic assemblages comprised of Mesozoic granite (gr), Pre-Cretaceous metamorphics (m), and Paleozoic

Similar evidence of potential alteration is suggested by the dark blue tonal anomaly located at the northern end of the Little Maria Mountains. The tonal pattern is definitely related to the Paleozoic marine (IP-limestone) unit that is in contact with Mesozoic granitic (gr) units.

To the southeast, additional dark green and dark blue anomalies occur in a contact zone characterized by Paleozoic marine (IP-limestone) and Mesozoic granites (gr).

No distinct tonal anomalies occur in the Granite Mountains, and only one isolated tonal anomaly is apparent in the Coxcomb Mountains to the west. The latter pattern occurs along a contact zone separating Pre-Cretaceous metasedimentary rocks (ms) and Pre-Cretaceous metavolcanic units.

In the Eagle Mountains, relatively few distinct tonal anomalies are evident, although a considerable number of small, dark blue and dark green anomalies occur. There is, however, a very large (6 km wide) light blue tonal anomaly directly related to the contact between Pre-Cretaceous sedimentary rocks and Mesozoic granites (gr), in the vicinity of the Black Eagle Mines.

3.3.3.1 Correlation Between Tonal Anomalies and Known Faults

Visual interpretation indicates a relatively good correlation between tonal anomalies and known faults. Spatial trends are especially favorable in the Chocolate Mountains (NW fault trend) area in the southwestern corner of Area 3. Favorable correlations also occur in the Little Chuckawalla Mountains (NE fault trend), Granite Mountains, and the Big Maria Mountains (NW fault trend). A moderate correlation is evident in the Eagle Mountain area, where a dark green tonal anomaly appears related to a NNE-SSW and a NE-SW trend.

3.3.3.2 Correlation Between Tonal Anomalies and Known Metallic Mineralization

Very little correlation is evident between known mineralization and tonal anomalies in Area 3. Favorable areas consist primarily of the McCoy Mountain area (gold and copper deposits in the northern end of the mountain range) and the southeastern portion of the Chuckawalla Mountains (gold and silver deposits).

3.4 CORRELATION BETWEEN LINEAMENTS AND TONAL ANOMALIES

One of the major objectives of this project consisted of the identification of areas having potential mineralization using two different analysis techniques: (1) "spatial"; and (2) "statistical" analysis. The "spatial" analysis approach as discussed in this section concerns an analysis of the spatial relationship between tonal anomalies and lineaments. (The "statistical" approach is discussed in Section 3.5.)

The major objective of the "spatial" analysis task focused on the spatial relationship between lineaments and tonal anomalies: i.e., what is the structural correlation between lineament features as mapped from Landsat, Skylab, aerial or published data and tonal anomalies? If a structural correlation could be defined between these features and if the tonal anomalies evident on the ratioed-stretched Landsat images proved to be hydrothermally altered areas (based on field verification), then the identification of additional areas likely to have hydrothermal alteration would be possible. Development of a model of this type for the California Desert Conservation Area would considerably enhance field reconnaissance and evaluation of the areas' mineral potential.

Three types of correlations were developed in order to determine whether any significant pattern or trend could be detected which would assist in analysis of the metallic mineral exploration potential of each project area.

Correlation #1 considers the spatial correlation between lineaments and tonal anomalies. Correlation #2 considers the angle of lineament intersection for those intersecting lineaments located on or near a tonal anomaly. Correlation #3 considers the possibility that certain sets of intersecting lineaments have favorable spatial correlations with tonal anomalies.

Appendices D, E, and F show the data sheets developed for Correlation #1, Correlation #2, and Correlation #3, respectively.

3.4.1 AREA 1 LINEAMENT/TONAL ANOMALY CORRELATION

3.4.1.1 Correlation #1 Discussion

3.4.1.1.1 Landsat Lineaments (all) and Tonal Anomalies

In the discussions that follow (Sections 3.4.1.1, 3.4.2.1, 3.4.3.1) the "alarms" and "grouping" are frequently used. For each situation where a tonal anomaly is located "on" or "close" to a lineament, an "alarm" is recorded. Visual inspection of Appendix D data sheets notes each of the alarms recorded for each type of lineament/tonal anomaly relationship recorded. A clustering of an unusually high number of alarms in a particular range of trends (e.g., between N45-50W) is referred to as a "grouping".

To reiterate other terminology to be used, the "on", "close" and "combined" categories summarize the relationship between those anomalies: i.e., (1) located on (or directly next to) a Landsat lineament, (2) those anomalies located within 0.6 km of the lineament; and (3) "combined", that is, on or within .6 km. Table 3-8 shows the results of the lineament/tonal correlation for Area 1. For the Landsat lineaments (all) category, a total of 149 lineaments and 110 tonal anomalies were mapped. Only 14 tonal anomalies did not meet one of these two categories in Area 1. A total of 184 "alarms" (defined as those instances where a spatial Landsat lineament/tonal anomaly relationship was evident) were recorded in Area 1, 115 of which fall in the "on" category and 69 in the "close" category.

For the "on" category, the most distinct peaks occur in the NW trend. Distinct peaks occur at N45-48W (12 alarms), N90W (8), N1W (7), N22-25W (7), N30-35E (12), and N45-48E (10).

For the "close" category, a total of 69 "alarms" were recorded. The three primary peaks occur at N45-48W (10 alarms), N40-48E (10) and N10W (5).

For the "combined" category, a total of 184 alarms were recorded. Similar to the above results, distinct peaks occur at N45-48W (22 alarms), N90W (13), N30-35E (17), and N45-48E (15).

3.4.1.1.2 Major Landsat Lineaments and Tonal Anomalies

A total of 43 major Landsat lineaments were mapped in Area 1. Forty-five of the 110 tonal anomalies detected have no spatial correlations (located on or within 0.6 km) with a major Landsat lineament. Forty-five alarms were recorded for the "on" category. The largest percentage of alarms occur at N45-48W (13 alarms) and at N90W (9). Thirty-four alarms were recorded for the "close" category; the only distinct grouping of alarms occurs at N45-48W (11 alarms). For the "combined" category, the largest percentage of alarms occur at N45-48W (24 alarms) and N90W (13).

Table 3-8. Lineament/Tonal Anomaly Correlations (Area 1)

				"ON"			Within 0.6 km			"COMBINED"		
	Total Number of Lineaments Mapped in Area 1	Total Number of Anomalies Mapped in Area 1	Number of Anomalies Having no Spatial Correlation with Lineaments	Number of Alarms Recorded for "ON" Category	Major Lineament Trend(s)	Number of Alarms Per Trend	Number of Alarms Recorded for "CLOSE" Category	Major Lineament Trend(s)	Number of Alarms Per Trend	Number of Alarms Recorded for "Combined Category"	Major Lineament Trend(s)	Number of Alarms Per Trend
LINEAMENTS (ALL)	149	110	14	115	N45-48W N30-35E N90W N1W N22-25W N45-48E	12 12 8 7 7 10	69	N45-48W N40-48E N90W	10 10 5	184	N45-48W N30-35E N45-48E N90W	22 17 15 13
LANDSAT (MAJORS)	43	110	45	45	N45-48W N90W	13 9	34	N45-48W	11	79	N45-48W N90W	24 13
SKYLAB	81	110	27	80	N23-34E N45-49W N14W	15 11 7	36	N45-49W N20E	11 6	116	N28-34E N45-49W	20 16
LEVELS 1, 2, 4	121	110	49	42	N14W	8	27	N37-40W	9	69	N37-40W N14-16W	13 12

3.4.1.1.3 Skylab Lineaments and Tonal Anomalies

A total of 81 Skylab lineaments were mapped in Area 1. Twenty-seven of the 110 tonal anomalies mapped in this area have no spatial correlation with Skylab lineaments.

Eighty "alarms" were recorded for the "on" category. The largest percentage of alarms occur at N23-34E (15 alarms), N45-49W (11) and N14W (7). For the "close" category, 36 alarms were recorded; eleven (11) alarms occur at N45-49E (11 alarms) and six (6) at N20E. For the "combined" category, the N28-34E trend (20 alarms) and the N45-49W trend (16) are dominant.

3.4.1.1.4 Levels 1, 2, and 4 Lineaments and Tonal Anomalies (No Level 3)

A total of 121 lineaments are included in the Levels 1, 2 and 4 category. Of the 110 tonal anoamlies mapped for Area 1, 49 did not fall in the "on" or "close" category. Forty-two alarms were recorded for Area 1 in the "on" category. The only distinct grouping of alarms occurs at N14W (8 alarms). For the "close" category, only 27 alarms were recorded. The only distinct grouping in this category occurs at N37-40W (9 alarms). For the "combined" category, two distinct groupings occur at N37-40W (13 alarms) and N14-16W (12).

3.4.1.1.5 Summary

Figure 3-1 shows the primary trends recorded for those lineaments having a higher than usual correlation with tonal anomalies. These trends for each of the five individual lineament types were combined and are shown as a fifth line, labeled "composite".

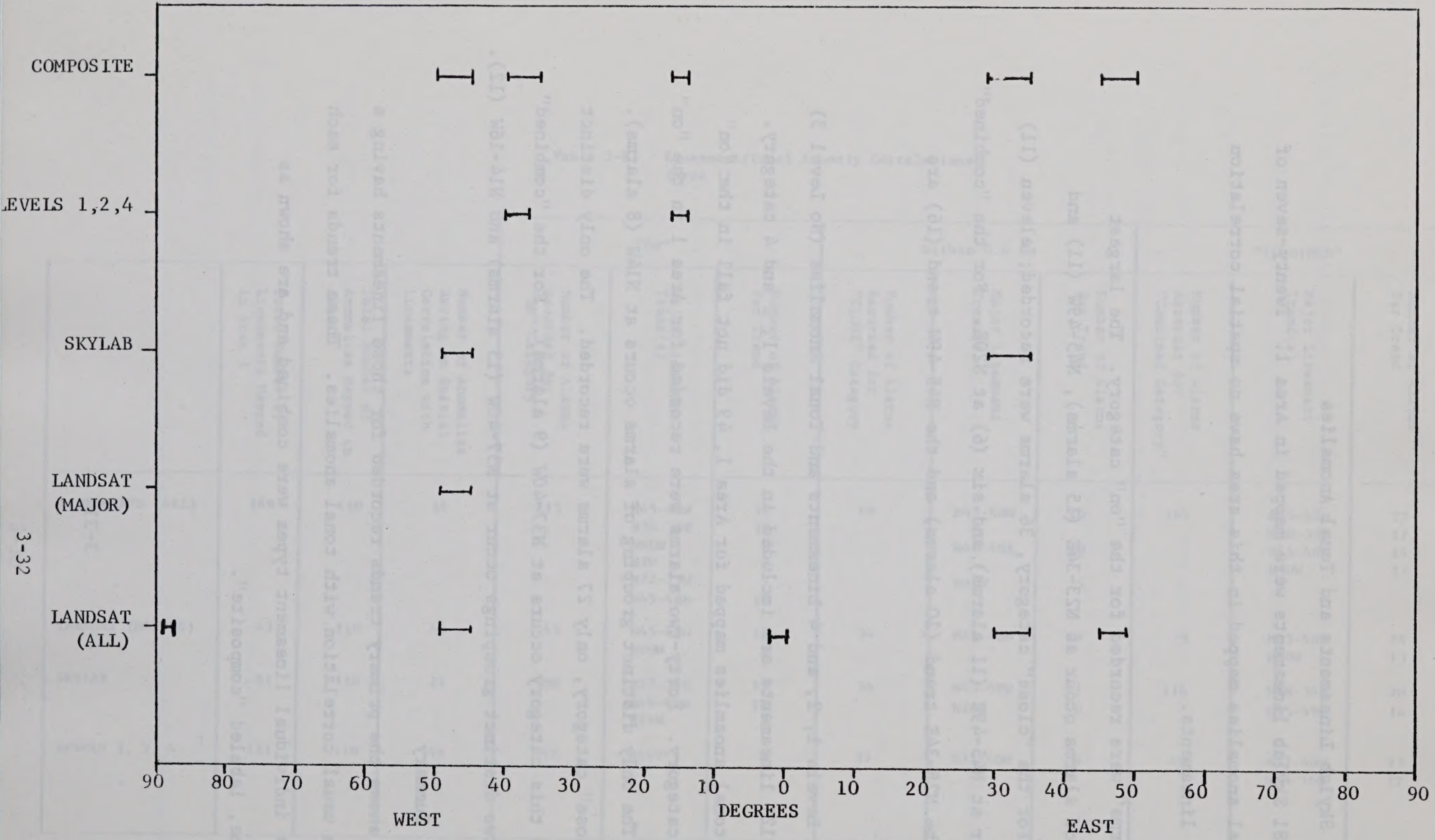

Figure 3-1. Lineament/Tonal Anomaly Correlation Results (Area 1)
(Most Alarms Occurred at the Areas Indicated by Brackets)

The results of this correlation generally indicate that tonal anomalies cluster more frequently than usual (relative to their overall distribution) along certain lineaments trends, including: N45-48W; N45-48E; N90W; N1W-N1E; and N30-35E. Should the Landsat-identified tonal anomalies represent hydrothermal alteration areas, then, based on this information only, the optimum areas to locate additional candidate altered areas would be along these particular trends.

3.4.1.2 Correlation #2 (Lineament Intersection Angles)

Figure 3-2 shows the histogram data compiled for Area 1 showing angles of intersecting lineaments associated with tonal anomalies. The most distinct peaks evident in the five histograms compiled occur in the major Landsat lineaments category at 35-50 and 115-130. For the Landsat lineament (all) intersections angle categroy, results are more widely distributed except for a broad peak at 70-110°, a distinct peak at 85°, and a more subtle peak at 35-55°.

Based on these data, tonal anomalies appear to be located more frequently than usual at lineament intersection angles of: (1) 35-50°; and (2) 70-110°.

3.4.1.3 Correlation #3: Lineament Sets

A review of the four matrices (Appendix E, Figures E-1 to E-4) prepared as part of this correlation for Area 1 suggests some grouping of "data points." (Data points represent the occurrence of a tonal anomaly located at the intersection of two lineaments.) Results vary somewhat for each of the four lineament categories considered (Landsat-all, Landsat-major, Skylab, and Levels 1, 2, 4). Results do indicate several repetitive patterns, and, perhaps as significant, indicate areas where low correlations (indicated by absence of data points on the matrix) exist. The general collection

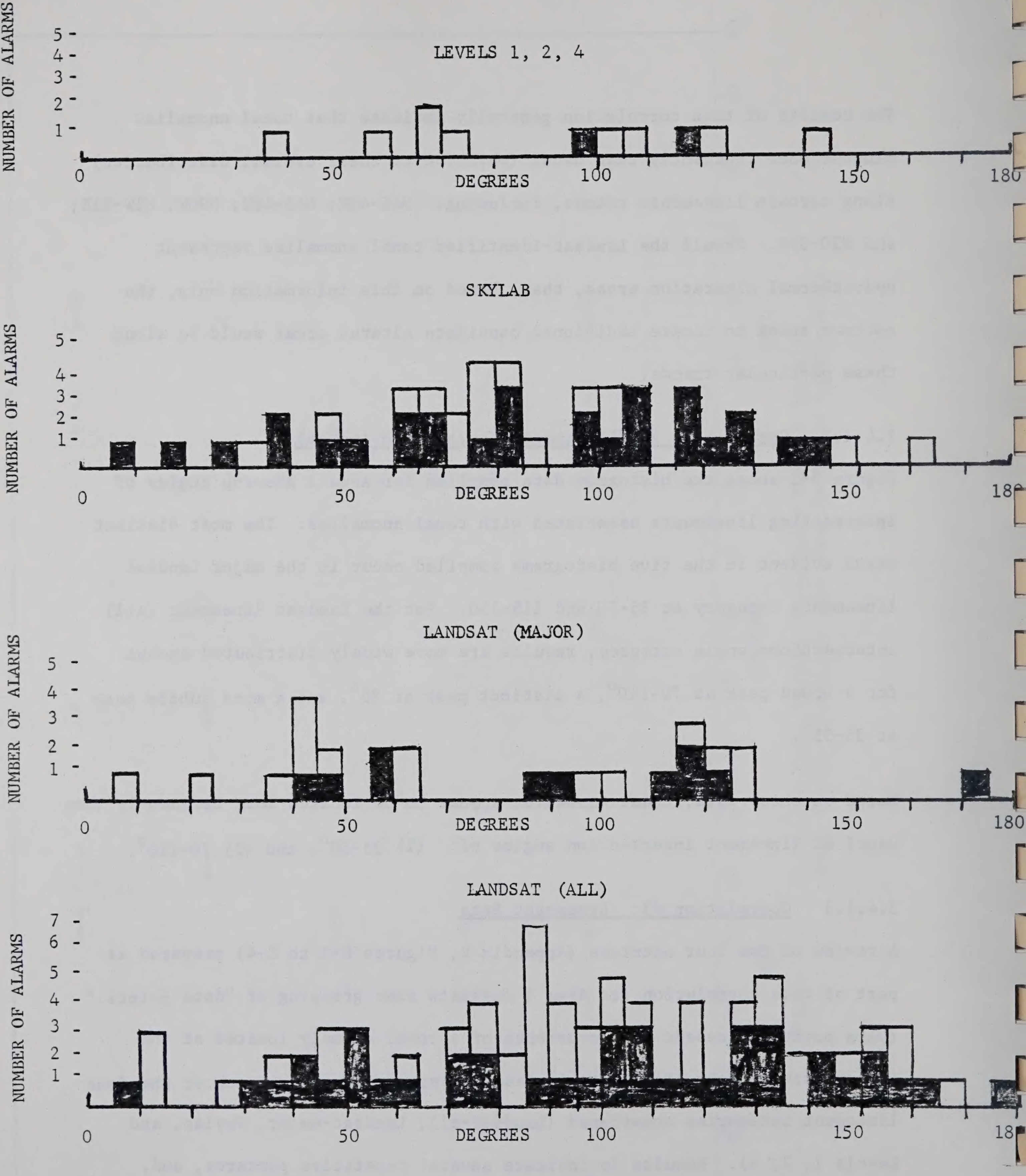
LEVELS 1, 2, 4

SKYLAB

LANDSAT (MAJOR)

LANDSAT (ALL)

Figure 3-2. Variation in Lineament Intersection Angles: Area 1

of data points in a regional area is defined as a "group". The collection of several data points about a localized area (at least three data points in a $5^{\circ} \times 5^{\circ}$ area) is defined as a "cluster". These features have been outlined on some of the matrices to emphasize potentially important areas. It is important to note that the outlining of these clusters was done on a subjective basis. Some of the clusters are much better defined (i.e., more localized) than others; the more centralized and the more data points contained within a cluster, the relatively better the possible significance. These higher potential "clusters" are indicated by solid lines; the lower potential "groups" by a dashed line. The salient characteristics of each of the matrices compiled for this correlation are described in the following subsections.

3.4.1.3.1 Intersections of Landsat Lineament (all) with Tonal Anomalies

The ten major clusters for the Landsat lineament (all) and tonal anomalies are shown in Figure E-1 of Appendix E. The three major "groups" occur at the upper left corner of the matrix (Group 1), the bottom center (Group 2), and at the lower right (Group 3).

Group 1 is considered of low potential because of the widely spaced data points. Group 2 is considered the most significant because of the number of distinct clusters (6) occurring in this area. Group 3 is considered of relatively low significance.

The several clusters within Group 2 suggest that most of the tonal anomalies/lineament intersection correlations occur within a zone generally partitioned between N10-50W and N40-90E, and more specifically, between N10-50W and N45-70E.

3.4.1.3.2 Intersections of Landsat (Major) with Tonal Anomalies

Salient features of this matrix (Figure E-2) include a distinct (but large) grouping between N40-55W and N45-90E. The most distinct cluster is located at N45-50W/N85-90E and correlates with one of the clusters in Group 2 for Landsat (all) lineaments.

3.4.1.3.3 Intersection of Skylab Lineaments with Tonal Anomalies

Salient features of this matrix (Figure E-3) include two distinctly identifiable clusters; in general, most of the data points are randomly scattered. Clusters occur at: (1) N50-55W/N25-30E; (2) N40-55W/N65-70E; (3) N85-90W/N20-30E; and (4) N20-30E/N55-70E.

3.4.1.3.4 Intersection of Levels 1, 2, and 4 Lineaments with Tonal Anomalies

Data points are generally scattered.

3.4.1.3.5 Summary

The results of Correlation #3 do not indicate the existence of any particular set of intersecting lineaments that have distinct correlation with tonal anomalies. Many factors may account for the relatively random distribution of data points in each of the matrices prepared; nevertheless some potentially significant observations can be made based on these data:

(1) Figure E-1 indicates a relatively good clustering of data points at the intersection of lineaments trending N40-50W/N85-90E (5 points).

(2) Figure E-1 also indicates that clusters occur at the intersection of lineaments trending N10-30W and N45-50E (7 points) and at N30-50E/N80-85E (Group 3 - 6 points).

(3) Figure E-1 indicates a notable absence of data points in a very large region in the N0-N40E/N0-N90W region.

(4) Only a few scattered data points (Group 1) occur in another rather large area of this matrix in the upper third (N0-90W/N0-90W) region (to the left of the diagonal line).

(5) The clustering of data points noted in item #1 above (at N40-50W/N85-90E) is also evident on Figure E-2.

(6) In contrast to that comment noted in item #3 above, Figure E-3 (Skylab) indicates a number of data points occur in this same area.

3.4.2 AREA 2 LINEAMENT/TONAL ANOMALY CORRELATION

3.4.2.1 Correlation #1 Discussion

3.4.2.1.1 Landsat Lineaments (All) and Tonal Anomalies

Table 3-9 shows that a total of 145 Landsat lineaments and 118 tonal anomalies were mapped in Area 2. Only twenty-nine out of the total of 145 tonal anomalies have no spatial relationship to the Landsat lineaments. The "on", "close", and "combined" categories summarize the salient features evident in the recorded data.

A total of 154 "alarms" - or instances where a tonal anomaly was located on or close to a Landsat lineament - occur in Area 2. Seventy-nine of these fall in the "on" category and 75 in the "close" category.

For the "on" category, the largest percentage of alarms occur at N22-29E (11 alarms), N37-41E (10) and W40-43W (10).

Results vary somewhat for the "close" category. Alarms occur at N40-43W (10 alarms), N47-48E (7), and N70-72E (6). Other data points evident in this category are generally scattered.

The "combined" category shows the largest percentage of alarms at N40-43W (20 alarms). Other distinct groupings of alarms occur at N22-29E (14), N37-41E (14), N12-14E (12), N47-49E (11), and N70-72E (10).

Table 3-9. Lineament/Tonal Anomaly Correlations
(Area 2)

				"ON"			Within 0.6 km			"COMBINED"		
	Total Number of Lineaments Mapped in Area 2	Total Number of Anomalies Mapped in Area 2	Number of Anomalies Having no Spatial Correlation with Lineaments	Number of Alarms Recorded for "ON" Category	Major Lineament Trend(s)	Number of Alarms Per Trend	Number of Alarms Recorded for "CLOSE" Category	Major Lineament Trend(s)	Number of Alarms Per Trend	Number of Alarms Recorded for "Combined Category"	Major Lineament Trend(s)	Number of Alarms Per Trend
LANDSAT (ALL)	145	118	29	79	N22-29E N37-41E N40-43W	11 10	75	N40-43W N47-48E N70-72E	10	154	N40-43W N37-41E N22-29E N12-14E N70-72E	20 14 14 12 10
LANDSAT (MAJOR)	18	118	72	27	N49-51W N43-44W N40E	6 5 4	34	N49-51W N43W N67W N40E	6 5 5 5	61	N45-51W N43-44W N40E	12 11 9
SKYLAB	88	118	55	38	N18E N25E	7 6	44	N15-18E	10	82	N15-18E N53-60W	19 12
LEVELS 1, 2, 3	107	118	68	26	N58-63W N28E	6 4	36	N30-31W N43-44W	5 4	62	N60-63W N43-48W N30-31W	8 7 6
AERIAL	126	118	46	59	N60-62W N 8-13W N50-52W	9 8 6	61	N 8-13W N50-52W	11 8	120	N 8-13W N50-52W N60-61W	19 14 13

3.4.2.1.2 Major Landsat Lineaments and Tonal Anomalies

Eighteen major Landsat lineaments were mapped in Area 2. Of the total of 61 alarms recorded, 27 occur in the "on" category and 34 in the "close" category. Seventy-two of the tonal anomalies have no spatial correlation with major Landsat lineaments. The largest percentage of alarms in the "on" category occur at N49-51W (6 alarms), N43-44W (5), and N40E (4).

The largest grouping of alarms in the "close" category occur at N49-51W (6 alarms), N43W (5), N67W (5) and N40E (5).

In the "combined" category, the primary grouping of alarms occur at N49-51W (12 alarms), N43-44W (11), and N40E (9).

3.4.2.1.3 Skylab Lineaments and Tonal Anoamlies

A total of 88 Skylab lineaments were mapped in Area 2. Fifty-five of the 118 tonal anomalies mapped have no spatial correlation to Skylab lineaments.

Few significant groupings of alarms occur for either the "on" or "close" categories. For the "on" category, 38 alarms were recorded; the only groupings occur at N18E (7 alarms) and N25E (6). The only distinct grouping in the "close" category occurs at N15-18E (10 alarms).

The "combined" category shows one distinct peak at N15-16E (19 alarms) and one more widely-spread grouping located at N53-60W (12).

3.4.2.1.4 Levels 1, 2, and 3 Lineaments and Tonal Anomalies

A total of 107 Levels 1, 2 and 3 lineaments were mapped in Area 2. Sixty-eight of the 118 tonal anomalies have no spatial correlation to Skylab lineaments.

No well defined groupings of alarms are evident for either the "on", "close", or "combined" categories. The primary groupings for the "on" category (26 alarms recorded) occur at N58-63W (6 alarms) and N28E (4).

For the "close" category, (36 alarms recorded), relatively insignificant groupings occur at N30-31W (5 alarms) and N43-44W (4).

For the "combined" category, groupings are located at N60-63W (8 alarms), N43-48W (7), and N30-31W (6).

3.4.2.1.5 Aerial Lineaments and Tonal Anomalies

A total of 126 aerial lineaments were mapped in Area 2. Forty-six of the 118 tonal anomalies have no correlation with aerial lineaments.

Several well defined groupings of alarms occur in both the "on" and "close" categories. For the "on" category, of the 59 alarms recorded, distinct groupings occur at N60-62W (9 alarms), N8-13W (8), and N50-52W (6).

For the "close" category, of the 61 alarms recorded, distinct groupings occur at N8-13W (11 alarms) and N50-52W (8).

For the "combined" category, distinct groupings occur at N8-13W (19 alarms), N50-52W (14), and N60-61W (13).

3.4.2.1.6 Summary

Figure 3-3 shows the primary trends recorded for those lineaments having a higher than usual correlation with tonal anomalies. The trends for each of the five individual lineament types were combined and are shown as the sixth line, labeled "composite".

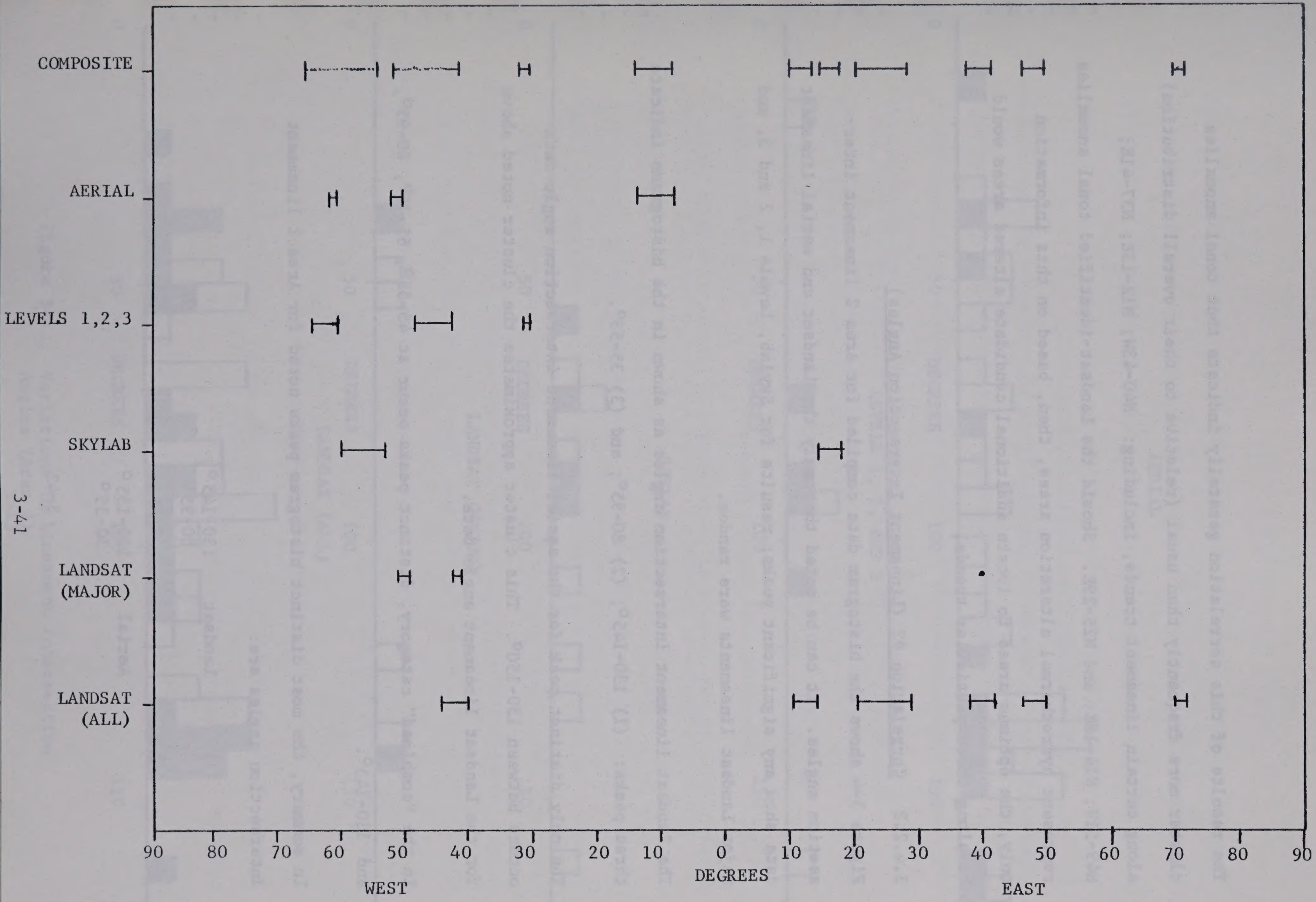

Figure 3-3. Lineament/Tonal Anomaly Correlation Results (Area 2)

The results of this correlation generally indicate that tonal anomalies cluster more frequently than usual (relative to their overall distribution) along certain lineament trends, including: N40-43W; N12-13E; N37-41E; N49-51W; N14-18E; and N25-29E. Should the Landsat-identified tonal anomalies represent hydrothermal alteration areas, then, based on this information only, the optimum areas to locate additional candidate altered areas would be along these particular trends.

3.4.2.2 Correlation #2 (Lineament Intersection Angles)

Figure 3-4 shows the histogram data compiled for Area 2 lineament intersection angles. It can be noted that only the Landsat and aerial lineament data show any significant peaks; results for Skylab, Levels 1, 2 and 3, and major Landsat lineaments were random.

The Landsat lineament intersection angles as shown in the histograms indicate three peaks: (1) 130-145°; (2) 80-95°; and (3) 35-55°.

The only distinct peak for the aerial lineament intersection angle data occurs between 130-150°. This cluster approximates the cluster noted above for the Landsat lineament angle data.

In the "combined" category, distinct peaks occur at 45-55°, 65-75°, 80-95°, and 130-145°.

In summary, the most distinct histogram peaks noted for Area 2 lineament intersection angles are:

Landsat	130-145°
	80-95°
	35-55°
Aerial	130-155°
	30-35°

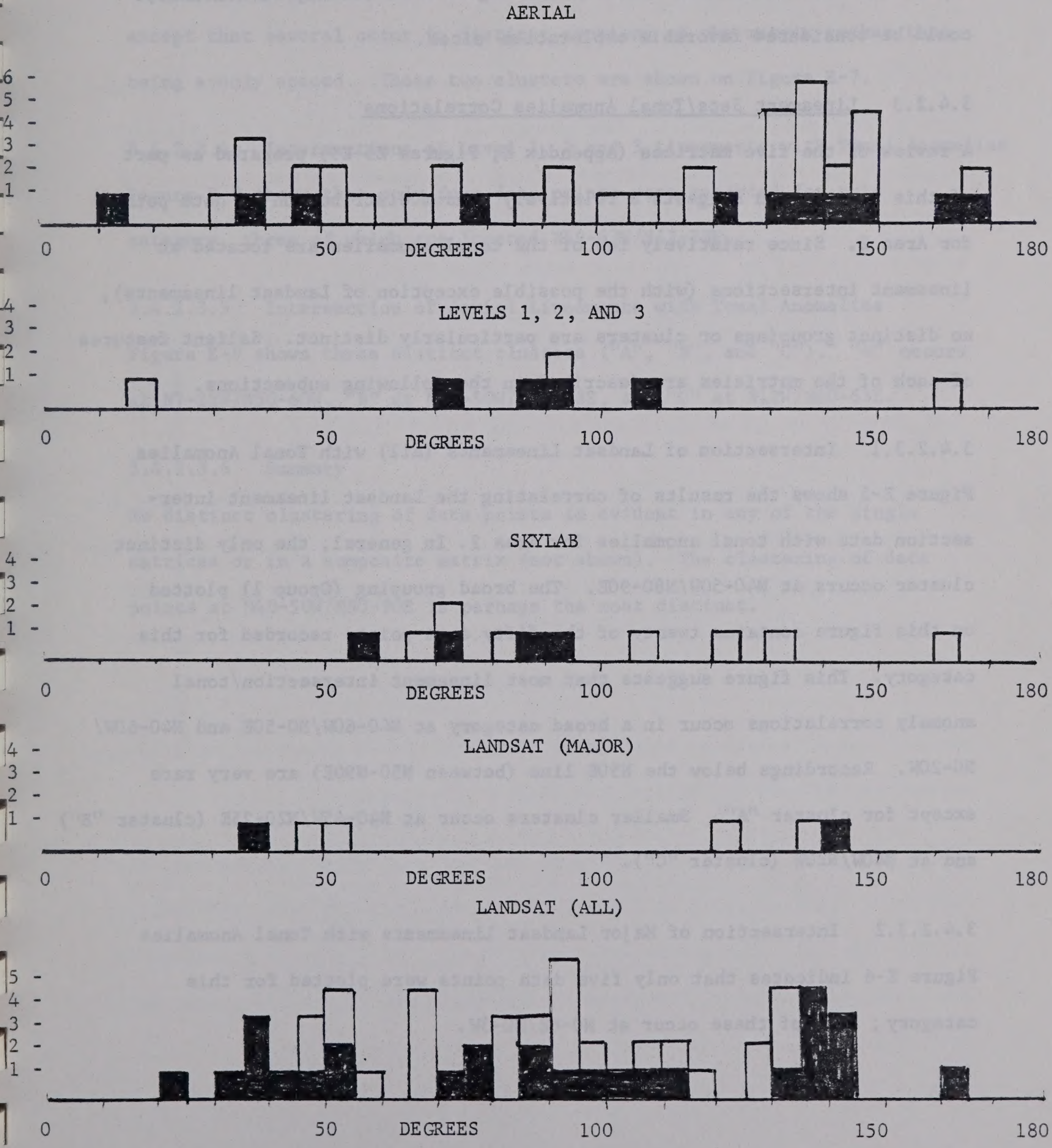

Figure 3-4. Variations in Lineament Intersection Angles (Area 2)

Thus, in Area 2, based on the data shown in the histograms, an area having one of the above lineament intersection angle/tonal anomaly relationships could be considered favorable exploration sites.

3.4.2.3 Lineament Sets/Tonal Anomalies Correlations

A review of the five matrices (Appendix E, Figures E5-E9) prepared as part of this correlation suggests a relatively random distribution of data points for Area 2. Since relatively few of the tonal anomalies are located at lineament intersections (with the possible exception of Landsat lineaments), no distinct groupings or clusters are particularly distinct. Salient features of each of the matricies are described in the following subsections.

3.4.2.3.1 Intersection of Landsat Lineaments (all) with Tonal Anomalies

Figure E-5 shows the results of correlating the Landsat lineament intersection data with tonal anomalies for Area 2. In general, the only distinct cluster occurs at N40-50W/N80-90E. The broad grouping (Group 1) plotted on this figure contains twenty of the fifty data points recorded for this category. This figure suggests that most lineament intersection/tonal anomaly correlations occur in a broad category at N40-60W/N0-50E and N40-60W/N0-20W. Recordings below the N50E line (between N50-N90E) are very rare except for cluster "A". Smaller clusters occur at N40-45W/N20-25E (cluster "B") and at N40W/N20W (cluster "C").

3.4.2.3.2 Intersection of Major Landsat Lineaments with Tonal Anomalies

Figure E-6 indicates that only five data points were plotted for this category ; four of these occur at N0-6E/N0-3W.

3.4.2.3.3 Intersection of Skylab Lineaments with Tonal Anomalies

The nine data points plotted for this category appear randomly distributed except that several occur in distinct sections of the matrix rather than being evenly spaced. These two clusters are shown on Figure E-7.

3.4.2.3.4 Intersections of Level 1, 2 and 3 Lineaments with Tonal Anomalies

Figure E-8 shows that only four data points were recorded for this category, three of which are located N59-63W/N17-28E.

3.4.2.3.5 Intersection of Aerial Lineaments with Tonal Anomalies

Figure E-9 shows three distinct clusters ("A", "B", and "C"). "A" occurs at N7-22W/N50-60W, "B" at N40-50W/N85-88E, and "C" at N12W/N60-63E.

3.4.2.3.6 Summary

No distinct clustering of data points is evident in any of the single matrices or in a composite matrix (not shown). The clustering of data points at N40-50W/N80-90E is perhaps the most distinct.

3.4.3 AREA 3 LINEAMENT/TONAL ANOMALY CORRELATIONS

3.4.3.1 Correlation #1 Discussion

3.4.3.1.1 Landsat Lineaments (All) and Tonal Anomalies

Table 3-10 shows that a total of 149 Landsat lineaments and 112 tonal anomalies were mapped for Area 3. The categories "on", "close", and "combined" summarize the relationships between those tonal anomalies that are located on or near a single Landsat lineament. Only 21 tonal anomalies were not located either "on" or "close" to a Landsat lineament.

A total of 158 "alarms" - or instances where this Landsat lineament/tonal anomaly relationship were valid - occur in Area 3, 88 of which fall in the "on" category and 70 of which occur in the "close" category.

For the "on" category, results were generally mixed and no distinct peaks are evident. Table 3-10 shows that some clusters do occur in the N36-40E category (12 alarms), N69-76E (11), N84-85E (8), and N53W (7). The 46 alarms noted in these four categories represent approximately 52% of the total number of alarms detected in the "on" category.

For the "close" category, results are generally random except in two lineament categories, N34-40E (12 alarms) and N51-55W (10 alarms).

By combining the individual results of the "on" and "close" categories, the four major clusters occur at N33-40E (26 alarms), N51-55N (19), N69-76E (17), and N84-85E (11). The alarms detected in these four lineament groupings in the "combined" category, represent approximately 50% of the 158 alarms noted in Area 3.

Table 3-10. Lineament/Tonal Anomaly Correlations (Area 3)

				"ON"			Within 0.6 km			"COMBINED"		
	Total Number of Lineaments Mapped in Area 3	Total Number of Anomalies Mapped in Area 3	Number of Anomalies Having no Spatial Correlation with Lineaments	Number of Alarms Recorded for "ON" Category	Major Lineament Trend(s)	Number of Alarms Per Trend	Number of Alarms Recorded for "CLOSE" Category	Major Lineament Trend(s)	Number of Alarms Per Trend	Number of Alarms Recorded for "Combined Category"	Major Lineament Trend(s)	Number of Alarms Per Trend
LANDSAT (ALL)	149	115	21	88	N36-40E N69-76E N84-85E N53W	12 11 8 7	70	N51-55W N34-40E	10 12	158	N33-40E N51-55W N69-76E N84-85E	26 19 17 11
LANDSAT (MAJOR)	9	115	89	13	N76E N84-85E	44 8	11	N84-85E	8	24	N84-85E N76E	16 4
SKYLAB	90	115	24	73	N63E N73-76W N36-42E	13 10 11	55	N60-66E N44-47W N21-27W N53E	10 7 6 4	128	N60-63E N36-47E N73-76W N44-47W	22 17 13 12
LEVELS 1, 2, 3	123	115	32	55	N63-65E N54-60W N73-74E	8 7 6	47	N43-48W N53-57E N74-75W	8 5 5	102	N39-48W N53-60W N63-65E N73-76W	19 11 10 10
AERIAL	107	115	54	65	N55-60W N86-90W N75-79E	10 8 6	38	N58-62E N55-60W	7 5	103	N55-60W N80-90W N58-65E N78-81W	15 11 11 8

3.4.3.1.3 Landsat Lineaments (Major) and Tonal Anomalies

A total of 24 "alarms" occur in Area 3 for the major Landsat lineament/tonal anomaly category, 13 of which fall in the "on" category and 11 of which occur in the "close" category.

For the "on" category, two distinct peaks occur at N76E (4 alarms) and N84-85E (8 alarms). For the "close" category, the N84-85E trend (8 alarms) is distinct. In the "combined" category, the alarms detected at N84-85E (16 alarms) and at N76E (4) represent 83% of the total alarms noted in Area 3.

3.4.3.1.3 Skylab Lineaments and Tonal Anomalies

A total of 90 Skylab lineaments and 115 tonal anomalies were mapped for Area 3. A total of 128 alarms occur in Area 3 for Skylab lineament tonal anomaly category. Seventy-three alarms fall within the "on" category and 55 fall within the "close" category. Twenty-four of the 115 tonal anomalies detected on the ratio-stretch enhancements have no spatial correlation with the Skylab lineament data.

For the "on" category, three distinct clusters were evident at N67E (13 alarms), N73-76W (10), and N36-42E (11). For the "close" category, fewer distinct clusters were evident for the 55 alarms noted. The largest percentage of alarms occur at N60-63E (10 alarms), N44-47W (7), N21-27W (6) and N53E (4).

For the "combined" category, four distinct groupings of alarms occur at N60-63E (22 alarms), N36-42E (17), N73-76W (13) and N44-47W (12). The 64 alarms noted in these four lineament trend clusters represent 50% of the total number of alarms noted in the area.

3.4.3.1.4 Levels 1, 2, and 3 Lineaments and Tonal Anomalies

Table 3-10 shows that a total of 123 Level 1, 2, and 3 lineaments were identified in Area 3. Thirty-two of the 115 tonal anomalies identified in Area 3 have no spatial correlation with this lineament category.

A total of 102 alarms occur in Area 3 for this category, 55 of which fall in the "on" category and 47 in the "close" category. For the "on" category alarms were randomly distributed. The three most noticeable groupings occur at N63-65E (8 alarms), N54-60W (7), and N73-74E (6).

For the "close" category, results were also randomly distributed. The three most distinct groupings occur at N43-48W (8 alarms), N53-57E (5), and N74-75W (5).

For the "combined" category, the most distinct clusters occur at N39-48W (19 alarms), N53-60W (11), N63-65W (10) and N73-76W (10). The 50 alarms noted in these four categories represent slightly less than 50% of the total number of alarms noted in Area 3.

3.4.3.1.5 Aerial Lineaments and Tonal Anomalies

Table 3-10 shows that a total of 107 aerial lineaments were identified in Area 3. Fifty-four of the 115 tonal anomalies identified in Area 3 have no spatial correlation in this lineament category.

A total of 103 alarms occur in Area 3 for this category, 55 of which fall in the "on" category and 47 in the "close" category. For the "on" category, the distribution of alarms appears random. Major alarm groupings occur at N55-60W (10 alarms), N86-90W (8), and N75-79E (6).

For the "close" category, alarms are randomly distributed except for one significant grouping located at N58-62E (7 alarms). A second broader cluster occurs at N55-60W (5 alarms).

For the "combined" category, the most distinct alarm groupings occur at N55-60W (15 alarms), N86-90W (11), N58-65E (11), and N78-81W (8). These four alarm clusters represent slightly less than 50% of the total number of alarms noted in Area 3.

3.4.3.1.6 Summary

Figure 3-5 shows the primary trends recorded for each of the five lineament categories discussed. The "composite" lineament category combines the data from each lineament category onto a single line.

The results of this correlation generally indicate that tonal anomalies cluster more frequently than usual (relative to their overall distribution) along certain lineament trends, including: N51-55W (20 alarms), N33-40E (26 alarms), and N69-76E (17 alarms). Should the Landsat-identified tonal anomalies represent hydrothermal alteration areas, then, based on this information only, the optimum areas to locate additional candidate altered areas would be along these particular trends.

3.4.3.2 Correlation #2 (Lineament Intersection Angles)

Figure 3-6 shows the histogram data compiled for Area 3 lineament intersection angles. The most distinct peaks evident in the five histograms compiled occur in the Landsat lineament intersection category, where intersection angles of 50-60°, 85-90°, and 135-140° are predominant. For Skylab lineament intersection angles, the most pronounced peak occurs at 115-120°, and a large cluster is evident at 30-50°. Aerial lineament intersection angles data show distinct peaks at 50-75° and 145-155°.

To summarize, the most distinct histogram peaks noted for lineament intersection angles in Area 3 are:

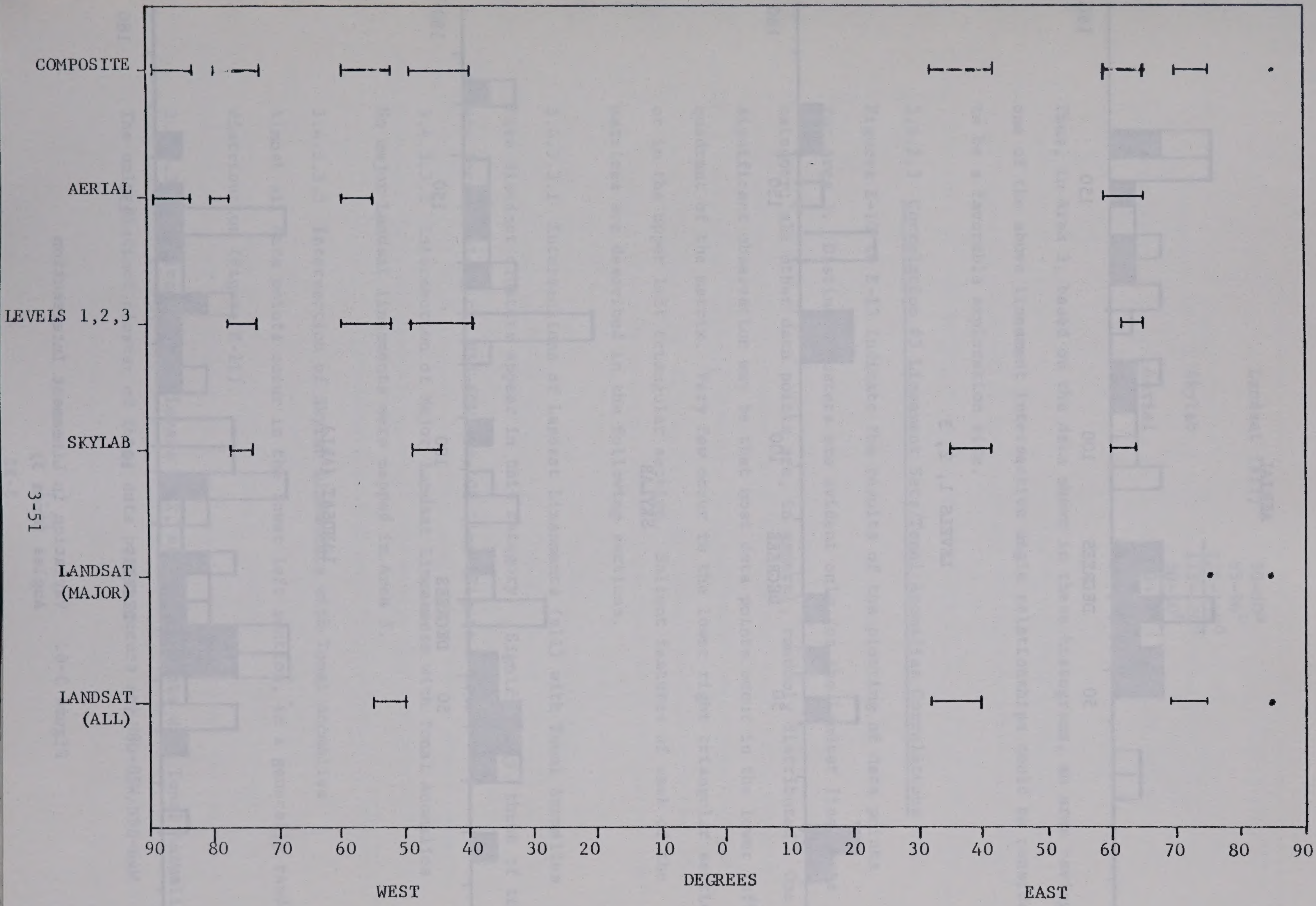

Figure 3-5. Lineament/Tonal Anomaly Correlation Results (Area 3)

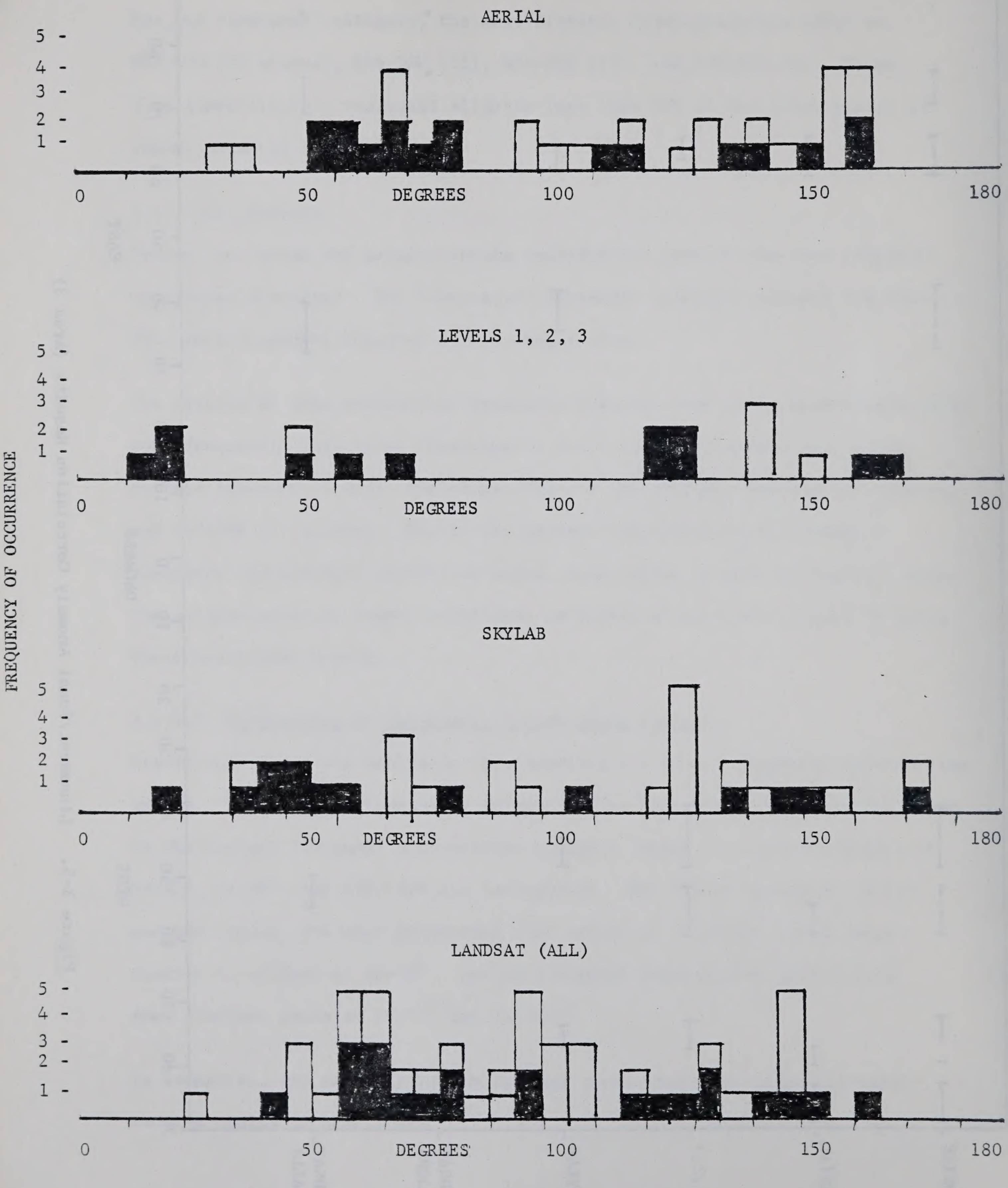
AERIAL

LEVELS 1, 2, 3

SKYLAB

LANDSAT (ALL)

Figure 3-6. Variation in Lineament Intersection Angles (Area 3)

Landsat (all)	50-60°
	85-90°
	135-140°
Skylab	115-120°
	30-50°
Aerial	50-75°
	145-155°

Thus, in Area 3, based on the data shown in these histograms, an area having one of the above lineament intersection angle relationships could be considered to be a favorable exploration site.

3.4.3.3 Correlation #3 Lineament Sets/Tonal Anomalies Correlations

Figures E-10 to E-13 indicate the results of the plotting of data points for Area 3. Distinct clusters are evident only for the Landsat lineaments category; all other data points are, in general, randomly distributed. One significant observation may be that most data points occur in the lower left quadrant of the matrix. Very few occur in the lower right triangular section or in the upper left triangular section. Salient features of each of the matrices are described in the following sections.

3.4.3.3.1 Intersections of Landsat Lineaments (all) with Tonal Anomalies

Five distinct clusters appear in this category. Significantly, three of these are located along the N55-60W/N34-40E line (Figure E-10).

3.4.3.3.2 Intersection of Major Landsat Lineaments with Tonal Anomalies

No major Landsat lineaments were mapped in Area 3.

3.4.3.3.3 Intersection of Skylab Lineaments with Tonal Anomalies

Almost all data points occur in the lower left section, in a generally random distribution (Figure E-11).

3.4.3.3.4 Intersection of Levels 1, 2, and 3 Lineaments with Tonal Anomalies

The only distinct cluster of these data points occurs at N80-85W/N58-64W

(Figure E-12).

3.4.3.3.5 Intersection of Aerial Lineaments with Tonal Anomalies

The only two distinct clusterings of data points occur at N70-80W/N55-65E.

3.4.4 SUMMARY OF CORRELATION RESULTS

Table 3-11 summarizes the results described in the above sections (3.4.1, 3.4.2 and 3.4.3). Three correlation categories shown are (1) lineament/tonal anomaly correlations; (2) lineament intersection angles, and (3) lineament set intersection/tonal anomaly correlations.

In Area 1, Correlation #1 results show that a N45-50W Landsat trend is dominant; this trend parallels the major known fault trend of this area. This lineament trend intersects with a N85-90E lineament trend where a number of tonal anomalies were mapped (Correlation #3). Correlation #2 shows that the primary lineament intersection angle detected is 75-110/degrees.

In Area 2, Correlation #1 results show that the primary Landsat lineament trend is N40-43W. As with Area 1, Correlation #3 shows that lineaments having this lineament intersect with a N83-90E lineament set; where a number of tonal anomalies were mapped having this particular relationship. The 130-145° lineament intersection angle agrees with the angle between these two lineament sets recorded in Correlation #3 (for Landsat lineaments).

In Area 3, Correlation #1 results show a variety of primary lineament trends; no particular trend is dominant. Correlation #3 results show that tonal anomalies are located at the intersection of three lineament sets; (1) N50-60W/N65-75E; (2) N50-60W/N35-40E; and N3-5W/N40E. In general, results derived for Area 3 are random.

Table 3-11. Summary of Correlation Results

	CORRELATION #1	CORRELATION #2	CORRELATION #3
	PRIMARY LINEAMENT/TONAL ANOMALY CORRELATIONS ("COMBINED" CATEGORY)	PRIMARY LINEAMENT INTERSECTION ANGLES	PRIMARY LINEAMENT SETS
AREA 1	(L) N45-48W N30-35E (LM) N45-48W (S) N45-49W N28-34E (L124) N37-40W N14-16W	(L) 75-110° (LM) 40-50 (S) - (L124) - (A) -	(L) N45-50W/N85-90E N10-15W/N45-50E (LM) N85-90W/N85-90E (S) - (L124) -
AREA 2	(L) N40-43W N37-41E N22-29E (LM) N45-51W (S) N15-18W (L124) N60-63W (A) N 8-13W	(L) 130-145° 80-90° (LM) - (S) - (L123) - (A) 130-155° 30-45°	(L) N45-50W/N85-90E (LM) - (S) - (L123) - (A) N40-50W/N85-90E
AREA 3	(L) N33-40E N51-55W (LM) N84-85E (S) N60-63E (L123) N39-48W (A) N55-60W	(L) 50-60° 85-90° 135-140° (LM) - (S) 115-120° (L123) - (A) 145-155°	(L) N50-60W/N65-75E N50-60W/N35-40E N 3- 5W/N40E (LM) - (S) - (L123) - (A) -

KEY

(L) = Landsat (all)
(LM) = Landsat (major)
(S) = Skylab
(L123) = Levels 1,2, 3
(A) = Aerial

3.5 RELATIVE POTENTIAL EVALUATION (OVERLAYS 1C, 2C, 3C)

Available geologic information and information derived from remotely sensed data were utilized in the development of the relative potential evaluation of the three project areas. Specifically, the four geologic factors evaluated were:

1) Lineaments: As detected and plotted from Landsat, Skylab, aerial photography, and published geophysical lineament data. These data were integrated with existing (published) fault data, and all inputs were combined into a comprehensive lineament overlay.
2) Known metallic mineral occurrences: as shown on published 1:250,000 scale maps available from the U.S. Bureau of Mines.
3) Lithology: as shown on the 1:250,000 scale geologic map published by the California Division of Mines and Geology.
4) Tonal Anomalies: as interpreted from ratioed-stretched Landsat images.

These four geologic indicators were subjectively quantified and totaled into a resource potential evaluation score for each of the over 2000 2 x 2 km grid cells making up each project area. Each data input was uniformly available for the entire CDCA. Thus, final scores calculated reflect a relative measure of potential metallic mineral endowment, in relationship to each of the other grid cells.

The final total scores for each project area for each grid cell were plotted as a histogram and resource potential categories were then selected. The purpose of the "Relative Potential" overlay was to provide a measure of detail for mineral resource evaluation for each project area. Therefore, five relative potential categories have been developed based on the histogram: A, B, C, D, or E.

Category "A" consists of those grid cells whose total score represented the top 5% of all total scores as shown on the histogram. Category "B" represents the next 5% group (between 5-10%); "C" represents the next 10% group (between 10-20%); "D", the next ten percent (20-30 percent), and "E" below the 30% grouping.

The results of this subjective statistical evaluation are shown in Figures 3-7 through 3-9 and Tables 3-12 through 3-14 for the three project areas.

3.5.1 AREA 1

For Area 1, the range of scores for the grid cells evaluated for relative potential are:

CATEGORY	RANGE OF SCORES	PERCENTAGE
A	58-86	Top 5%
B	52-57	5-10%
C	43-51	10-20%
D	36-42	20-30%
E	< 36	< 30%

Figure 3-7 shows the histogram of the resulting scores. Table 3-12 identifies the top five percent grid cells from Area 1, their location, their general geographic area, and predominant lithology.

Category "A" (High Potential) grid cells represent the top five percent of the over 2000 grid cells evaluated for each project area, based on total scores. As expected, because of the types of geologic factors selected for evaluation in this project, high potential grid cells are, in general, geographically located in areas of exposed bedrock. However, the total number of grid cells classified as category "A" represent only a percentage of the total number of grid cells located within exposed bedrock areas. Of the over 100 grid cells classified as category "A" the greatest number are located in one of four primary

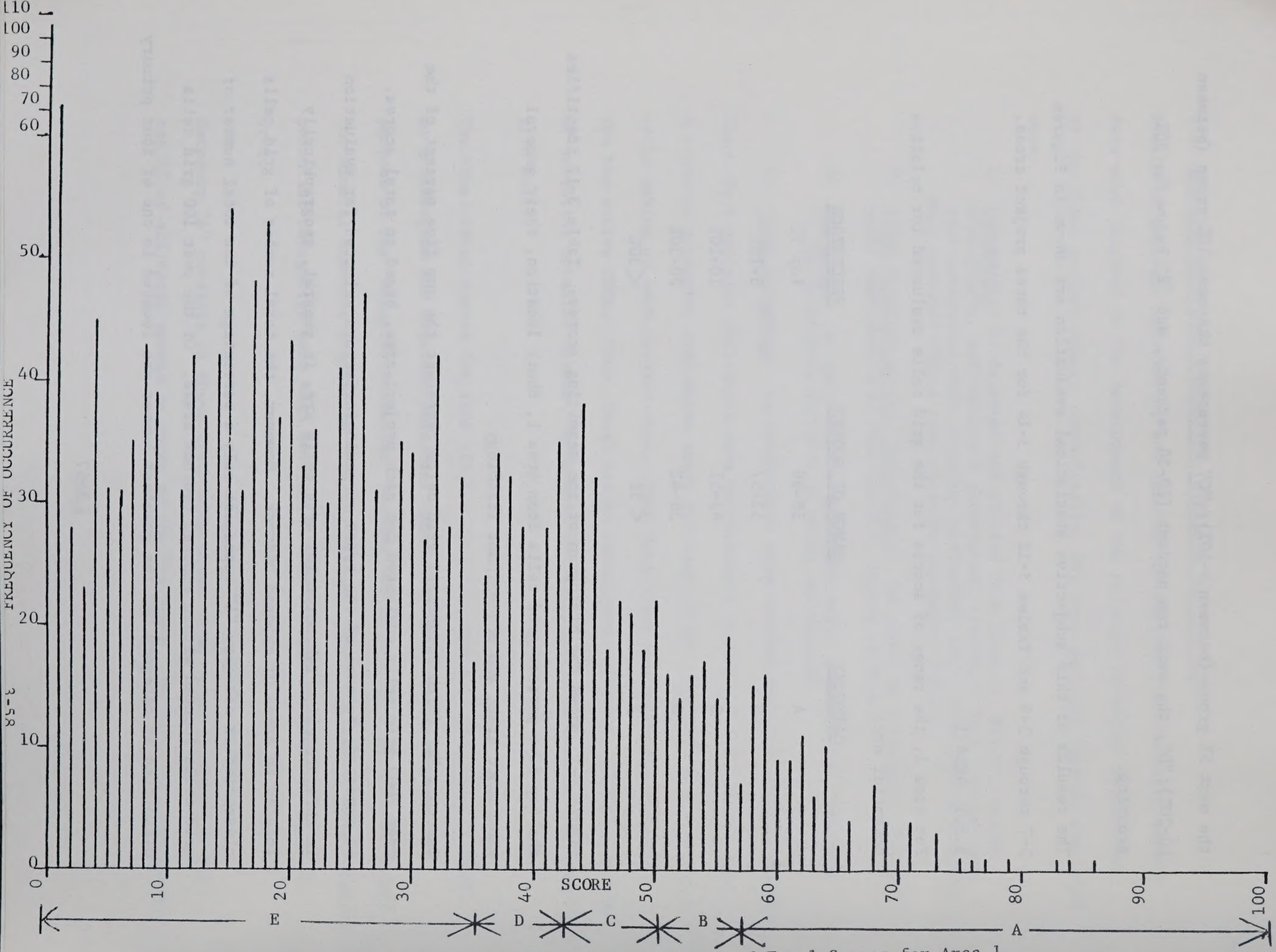

Figure 3-7. Histogram Showing Distribution of Total Scores for Area 1

Table 3-12. Top 5 Percent Grid Cells for Area 1

UTM BLOCK	GRID CELL LOCATION	GENERAL GEOGRAPHIC AREA	LITHOLOGY
B7	8,9,12,13,14,18,19,24	Silver Mountains	JTrv
C5	24	Silver Mountains (N.)	gr[a]
C6	20,22	Stoddard Mountains	gr, JTrv
C7	1, 21	Stoddard, Sidewinder Mnts.	JTrv, Pm, gr
D4	3	Calico Mountains (N.)	Ti, gr
D7	4, 5, 8, 9	Stoddard Mountains	JTrv
	13,14,16,17,23,25	Sidewinder Mountains	gr, JTrv
D8	7, 8, 9, 12, 18	Granite/Sidewinder (along Helendale Fault	gr, JTrv
E1	23	Lane Mountain (N.)	bi
E2	8	Lane Mountain (N.)	bi
E4	1, 5, 12, 13, 16	Calico Mountains (W.)	Ti, pЄg?
E6	3	Daggett Ridge	Mv[b]
E7	3, 11, 12, 19, 20		gr, bi, pЄg
F2	14, 15	Lane Mountains	bi
F3	16, 17, 23, 24	Calico Mountains	Ti[a], Muc
F4	2,3,4,5,6,7,8,11	Calico Mountains	Mv[a], Ti[a]
F5	25	Daggett Ridge (N.)	Mc
F6	2,3,4,5,6,8,9,15,19	Newberry Mountains (W.)	Mvb, JTrv
	21, 22, 23, 24	Ord Mountains (N.)	gr, JTrv

Table 3-12. Top 5 Percent Grid Cells for Area 1 (Con't.)

UTM BLOCK	GRID CELL LOCATION	GENERAL GEOGRAPHIC AREA	LITHOLOGY
F7	2,3,6,7,8,13,14,16,18	Ord Mountains	gr, JTrv
G5	22	Newberry Mountains (E.)	Ti^r, JTrv
G6	9, 12, 19, 20	Newberry Mountains (S.)	Ti^r, Mv^a, Mc
G7	2, 16	Rodman Mountains	JTrv
	21, 25	Ord Mountains	JTrv
G8	8, 12	Johnson Valley (W.)	gr^i gr^a
H2	19	Alvord Mountains (S.)	Mv^b
H3	2	Alvord Mountains	gr^a
I6	25	Newberry Mountains	Mv^b Mc
I7	2, 8, 25	Newberry Mountains	gr^a
I8	4, 5, 6, 7	Iron Ridge	gr^a
I9	4, 8	Johnson Valley (E.)	gr^a, bi

bedrock areas located generally in the central portion of the project area. The four primary high potential areas include: (1) Silver Mountains (8 cells); (2) Stoddard Mountains/Sidewinder Mountain areas (19 cells); (3) Ord Mountains (21 cells) and (4) Calico Mountains (11 cells). Virtually no areas located on the periphery of Area 1 are classified as category "A".

The combination of favorable lithology, extent of known faulting, high lineament density, widespread tonal anomalies, and considerable known metallic mineralization in the vicinity make the Calico Mountain area one of the best exploraton sites in Area 1, based on the results of relative potential evaluation.

Although few tonal anomalies occur within the Silver Mountain area, favorable lithology, mineralization and lineament density characteristics resulted in this area's high classification. However, grid cells containing little or no evidence of tonal anomalies in this area could be considered to have a lower level of mineral potential.

A considerable number of grid cells are classified as category "A" in the Stoddard Mountains/Sidewinder Mountains in spite of relatively little evidence of tonal anomalies. The only predominant area of tonal anomalies occurs at the western end of Stoddard Ridge.

As with the Silver Mountains and Calico Mountains, the abundance of lineament intersections, favorable lithology, and abundance of known mineralization resulted in a number of category "A" areas within the Ord Mountains. However, this area has limited potential for surface alteration because few anomalies appear except at the southern end of these mountains.

An abundance of tonal anomalies are evident along the eastern portion of the Newberry Mountains. However, insufficient correlation of these areas with known mineralization, plus a relatively mixed lithologic and fracture assemblage, results in the lower classification of this area.

3.5.2 AREA 2

For Area 2, the range of scores for the 2057 grid cells evaluated for relative potential are:

CATEGORY	RANGE OF SCORES	PERCENTAGE
A	57-81	Top 5%
B	49-56	5-10%
C	38-48	10-20%
D	28-37	20-30%
E	<28	$<30\%$

Figure 3-8 shows the histogram of the resulting scores.

Table 3-13 identifies the top five percent grid cells for Area 2, their specific grid cell location, their general geographic location, and predominant lithology at this location.

Category "A" (High Potential) grid cells represent the top five percent of the over 2000 grid cells evaluated for Area 2 based on total scores. As expected, because of the types of geologic factors selected for evaluation in this project, high potential grid cells are in general geographically located in areas of exposed bedrock. However, the total number of grid cells classified as category "A" represent only a percentage of the total number of grid cells that are located within exposed bedrock areas.

Of the 94 grid cells classified as category "A", by far the greatest number of these (approximately 24) are located in the extreme western portion of the project area (Bristol Mountains) or within the central and southern portion of the N-S trending Old Woman Mountains, located in the eastern third of the

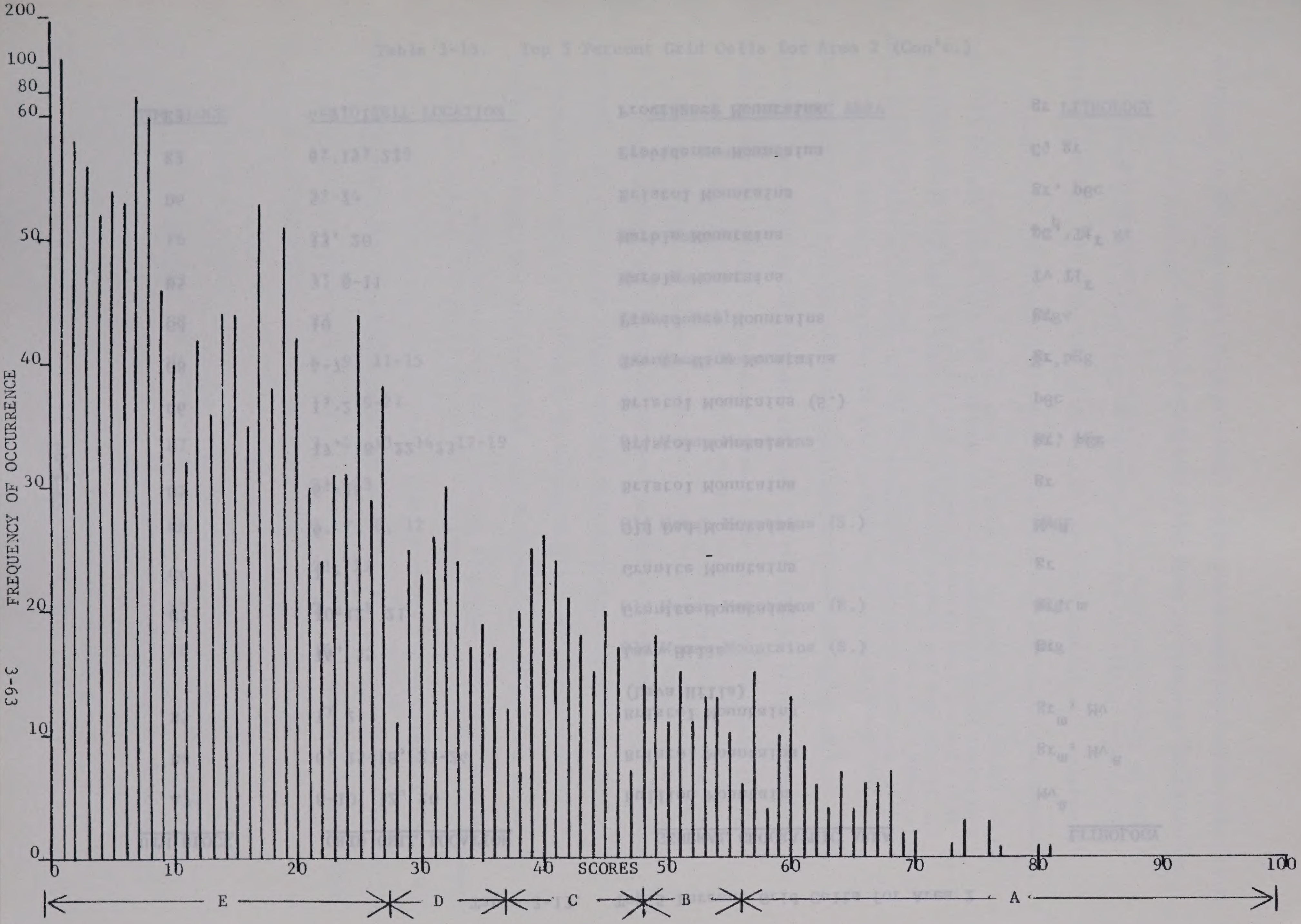

Figure 3-8. Histogram Showing Distribution of Total Scores for Area 2

Table 3-13. Top 5 Percent Grid Cells for Area 2

UTM BLOCK	GRID CELL LOCATION	GENERAL GEOGRAPHIC AREA	LITHOLOGY
A7	8-10, 12, 20	Bullion Mountain	Mv[a]
B4	6, 15-18, 21-24	Bristol Mountains	gr[m], Mv[a]
B5	1, 2	Bristol Mountains (Lava Hills)	gr[m], Mv
	14, 15	Lava Hills	gr
C3	10-12, 21	Granite Mountains	gr, m
C4	1	Granite Mountains	gr
	6	Old Dad Mountains	Mv[a]
C5	6, 15	Bristol Mountains	gr
	17, 18, 22, 23	Bristol Mountains	gr, pCc
C6	1, 2	Bristol Mountains (S.)	pЄc
C8	4-7	Twenty-Nine Mountains	gr
Cd	10	Providence Mountains	gr
D5	3, 8-11	Marble Mountains	Tv Ti[r]
	13, 20	Marble Mountains	pC, Ti[r]
D6	5, 7	Bristol Mountains	gr, pЄc
E2	6, 15, 22	Providence Mountains	C, gr
E3	4-7, 17	Providence Mountains	gr

Table 3-13. Top 5 Percent Grid Cells for Area 2 (Con't.)

UTM BLOCK	GRID CELL LOCATION	GENERAL GEOGRAPHIC AREA	LITHOLOGY
F4	12, 17, 19 22-24	Clipper Mountains	Tv
F6	21	Ship Mountains	Tv^b, Ꞓ, gr
F7	1, 2	Ship Mountains	
G8	23	Kilbee Hills	pꞒgv
H6	6, 9, 11-15 17, 19-21	Old Woman Mountains	gr,pꞒg
H7	3, 4, 13, 14, 17-19 22, 23	Old Woman Mountains	pꞒ, pꞒg
H8	3, 7, 8, 12 21, 22	Old Woman Mountains (S.)	pꞒgr
I7	2-4, 8	Old Woman Mountains (E.)	pꞒgr
I8	16	Old Woman Mountains (S.)	pꞒg

project area (approximately 31). These two areas represent 60% of the total number of category "A" grid cells identified in Area 2.

Other areas containing several category "A" grid cells include: Marble Mountains (7), Clipper Mountains (6), Granite Mountains (6), and the Providence Mountains (11).

A distinct NW-SE trending pattern of category "A" grid cells appears in both the Bristol and the Marble Mountains. This trend is thought to be largely due to the NW-SE trending characteristic of the exposed bedrock in these areas.

The occurrence of numerous distinct tonal anomalies within the Bristol Mountains area as well as favorable lithologic, known mineralization and lineament density characteristics are the primary features responsible for the category "A" classification of this area.

In contrast, however, few distinct tonal anomalies occur within the portion of the Old Woman Mountain area that are classified as category "A". Farther to the north, numerous tonal anomalies occur in the Old Woman Mountain area, but no grid cells are classified "A". Nevertheless, these grid cells should be considered good candidate sites for more detailed mapping.

3.5.3 AREA 3

For Area 3, the range of scores for the 2026 grid cells evaluated for relative potential are:

CATEGORY	RANGE OF SCORES	PERCENTAGE
A	63-89	Top 5%
B	56-62	5-10%
C	45-55	10-20%
D	36-44	20-30%
E	<36	<30%

Figure 3-9 shows the histogram of the resulting scores. Table 3-14 identifies the top five percent of these grid cells for Area 3, their specific location, their general geographic location, and the predominant lithology at this location.

Category "A" (High Potential) grid cells represent the top five percent of the over 2000 grid cells evaluated for Area 3. As expected, because of the types of geologic factors selected for evaluation in this project, high potential grid cells are, in general, geographically located in areas of exposed bedrock. However, the total number of grid cells classified as category "A" represent only a percentage of the total number of grid cells located within exposed bedrock areas.

Of the approximately 90 grid cells classified as category "A", by far the greatest number of these (approximately 41) are located in the southwest portion of the project area, within the Chuckawalla Mountains. Although relatively few tonal anomalies occur in this area, the level of fracturing (lineament density), favorable lithology and know mineralization potential suggests that this area is a good exploration site.

Other category "A" grid cells located in areas of exposed bedrock are scattered throughout the project area. These areas include: (1) the Big Maria Mountains (11 grid cells); (2) Palen Mountains (7 grid cells); (3) McCoy Mountains (4 grid cells in the extreme southern portion and 3 in the extreme northern end); and (4) Little Maria Mountains (7 cells).

Evidence of widespread tonal anomalies in the extreme southwest corner of project Area 3 (Chocolate Mountains) suggests this area's high potential. However, few areas of known mineralization and lower values in the lineament

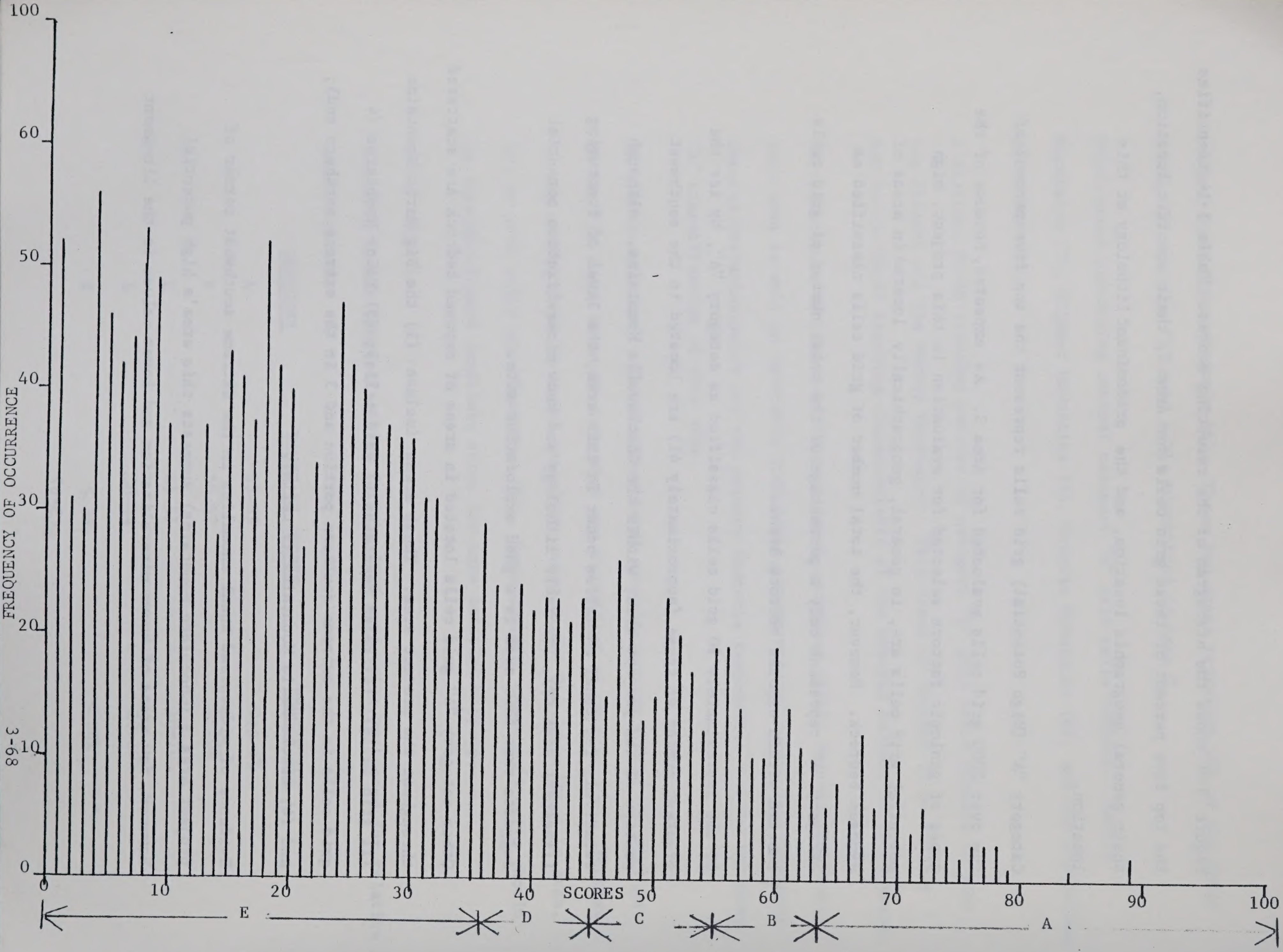

Figure 3-9. Histogram Showing Distribution of Total Scores for Area 3

Table 3-14. Top 5 Percent Grid Cells for Area 3

UTM BLOCK	GRID CELL LOCATION	GENERAL GEOGRAPHIC AREA	LITHOLOGY
B4	21,22	Eagle Mountains (N.)	gr[a]
B5	17	Eagle Mountains (N.)	pC
B6	3	Eagle Mountains (S.)	pЄc
	16	Eagle Mountains (S.)	gr, Ti
B7	16, 17	Orocopia Mountains (E.)	gr, pЄg
B10	4, 5	Chocolate Mountains	pЄc
C7	8-11, 14	Chuckawalla Mountains	gr
	14, 17	Chuckawalla Mountains	pЄg
	19, 21, 22		gr, pЄg
C8	3, 6-8, 11, 12	Chuckawalla Mountains (S.)	pЄg
	21		pЄg
D3	17, 18	Coxcomb Mountains	gr[g], m
D7	5, 6	Chuckawalla Mountains	gr
	12, 16, 7	Chuckawalla Mountains	gr, pЄc
	21-25	Chuckawalla Mountains	gr
D8	1,	Chuckawalla Mountains	pCc, gr
	4, 5, 7, 8	Chuckawalla Mountains	gr
	13, 15	Chuckawalla Mountains (Pilot Mountain/Black Butte)	pЄg

Table 3-14. Top 5 Percent Grid Cells for Area 3 (Con't.)

UTM BLOCK	GRID CELL LOCATION	GENERAL GEOGRAPHIC AREA	LITHOLOGY
D9	1	Chuckawalla Mountains (S.)	ms, Ti
D10	21-23	Chocolate Mountains	pЄc, pЄg
E8	15	Chuckawalla Mountains	pЄc
E9	5, 7-9	Chucawalla Mountains	Ti, pЄc,pЄg
F4	11, 20	Granite Mountains	gr, IP, m
F5	19-21	Palen Mountains	ms
F6	13, 17	Palen Mountains	ms
F9	11	Little Chuckawalla Mountains	pЄgr
F10	21	Little Chuckawalla Mountains	Ti
G4	11	Little Maria Mountains	pЄc
G8	15	Palen Mountains (E.)	mv
	25	Palen Mountains (E.)	ms
G10	11	Black Hills	Tv^{p}
H4	14, 15	Little Maria Mountains	m
	17, 22-24		IP, m
H5	17, 23, 24	McCoy Mountains (N.)	gr
H7	17, 23, 24	McCoy Peak	ms

Table 3-14. Top 5 Percent Grid Cells for Area 3 (Con't.)

UTM BLOCK	GRID CELL LOCATION	GENERAL GEOGRAPHIC AREA	LITHOLOGY
I7	5, 6, 13	McCoy Peak	ms
I8	25	Mule Mountains	pЄgr
I10	16, 24, 25	Palo Verde Mountains	Tv
J4	21, 22, 25	Big Maria Mountains	pЄg
J5	1-5, 10, 13, 19	Big Maria Mountains	pЄg, IP

density category resulted in the identification of only 2 target areas as category "A".

The tonal anomalies in the Chocolate Mountains region within Area 3 appear to be strongly affected by the well-defined NW-SE trending fracture pattern of this area.

Another observation noted is the relatively low correlation between tonal anomalies and category "A" grid cells in Area 3. This observation is especially valid for the Chuckawalla Mountains category "A" grid cells.

3.6 AREAS HAVING MINERAL POTENTIAL (OVERLAYS 1D, 2D, and 3D)

Overlays have been prepared to show areas having mineral potential within the three project areas. Six "levels" of metallic mineralization potential have been identified, in an decreasing order of priority. The information utilized to develop this particular overlay included information previously prepared for overlays A, B, and C, namely, major lineament intersection areas (from Overlay A), tonal anomalies (from Overlay B), and areas having the highest relative potential (from Overlay C).

3.6.1 MINERAL POTENTIAL AREAS IN PROJECT AREA 1

Level 1 areas are primarily located within the Ord Mountains and Dagget Ridge area; the nineteen Level 1 categories that are evident occur in a general north-south trend. Clusters of other Level 1 areas are considerably fewer: four occur in the Silver Mountains, and six within the Calico Mountains. The only other area having Level 1 areas is a broad region encompassing portions of the Stoddard, Sidewinder and Granite Mountains.

Level 2 areas are grouped in small clusters throughout the area. Principal areas include the Rodman Mountains (5 areas along the Camp Rock fault), Silver Mountains (4 areas), Calico Mountains (6 areas), Newberry Mountains (3 areas along the Camp Rock fault), and the Sidewinder Mountains (5 areas).

Level 3 areas are generally scattered throughout Area 1. Three areas occur on the east flank of the Silver Mountains, and three are located along the West Calico fault on the southwest flank of the Lava Mountains. Six areas are scattered throughout the Granite Mountains.

Level 4 areas occur on the north flank of the Newberry Mountains (3 areas) and on the west flank of the Ord Mountains (1 area).

Level 5 areas are scattered in an apparent random manner throughout the area. Several larger Level 6 areas occur at Stoddard Valley, along the Lenwood fault south of the Ord Mountains, on the north flank of the Newberry Mountains, and along the southwest flank of the Cady Mountains.

3.6.2 MINERAL POTENTIAL AREAS IN PROJECT AREA 2

Clusters of Level 1 areas are scattered throughout Project Area 2. The largest cluster occurs in the Old Woman Mountains (13 areas); the second largest cluster occurs along the NW-SE axial trend of the Bristol Mountains (13 areas). Other less notable clusters occur at: (1) northeast portion of the Twenty-Nine Palms (4 areas); (2) Lead Mountains (4 areas); (3) Copper Mountains (3 areas); (4) and along the eastern flank of the Old Woman Mountains (3 areas), within the Precambrian granite outcrops.

Level 2 areas occur primarily within the Bristol Mountains (11 areas), Granite Mountains (6 areas), and the southern portion of the Providence Mountains (6 areas).

Level 3 areas are scattered throughout the project area. The largest clusters occur within the Piute Mountains (9 areas). Iron Mountains (6 areas), and the Clipper Mountains (7 areas). Scattered Level 3 areas occur within the Old Woman Mountains (6 areas), Granite Mountains (6 areas), and Twenty-Nine Palms (9 areas).

Level 4 areas occur only in the northern end of the Clipper Mountains. The absence of Level 4 areas is due to some degree to the inclusion of these areas in a higher level (Levels 1, 2, and 3) category. Also, to some extent, the absence suggests a relatively low correlation between major lineament intersection areas and tonal anomalies.

Level 5 areas occur primarily within the Granite and Marble Mountains area. Other notable Level 6 areas include the Iron and the Piute Mountains.

Level 6 areas represent tonal anomalies that were not already combined within a higher level category. The largest grouping (30 areas) of this particular category occurs within the northeast quadrant, primarily within the Piute and Little Piute Mountains. Other Level 5 areas occur at north flank of the Bristol Mountains, north flank of the Marble Mountains, east flank of the Old Woman Mountains, in the Clipper Mountains, and several isolated areas in the Old Dad Mountains.

3.6.3 MINERAL POTENTIAL AREAS IN PROJECT AREA 3

Level 1 areas occur primarily within the Chuckawalla Mountains (2 areas) or Big Maria Mountains (9 areas). Other Level 1 areas include: Little Maria Mountains (5 areas), northern portion of the McCoy Mountains (3 areas), and the central portion of the Palen Mountains (3 areas).

Level 2 areas occur primarily within the eastern portion of the Chuckawalla Mountains (10 areas). Three (3) areas occur in the western portion of these mountains. Other Level 2 areas in general are randomly scattered throughout Area 3.

The largest clustering of Level 3 areas occurs within the Chocolate Mountains; eighteen (18) areas are located in this area. Four (4) Level 3 target areas occur in the Big Maria Mountains. Four (4) Level 3 areas are loosely clustered in the Coxcomb Mountains region.

Level 4 areas (the coincidence of tonal anomalies with major fracture zones) are conspicuously absent in Area 3 (with the exception of a very small unit in the Chuckawalla Mountains). This result suggests that a direct correlation between fractures and tonal anomalies does not exist, at least within Area 3.

Level 5 areas represent any major fracture zones that have no spatial correlation with Level 1-4 categories. Level 5 areas occur principally in the northwest portion of the area (Coxcomb and northeast portion of Eagle Mountains), and in the southwest portion of the area (Palo Verde Mountains).

Level 6 areas represent tonal anomalies that did not have sufficient spatial correlation to be included with the Level 1-5 categories. Most Level 5 areas occur in the southern one-quarter of Area 3, principally within the Chocolate, Palo Verde, Little Chuckawalla, or southern portion of the Chuckawalla Mountains. Additional Level 5 categories occur in the Eagle, Granite, and Palen Mountains.

SECTION 4

SUMMARY AND CONCLUSIONS

In summary, results derived from the Landsat Enhancement Project can be incorporated into an on-going mineral potential evaluation program to identify potential mineralization areas within the three project areas. Results derived from this project can be incorporated with data already on file or currently being compiled to enhance future programs as well as to identify areas of similarities and discrepancies where further attention should be devoted. Data provided by this project can improve and refine on-going field mapping efforts by focusing them on primary areas.

Lineament maps prepared as a result of this project provide a valuable indication of the intensity of fracturing within each project area and allow identification of heavily fractured areas characterized by numberous intersections. Based on the hypothesis that mineral-rich fluids migrate more readily along zones of fracture and especially within areas of intense fracture intersections, the identification of these zones can provide further discrimination as to specific areas that should be field-checked in detail. In addition, identification of previously unmapped lineaments may provide information that will help explain certain field mapping problems.

The fracture (lineament) maps prepared as a result of this project should be evaluated and utilized with the understanding that they have not yet been field-checked or verified from other sources. The user should be aware that "Level 5" lineaments may or may not be valid; the assignment of a lineament to a category only indicates a relative confidence. And, in fact, some Level 5 lineaments may be just as valid as Level 1. Also, since detailed lineament interpretation of seasonal, low sun angle Landsat imagery has not yet been conducted, continued refinement of these maps could significantly alter future composite lineament maps.

One of the primary objectives of this project was the identification of potential hydrothermal alteration areas within the project areas. The identification of these areas was based on tonal information evident on ratioed-stretched color Landsat enhancements prepared by General Electric. Analysis of these enhancements has resulted in the detection of numerous tonal anomalies that are inferred to be potential hydrothermal alteration areas. Field checks will have to be made of these areas before a more precise classification can be made. The tonal anomalies appear on the ratioed-stretched Landsat enhancements as a variety of colors, typically dark blue, dark green, medium green, and lavendar. Typically, the areal extent of these anomalies is approximately one square km. In some cases these tonal anomalies appear to be related to certain lithologic or structural conditions, such as being located along a contact between an igneous intrusive and limestone, or being related to or affected by a particular structural trend.

Results of a detailed analysis of the spatial correlation between tonal anomalies and lineaments indicate a possible structural relationship between anomalies and certain single lineaments or sets of lineaments, or lineament intersections. In Area 1, for example, a large percentage of the tonal anomalies can be correlated with four specific Landsat lineament trends: N45-48W; N30-35E; N90W; and N45-48E. While the NW-SE (e.g., N45-48W) trend appears consistently in many of the histograms and graphs prepared for analysis, no one lineament trend is dominant. In fact, it appears that several (or numerous) trends are dominant, depending on whether the data reflect Landsat, Skylab, aerial, or known lineaments. Results of the analysis of the most common lineament intersection angles spatially related to tonal anomalies were generally negative. Histograms show a wide distribution of angles rather than one or two distinct angles.

Another analysis was conducted to determine whether tonal anomalies are related to a certain set (or sets) of intersecting lineaments. That is, it was hoped that histograms might show a clustering of tonal anomalies with certain intersecting Landsat lineament trends. Analysis of the matrices prepared showing the distribution of these particular structural/tonal anomaly relationships failed to indicate any dominant correlations. Results indicate that certain areas are devoid of data, however, and the absence of data is perhaps as significant as the presence of data. It was also observed that many tonal anomalies were not located at a lineament intersection. For example, in Area 2, only 50 of the 118 tonal anomalies mapped were located at a lineament intersection. Results do show, nevertheless, that certain areas have more favorable correlations than others. In Area 2, for example, a strong clustering of data points occurs at N40-50W/N80-90E (for Landsat lineaments).

The relative potential evaluation of metallic mineral resources within the project areas has resulted in the classification of five categories of mineral potential, based on the four geologic factors considered. Areas of "high", "moderate", "some", "low", and "no" potential have been identified. The highest priority grid cells--classified "A"--are characterized by : (1) numerous lineament intersections; (2) favorable lithologic assemblage, such as metavolcanics; (3) contain or are directly adjacent to known mineralization; and (4) contain tonal anomalies within the grid cell, and these anomalies have a favorable relationship to known faults and known mineral deposits. Grid cells devoid of lineaments, covered by unconsolidated alluvial deposits, not located near known mineralization, and/or devoid of tonal anomalies received relatively lower scores and, hence, a lower classification. Due to the wide expanses of alluvial cover contained in the three areas, many grid cells by definition received a low classification.

A fourth set of overlays provided in this project identifies the primary exploration sites within each project area. By definition, "high potential" grid cells identified in the relative potential evaluation represent favorable sites. In addition, grid cells containing tonal anomalies characterized by numerous lineament intersections would also be favorable sites. Prioritization of these areas was accomplished by identifying areas of commonality between the above factors.

SECTION 5

RECOMMENDATIONS

The results of the Landsat Enhancement Project should provide useful geologic information to BLM resource managers in their continuing metallic mineralization resources assessment program. Continued refinement of geologic interpretation techniques and tailoring of Landsat enhancements and other types of data to the particular geologic characteristics of the California Desert Conservation Area (CDCA) will result in additional improvement to the exploration model(s) being developed during this current phase.

The recent four-month effort devoted to the detailed photogeologic interpretation of satellite and other data in the BLM Landsat Enhancement Project has allowed GE geologists the opportunity to identify several areas where refinements can be made to the exploration model for metallic mineral resources. These recommendations are briefly described in the following discussion.

1. Processing and Interpretation of Low Sun Angle, Seasonal Landsat Data

GE's experience in photogeologic interpretation indicates that digitally enhanced, low sun angle, seasonal Landsat imagery should be utilized to achieve the optimum enhancement of lineament features. Although use of the single date Landsat data does provide useful information, verification of many questionable lineament features could be verified if seasonal data were available.

A related critical factor is the date of the Landsat imagery selected for digital enhancement. While the higher sun angle data (April-May), such as utilized in the current project, provide valuable geologic information, low sun angle data (November-March) have been shown to provide more information regarding structural geologic features.

2. Lineament Pattern Analysis

The next higher level step to take to improve the metallic mineral exploration model would be to utilize more sophisticated lineament analysis techniques, perferably using computer processing, to maximize efficiency and acquire optimum results. Manual interpretation of lineament features for trend, destination, intersection, etc. provides a useful first-cut analysis. Application of more sophisticated analysis techniques (such as standard deviations) could improve the analysis aspect and result in an improved relative potential evaluation. It would also allow utilization of a weighted factor and analysis approach, thereby improving the objectivity of the approach as well as enhancing the related subjective interpretations.

3. Updating Known Fault Maps

The published CDMG geologic maps at 1:250,000 scale provide the only single source of information regarding known faults in the entire CDCA. Incorporation of more up-to-date fault data are hindered by the unavailability of some published maps or the considerable effort required to extract the data from the voluminous maps or reports that are available. In addition, many of the faults shown on the CDMG maps have been mapped in local areas only (i.e., their length is relatively short). Attempts to compare Landsat lineaments with these faults is therefore complicated and generally results in low correlations.

4. Updating Mineral Resources Maps

A similar problem has been encountered with the metallic mineral resources maps utilized in the project. A comparison of U. S. Bureau of Mines data (MILS) and county maps showing known mineral resources showed a considerable number of discrepancies. The locations of the deposits as well as the type of mineralization at the various localities did not agree. Preparation of a single, reliable, mineral resource map at 1:100,000 scale is suggested.

2. Lineament Pattern Analysis

The next logical level step to take to improve the metallic mineral exploration model would be to utilize more sophisticated lineament analysis techniques, preferably using computer processing, to maximize efficiency and acquire optimum results. Manual interpretation of lineament features for trend, distribution, intersection, etc. provides a useful first-cut analysis. Application of more sophisticated analysis techniques (such as standard deviations) could improve the analysis effect and result in an improved relative potential evaluation. It would also allow utilization of a weighted factor and analysis approach, thereby improving the objectivity of the approach as well as enhancing the related subjective interpretations.

3. Updating Known Fault Maps

The published CDMG geologic maps at 1:250,000 scale provide the only single source of information regarding known faults in the entire CDCA. Incorporation of more up-to-date fault data are hindered by the unavailability of many published maps or the considerable effort required to extract the data from the voluminous maps or reports that are available. In addition, many of the faults shown on the CDMG maps have been mapped in local areas only. Since their length is relatively short, attempts to compare Landsat lineaments with these faults is therefore complicated and generally results in few correlations.

4. Updating Mineral Resources Maps

A similar problem has been encountered with the metallic mineral resources maps utilized in the project. A comparison of U. S. Bureau of Mines data (MILS) and county maps showing known mineral resources showed a considerable number of discrepancies. The locations of the deposits as well as the type

APPENDIX A

DIGITAL IMAGE ANALYSIS LABORATORY

General Electric used the Digital Image Analysis Laboratory (DIAL), located at its Beltsville, Maryland, facility to perform the Landsat image processing required for the BLM Landsat Enhancement Project.

DIAL is based on the IMAGE 100 System, but with considerable enhancements and augmentations, both in hardware and software, so that it represents the current state-of-the-art in operational image analysis systems. DIAL uses a DEC PDP 11/70 as the primary processing CPU, thus deriving the benefits of multitasking software, and permitting simultaneous operation in both batch and interactive modes. The software algorithms used for such functions as geometric correction, registration and feature classification have been shown to be the most cost effective of any currently available (Jayroe, Atkinson, et al, 1979). The laboratory includes extensive photographic product generation capability, as well as the capability to produce precision graphic overlays to any desired scale, including national mapping standards.

A.1 SYSTEM OVERVIEW

Figure A-1 is a block diagram of the DIAL system configuration, and Table A-1 lists the DIAL hardware complement.

The heart of the DIAL System is the IMAGE 100 Image Analysis Console. This console provides the analyst with the capability to use special purpose hardware circuitry to perform simple repetitive functions at high speed, thus providing high speed for these processes while at the same time freeing the PDP 11/70 CPU to handle more complex tasks.

The DIAL Operating System is RSX 11-D. Multi-tasking is employed extensively, and during such operations task priorities may be set as required. Interactive Analysis, Batch and software development tasks can run concurrently, but many other combinations are also employed. For Interactive Analysis, the minicomputer is required for as little as 10-15 percent of the time, so that utilization of the system for additional concurrent tasks is highly desirable for efficient operation. In addition to the system level software, DIAL uses a large library of specially-designed applications software. There are also diagnostics and utilities (such as tape copy) available.

Software development, and most Batch and Interactive Analysis Software, currently runs under RSX 11-D, version 6.2.

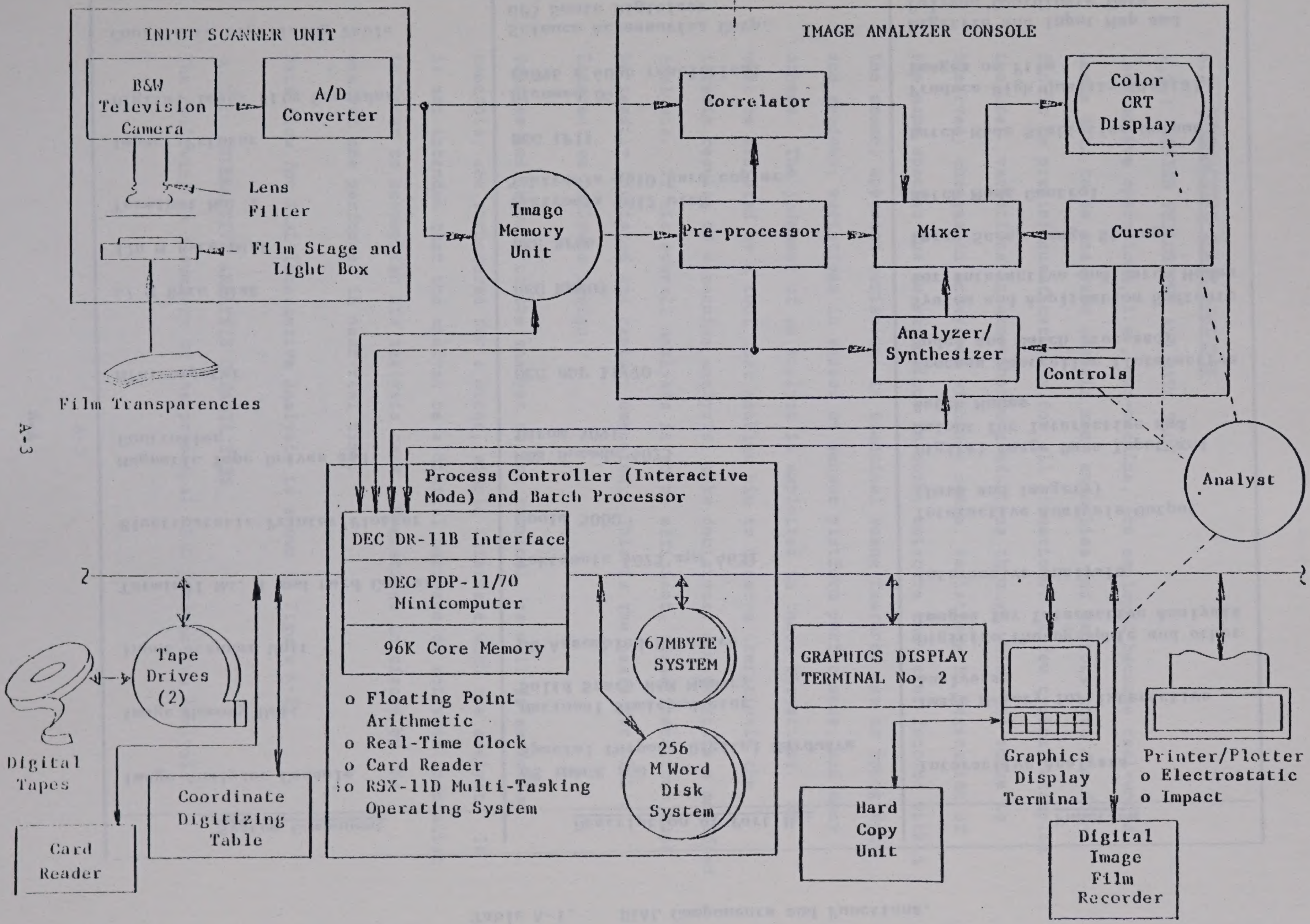
INPUT SCANNER UNIT
B&W Television Camera
A/D Converter
Lens
Filter
Film Stage and Light Box
Film Transparencies
Image Memory Unit
IMAGE ANALYZER CONSOLE
Correlator
Color CRT Display
Pre-processor
Mixer
Cursor
Analyzer/ Synthesizer
Controls
Analyst
Process Controller (Interactive Mode) and Batch Processor
DEC DR-11B Interface
DEC PDP-11/70 Minicomputer
96K Core Memory
o Floating Point Arithmetic
o Real-Time Clock
o Card Reader
o RSX-11D Multi-Tasking Operating System
67MBYTE SYSTEM
256 M Word Disk System
Tape Drives (2)
Digital Tapes
Card Reader
Coordinate Digitizing Table
GRAPHICS DISPLAY TERMINAL No. 2
Hard Copy Unit
Graphics Display Terminal
Digital Image Film Recorder
Printer/Plotter
o Electrostatic
o Impact

Figure A-1. Block Diagram of the Digital Image Analysis Laboratory

Table A-1. DIAL Components and Functions.

System Component	Description or Part No.	Function
Image Analyzer Console	GE IMAGE 100 Special Purpose Digital Hardware	Interactive Analysis
Image Memory Unit	National Semiconductor Solid State RAM Memory	Image Memory for Interactive Analysis
Input Scanner Unit	GE Assembled Hardware	Digitize Photographic and other Images for Interactive Analysis
Terminal No. 1 and Hard Copier	Tektronix 4025 and 4631	Interactive Analysis
Electrostatic Printer/Plotter	Gould 5000	Interactive Analysis Output (Data and Imagery)
Magnetic Tape Drives and Controller	MDS Bucode 4025 Datum 5091	Digital Image Data Input and Output for Interactive and Batch Modes
Minicomputer	DEC PDP 11/70	Process Controller (Interactive Mode) and Batch Processor
67 M Byte Disk	DEC RMW03	System and Application Software for Interactive and Batch Modes
176 M Byte Disk	DEC RP06	Large Scene Image Storage
Terminal No. 2	Tektronix 4012 with Tektronix 4610 hard copier	Batch Mode Control
Impact Printer	DEC LP11	Batch Mode Statistics Output
Digital Image Film Recorder	Dicomed D47 (4096 x 4096 resolution)	Produce High Quality Digital Images on Film
Coordinate Digitizing Table	Science Accessories Corp. GP3 Sonic Digitizer	Digitize and Input Map and Polygon Coordinate Data

A.2 INTERACTIVE IMAGE ANALYSIS

A.2.1 DESIGN PHILOSOPHY AND DATA FLOW

Interactive operations, i.e., man-machine, are employed because real-world image data to be analyzed contain many anomalies and factors that are difficult to predict quantitatively for all situations. A few typical examples include: variations in atmospheric conditions through which the scene is observed; changes in ecosystem within a scene; variations in vegetation of the same species due to variations in soil, moisture and other factors within the scene; apparent variations in identical scene features due to topography and shadows; variations in sensor or sensor platform performance; and many others. The judgment of an analyst is exploited in these situations. He must be assisted by a tool that enables him to observe iteratively the interim results of a machine analysis, make decisions, and initiate a modified analysis. If his overall analysis is to be efficient, these iterations must be readily initiated and rapidly executed. This is the basis for DIAL's Interactive Analysis design.

Queries and reports to the analyst at the terminal, as well as execution controls, are structured for a clear, simple interface with the analyst. It is not intended that the analyst be a digital hardware or software specialist in order to accomplish his analysis task. Operations initiated by the analyst are performed in near-real time.

Data flow for DIAL Interactive Analysis is shown in Figure A-2.

A.2.2 INTERACTIVE ANALYSIS CAPABILITIES

The following is a summary of the principal DIAL Interactive Analysis

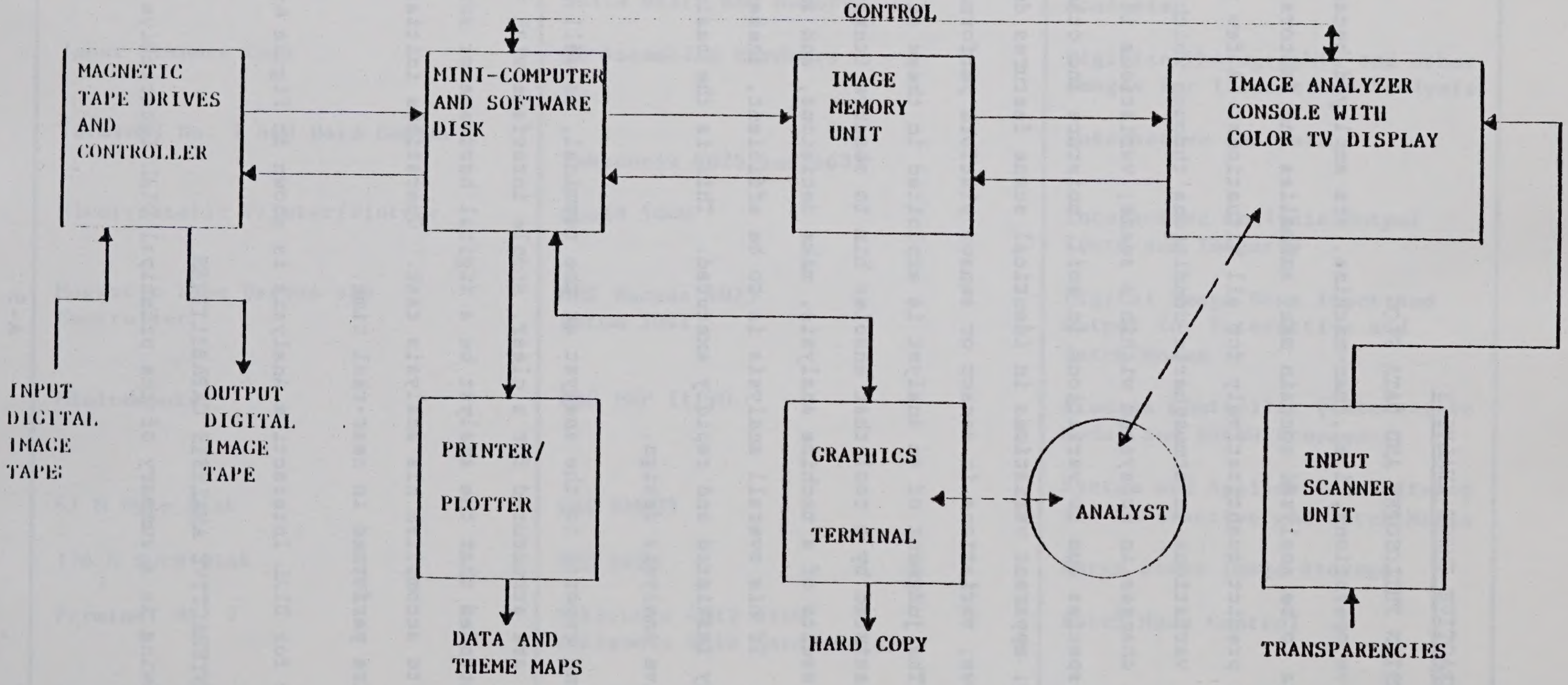
CONTROL
MAGNETIC TAPE DRIVES AND CONTROLLER
MINI-COMPUTER AND SOFTWARE DISK
IMAGE MEMORY UNIT
IMAGE ANALYZER CONSOLE WITH COLOR TV DISPLAY
INPUT DIGITAL IMAGE TAPE
OUTPUT DIGITAL IMAGE TAPE
PRINTER/ PLOTTER
GRAPHICS TERMINAL
ANALYST
INPUT SCANNER UNIT
DATA AND THEME MAPS
HARD COPY
TRANSPARENCIES

Figure A-2. DIAL Interactive Analysis

capabilities. Some are implemented solely via hardware, others through a combination of hardware and software.

- Image Input
  - All image input data are stored in the Image Memory Unit (see below)
  - Landsat CCT
    - 9-track 800 or 1600 bpi, BI2P format
    - Any size rectangular portion of the scene may be stored in any size rectangular region in the image plane of the Image Memory Unit. Capacity of the Image Memory Unit is 512 x 512 pixels, however. Over-, unity-, or under-sampling of the Landsat scene may be used. For example, sampling every fourth pixel and line in a 1024 x 1024 portion of a Landsat scene produces a 256 x 256 pixel array in the Image Memory Unit.
    - De-skewing available
    - Several separate regions of the scene may be stored side-by-side in the Image Memory Unit, forming a composite image to be analyzed.
  - Other digital image data on magnetic tape
    - Aircraft scanners
    - Other sensors (e.g., SMS)
    - Output from prior interactive analyses
    - Other (e.g., topographic data)
  - Transparency
    - Aerial photography
    - Thermal imagery
    - Radar imagery
    - Other
    - Multi-frame integration available to minimize effects of time-varying noise in the scanner-digitizer

- Shading correction available to compensate for non-uniformities across the field-of-view in the light table and TV scanner
- 8-bit digitizing for 512 x 512 pixels over the scanner optical field-of-view (ranges from 0.75 in x 0.75 in to 6 in x 6 in)

- Considering the effective spatial resolution of the transparency scanner/digitizer to be 375 elements over the optical field-of-view, the following is an example of the digitizing capability available.

  Scale of imagery - 1:15,840
  Scanner field-of-view on the image - 1.42 in. x 1.42 in.
  Corresponding field-of-view in the scene - 1874 ft. x 1874 ft.
  Effective resolution of digitized scene - 5.0 ft.

- For those infrequent occasions in which a large quantity of high-resolution image digitizing is required, DIAL employs an outside commercial digitizing service.
- Multi-Sensor, Multi-Date Image Data
  - 3 bands of Landsat + 1 band aerial photography for same scene
  - 3 bands of Landsat + 1 channel of topographic data for same scene
  - 2 bands of Landsat for one date + 2 bands of Landsat for second date, same scene
  - Numerous similar combinations
- Image Memory
  - 512 x 512 pixels, 5 overlaying channels, 8 bits/pixel/channel
  - 5th channel frequently used to store up to 8 binary map images (themes)

- Image Manipulations
  - For image data in any channel of the Image Memory Unit
  - Uses Affine Transform
  - Accomplishes registration of multi-date or multi-sensor imagery, and registration of map to image or image to map
- Radiometric Scaling and Resolution
  - Available for image data in the first four channels of the Image Memory Unit

- Band (Channel) Ratioing
  - Available for the first four channels of image data in memory
  - Pixel-by-pixel: direct ratio; two channel difference over sum; single channel over sum of channels
- Joystick Driven Cursor
  - Cursor operates in 3 modes: rectangle; 45° rotated rectangle; crosshair
  - Cursor may be controlled in size and position anywhere in the image plane in memory
  - Cursor also is computer driven
- Examination of Image Data in Memory
  - Densitometer (trace line defined by cursor position)
  - Histograms (pixel radiometric values vs. frequency of occurrence)
  - Video Gray Level Dump
  - Acquisition of 4-channel radiometric values for single pixel
  - Magnification (via pixel replication) of selected region of image
- Signature Extraction
  - Operates jointly on first four channels of memory
  - Based on partitioning 4-space using parallelepiped cells
  - 1-cell histogram (signature) acquisition
    - For any single or multiple region in the image plane
    - Recognition or alarm signal is produced and is visible in the scene display for all pixels in memory whose location in 4-space falls within the cell corresponding to the training (acquisition) region

    - Analyst may iteratively and rapidly modify histogram limits to cause recognition signal to correspond closely to ground truth
  - 2-channel, 2-dimensional histogram acquisition
    - For any analyst-defined region in the image plane
    - Analyst iteratively and rapidly sets rectangular boundaries in the histogram 2-space to cause recognition signals to correspond closely to ground truth
  - M-cell (multiple cells in 4 space) signature acquisition available when the most discriminating partitioning of 4-space is needed
- Clustering
  - Employs a "method of migrating means"
  - Partitions a user defined feature space into a selected number of classes
- Theme (Binary Map) Generation and Processing
  - Themes may be produced from the alarm (recognition) signal
    - 1-cell and M-cell signature acquisition
    - 1-cell signature limit input
    - Single channel level slicing
    - Clustering
  - Themes may be produced from the cursor
    - Joystick-controlled 3-mode cursor
    - Polygon cursor-a polygon defined by the analyst using the joystick-controlled cursor in crosshair mode
  - Themes may be produced from combinations of the above and from other themes
  - Theme Boolean operations and area measurement are available
  - Golay theme processing available
    - Edge, swell, shrink, fill, other

- Radiometric Enhancement
    - Linear, logarithmic and equi-density stretches available in all memory channels
    - Analyst sets amplitude limits of the data to be stretched (e.g., small amplitude range may be stretched to 8-bit range)
    - Enables visual detection of scene tonal features often not otherwise apparent
- Spatial Convolution
    - 10 menu-selected operations, including
        - Compass gradient
        - Noise filters
        - Edge, line, texture enhancement
        - User-defined kernel
    - Kernels up to 7 x 7
    - 1-2 minute execution time
    - Interactive spatial enhancement available using convolution
        - Produces a range of custom edge and texture enhancements without iterating a time-consuming process
        - Range of enhancements is under joystick control
- General Purpose Transform
    - Used to perform geometric transformations in 4-space (Eigenvector, Hadamard, other)
    - Enables linear combinations of multiple image channels (e.g., $Y_k = ax_1 + bx_2 + cx_3 + dx_4$)
- Output Products
    - Imagery
        - Image Memory contents on digital tape (BSQ format, 9-track, 1600 bpi)
        - A/N and binary theme maps via the electrostatic printer
        - Halftone print from memory image channel via electrostatic printer

        - Photography of color TV monitor display of image memory
        - Digital image recording on film of a Landsat image in memory is available under Batch mode
    - Graphics and Data
        - Histogram tabulations and plots (one-dimensional, 4-channel), including mean, variance and 4-channel parallelepiped boundaries
        - Two-dimensional, two-channel histogram plot with 2-D parallelepiped boundaries
        - Densitometer traces of image data lines in memory
        - Dump of pixel numerical amplitude values of any region of the image in memory
        - Areas of themes by pixel count and percent of scene
- Utility and Diagnostic Operations
    - Patch for bad lines in stored image
    - Video channel exchange
    - Test Patterns
    - Several similar operations

A.3 BATCH PROCESSING OF DIGITAL IMAGES

A.3.1 DESIGN PHILOSOPHY AND DATA FLOW

In general, DIAL Batch mode processing is concerned with large scenes (almost always greater than 512 x 512 pixels, and frequently the equivalent of a full Landsat scene). Further, the processing algorithms and parameter values have been established in advance--sometimes based on experience, but usually based on the results of a preceding Interactive Analysis session. This mode, then, is frequently a production activity, unattended except at initiation, with operation structured for high throughput. Depending on the tasks, multiple Batch processing jobs may be run concurrently, or the mixture may be Interactive Analysis plus Batch processing jobs.

Four image data files, each capable of accommodating a full Landsat scene (32 M Bytes), are available in the disk storage system. Except for thematic classification of Landsat CCTs, and a few other cases, all Batch mode processing of images begins by storing in one of the four disk image files the image data which is input via magnetic tape. Landsat CCT thematic classification begins in a similar manner.

Figures A-3 and A-4 depict the data flow for most DIAL Batch mode operations. Those operations not shown are included in the following discussion of DIAL Batch mode capabilities.

A.3.2 BATCH MODE CAPABILITIES

The following is a summary of the principal DIAL Batch mode capabilities.

- Landsat CCT Thematic Classification
  - Inputs
    - Up to 20 theme signatures derived from prior Interactive Analysis (Signatures are parallelepipeds in 4-space). Procedures exist to accommodate additional themes.
    - Coordinates of polygon regions in the scene in which specific signatures are to apply. (Avoids false classification in regions in scene where signature is known to be inapplicable.)
    - Coordinates of polygon regions in the scene in which theme areas are to be totaled (e.g., hectares of forest class X in watershed Y).

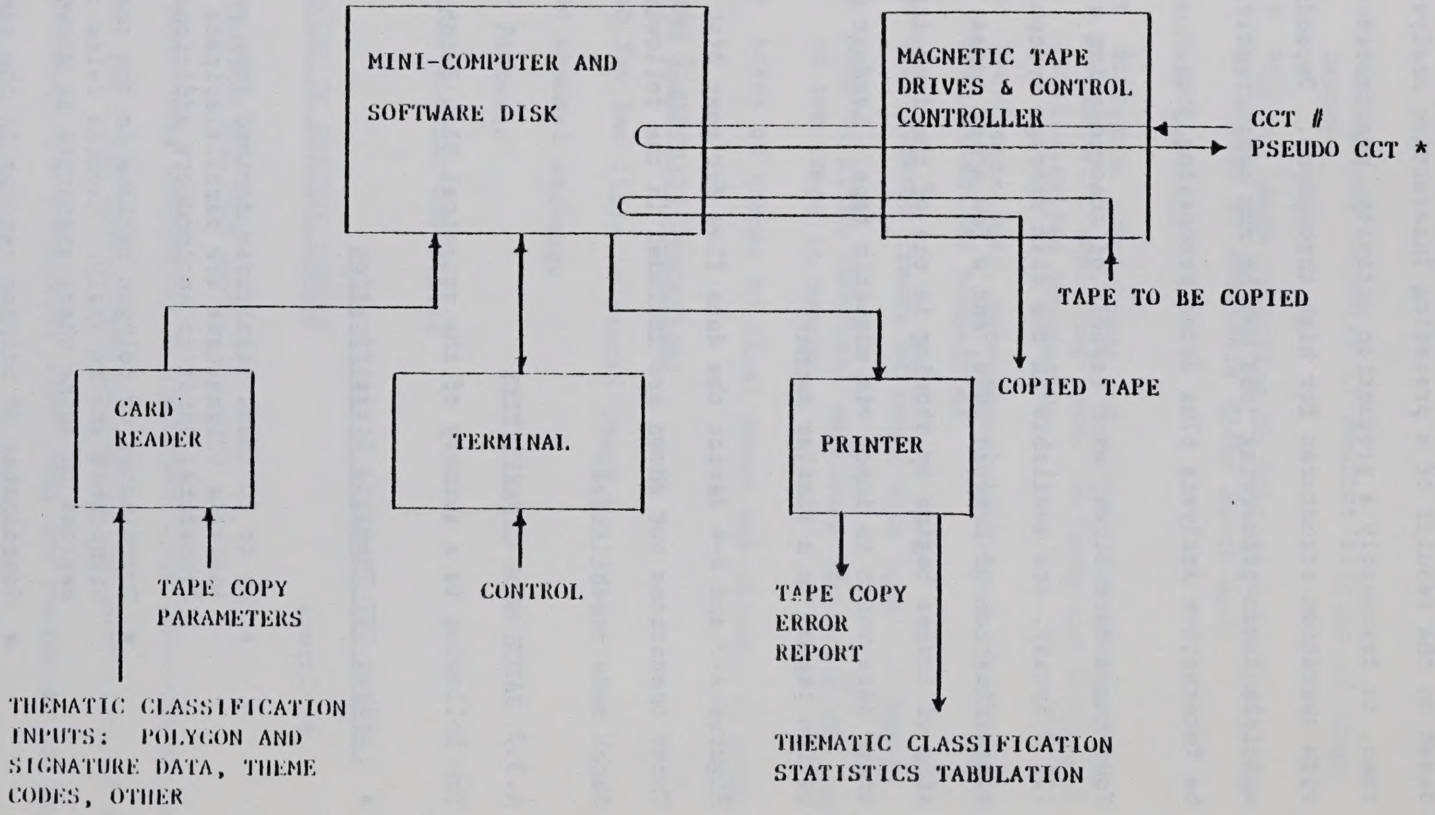
MINI-COMPUTER AND
SOFTWARE DISK
MAGNETIC TAPE
DRIVES & CONTROL
CONTROLLER
CCT #
PSEUDO CCT *
TAPE TO BE COPIED
COPIED TAPE
CARD
READER
TERMINAL
PRINTER
TAPE COPY
PARAMETERS
CONTROL
TAPE COPY
ERROR
REPORT
THEMATIC CLASSIFICATION
INPUTS: POLYGON AND
SIGNATURE DATA, THEME
CODES, OTHER
THEMATIC CLASSIFICATION
STATISTICS TABULATION

# 9-TRACK, 1600 BPI, BIZP FORMAT

* PSEUDO CCT IS A THEMATICALLY CLASSIFIED
CCT WITH SAME FORMAT AS A CCT

Figure A-3. DIAL Tape-to-Tape Batch Mode Operations

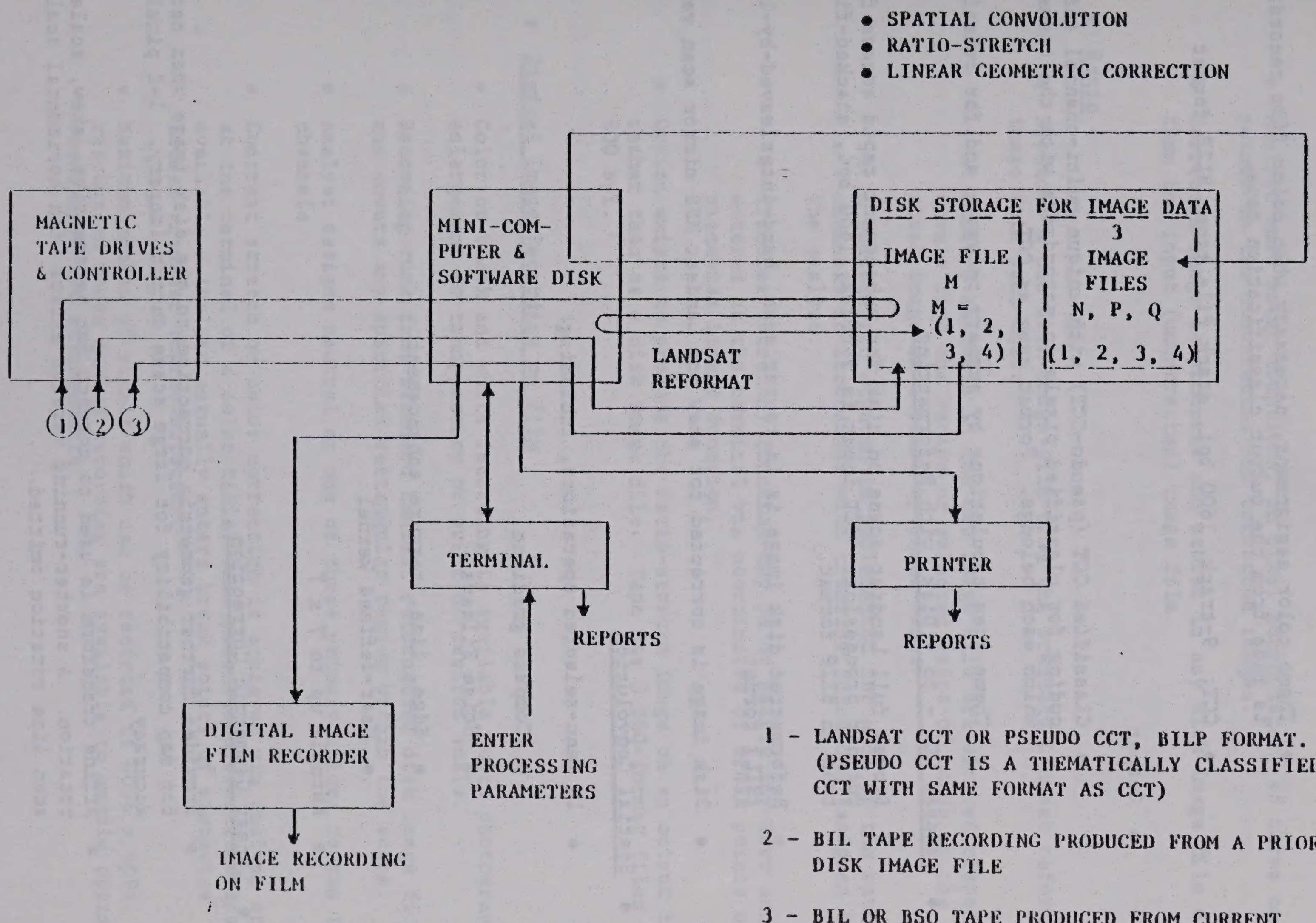
• SPATIAL CONVOLUTION
• RATIO-STRETCH
• LINEAR GEOMETRIC CORRECTION
MAGNETIC TAPE DRIVES & CONTROLLER
MINI-COMPUTER & SOFTWARE DISK
DISK STORAGE FOR IMAGE DATA
IMAGE FILE M
M = (1, 2, 3, 4)
3 IMAGE FILES N, P, Q
(1, 2, 3, 4)
LANDSAT REFORMAT
①
②
③
TERMINAL
REPORTS
PRINTER
REPORTS
DIGITAL IMAGE FILM RECORDER
ENTER PROCESSING PARAMETERS
IMAGE RECORDING ON FILM

1 - LANDSAT CCT OR PSEUDO CCT, BILP FORMAT. (PSEUDO CCT IS A THEMATICALLY CLASSIFIED CCT WITH SAME FORMAT AS CCT)

2 - BIL TAPE RECORDING PRODUCED FROM A PRIOR DISK IMAGE FILE

3 - BIL OR BSQ TAPE PRODUCED FROM CURRENT DISK IMAGE FILE. ALSO, "FAST VIDEO" FORMAT TAPE FOR INPUT TO INTERACTIVE ANALYSIS VIA IMAGE MEMORY UNIT

Figure A-4. DIAL Batch Mode Operations (Some Operations Not Included)

    - Theme color assignment, necessary when color film recording is made from the output classification tape.
    - CCT: 9-track, 1600 bpi, stack file tape, BI2P format
  - Output
    - Classified CCT (pseudo-CCT) with unique multi-channel intensity coding for classified pixels in accordance with the theme to which each belongs. Format same as CCT.
    - Theme area tabulations by summary polygon, and for overall scene.
- Landsat CCT - to - Disk, with Reformatting
  - Stores full Landsat scene on disk for subsequent rapid access for further processing. CCT input is 9-track, 1600 bpi, stacked-file tape in BI2P format.
  - Reformatted disk image is in raster scan, band-interleaved-by-line (BIL) format.
  - Disk image is corrected for skew and Landsat MSS mirror scan velocity.
- Spatial Convolution
  - 10 menu-selected operations, including:
    - Compass gradient
    - Noise Filters
    - Edge, line, texture enhancement
    - User-defined kernel
  - Kernels up to 7 x 7
- Linear Geometric Correction
  - Provides further geometric correction to the disk image when necessary for map compatibility for large scene output Imagery. 1-2 pixel accuracy.
  - Affine transform is used to correct for perspective, skew, scale and rotation. A shorter-running version exists with horizontal scale and scan line rotation omitted.

- Analyst must enter locations, in pixel coordinates, of three control points in the uncorrected and corrected images.
- Corrected image is produced and stored in any disk image file other than the input (uncorrected) image file.

- Ratio
  - Produces a new disk image file from the standard Landsat reformatted image file such that:
    - First 3 channels in the new image file are derived respectively from the ratios of selected pairs of bands in the original image on a pixel-by-pixel basis.
    - A radiometric stretch is implemented for each of the ratioed channels in accordance with transfer functions assigned by the analyst.
    - Transfer (stretch) function may be of nearly any form and is entered at the terminal via coordinates of break points of a piecewise linear function.
  - Option exists to produce the ratio-stretch image on an output tape rather than as a disk image file. Tape has 3 BSQ-format files at 800 bpi.

- Digital Image Recording on Film
  - Color or black and white recording is available, with photographic enlargement to transparency or print of desired scale.
  - Recording runs from standard Landsat reformatted disk image file and covers any specified rectangular region within the scene.
  - Analyst assigns neutral or one of three primary colors to the image channels.
  - Contrast stretch or color correction is achieved via analyst entry at the terminal of a color table. All possible corrections are available. Analyst actually enters break points of piecewise linear transfer characteristics.
  - Maximum number of pixels which can be recorded is 4096 x 4096. Three resolution modes during recording are available to enable optimum resolution for enlargements.

    - Option exists to make film recording from digital data on tape in 9-track, 800 bpi, BSQ format. Color correction, in this case, must be provided during production of the BSQ tape.

- Disk Image Data Transfer for Interactive Analysis

    - This capability enables an Interactive TV display and analysis check on performance of any Batch operation before proceeding to the next. It may be used also to facilitate extraction of geometric control points from a disk image.

    - Analyst specifies either the rectangular window of interest in the disk image, or the starting location and sampling ratios desired.

    - A 4-file (4-channel) BSQ image tape is produced, the image being a 512 x 512 pixel array. Format is such that it can be read under Interactive Analysis operations and stored in the Image Memory Unit.

- Coordinate Digitizing Operations

    - Enables maps, and points and polygons (e.g., a political boundary) on these maps, to be stored as binary map data in a disk image file in association with the corresponding Landsat image stored in the same file.

    - Use of analyst-selected control points in the maps and Landsat image enables the map data to be registered to the image.

    - Map boundaries and polygons are stored in outline form as themes.

    - Analyst is required to enter map corner points, polygon vertices, and control points using the coordinate digitizing table. He also must obtain control point locations in the image via an interactive mode operation, and enter other identification information via the terminal.

- Utility Operations

    - BIL Tape From Disk Image File

        - Enables disk image file to be recorded on tape for future use and/or for protection against accidental modification or loss on the disk.

        - Creates image output tape for users desiring the BIL format.

- Disk Image File From BIL Tape
  - Enables a previously created disk image file, stored on tape, to be restored to the disk.
- BSQ Image Tape From BIL Tape
  - Creates image output tape for users desiring the BSQ format.
- Tape Copy

  A versatile program which includes:

  - 800 to 1600, 1600 to 800, 800 to 800 and 1600 to 1600 bpi.
  - Copy any number of files or records.
  - Skip any number of files or records on the input or output tape.

APPENDIX B

BIBLIOGRAPHY

A bibliography of the published and available (but unpublished) sources describing geologic characteristics relevant to one or more of the three project areas is provided in the following listing. The cross reference matrix shown in Table B-1 describes in more detail the content (by geologic subdisciplines) of each publication.

1. Allen, C. R., C. F. Richter, J. M. Nordquist, Relationship Between Seismicity and Geologic Structure in the Southern California Region. Seismological Society of America Bulletin, V.55, p.753-797.

2. Alpha, A. G., Petroleum Potential of Sierra Nevada and Eastern Desert, California. 1971, American Association of Petroleum Geologists, Memoir No. 15, p.363-371.

3. American Association of Petroleum Geologists, California Fault Bibliography. 1962.

4. Anders, F. J., Sand Deposits as Related to Interactions of Wind and Topography in the Mojave Desert, Near Bartow, California. 1974, Master's Thesis, University of Virginia.

5. Anderson, D.N., First-and-Second Order Geothermal Project Survey, Imperial County, California. 1973-1974, Report #PB-261511/OWN; NTIS, Springfield, VA.

6. Anonymous, Mineral Industry of California. 1976, California Geology, Vol. 30, No.5, p.110.

7. Anonymous, Geothermal Energy in California: Status Report 1976. JPL Document 5040-25, California Institute of Technology, Pasadena, California.

8. Barca, R. A., Geology of the Northern Part of Old Dad Mountain Quadrangle, San Bernardino County, California. 1966, California Division of Mines and Geology-Map.

9. Bassett, A. and D. Kupfer, A Geologic Reconnaissance in the Southeastern Mojave Desert, California. 1964, California Division of Mines and Geology, Report 83.

10. Bassett, A. M., D. H. Kupfer, F. C. Barstow, Core Logs From Bristol, Cadiz and Danby Dry Lakes, San Bernardino County, California. 1959, USGS Bulletin 1045-D.

11. Bell, R. E., Geology and Ore Deposits of Shadow Mountains, San Bernardino County, California. 1971, Master's Thesis, University of San Diego.

12. Bell, R. E., Gravity Sliding in Shadow Mountains, Eastern Mojave Desert, California. 1971, Geological Society of America Abstracts, Vol. 3, No. 2, p.80.

13. Black, W. E., A Geophysical Investigation of the Yuha Desert, Imperial County, California. 1974, Master's Thesis, University of California at Riverside.

14. Bohannon, R. G. and A. L. Meier, Lithium in Sediments and Rocks from the California Desert Region. 1976, USGS Open File Report 76-693.

15. Bowen, O. E., Jr., Geology and Mineral Deposits of the Barstow Quadrangle, California. 1955, California Division of Mines and Geology Bulletin 165.

16. Briggs, P., F. Press and S. A. Guberman, Pattern Recognition Applied to Earthquake Epicenters in California and Nevada. 1977, Geological Society of America, Bulletin, Vol. 88, No. 2, p.161-173.

17. Byers, F. M., Jr., Geology of the Alvord Mountain Quadrangle, San Bernardino County, California. 1960, USGS Bulletin 1089-A.

18. California Dept. of Transportation, Dept. of Public Works, Division of Highways, California Aerial Photographic Coverage and Index of Aerial Photography. 1966.

19. California Division of Mines and Geology, Imperial County Map. 1976, Mines and Minerals.

20. California Division of Mines and Geology, San Bernardino County Map. 1954, Mines and Minerals.

21. California Division of Mines and Geology, San Francisco, Geologic Atlas of California. 1958, 27 Map Sheets 1:250.000.

22. California Division of Mines and Geology, Geology of the Mojave Desert. Mineral Information Service. 1970.

23. California Division of Mines and Geology, Salton-Mexicali Geothermal Province Mineral Information Service. 1967.

24. California Division of Mines and Geology, Geologic Structure in California: Three Studies with Landsat 1 Imagery. 1976, California Geology.

25. Calzia, J. P., Igneous Geology of a Part of the Southeastern Owlshead Mountains, San Bernardino County, California. Master's Thesis, University of Southern California.

26. Church, J. P. et al, Continuing Crustal Deformation in the Western Mojave Desert. 1974, GSA Abstracts Vol. 6, No. 7, p.687-688.

27. Clary, M. R., Geology of the Eastern Part of the Clark Mountain Range, San Bernardino County, California. 1967, California Division of Mines and Geology-Map.

28. Combs, J., and R. W. Rex, Geothermal Investigations in the Imperial Valley of California. 1971, Geological Society of America Abstracts, Vol. 3, No. 2, p.101-102.

29. Cooke, R. U., Morphometric Analysis of Pediments and Associated Landforms in the Western Mojave Desert, California. 1970, American Journal of Science, Vol. 269, No. 1.

30. Cooke, R. U. and A. Warren, Geomorphology in Deserts. 1973, University of California Press, 374 p.

31. Crowell, J. C., San Andreas Faults in Southern California. 1975, California Division of Mines and Geology, Special Report 118.

32. Cummings, D., Theory of Plasticity Applied to Faulting, Mojave Desert, Southern California. 1976, GSA Bulletin, Vol. 87, No. 5, p.720-724.

33. Dibblee, T. W., Preliminary Geologic Map of the Mojave Quadrangle. 1959, USGS Mineral Investigation - Map MF-219.

34. Dibblee, T. W., Jr., Geology of the Imperial Valley Region, California. 1954 California Division of Mines and Geology, Bulletin 170.

35. Dibblee, T. W., Jr., Areal Geology of the Western Mojave Desert, California. 1967, USGS Professional Paper 522.

36. Dibblee, T. W., Jr., Possible Large Lateral Displacement by the San Andreas Fault of Middle Tertiary Marine Unites of the Western Mojave Desert, California. 1975, GSA Abstract Programs Vol. 7, No. 3, p.310-311.

37. Dibblee, T. W., Jr., Tectonics of the Western Mojave Desert Near the San Andreas Fault. 1975, CDMG Special Report No. 118, p.155-161.

38. Dibblee, T. W., Jr., Geologic Map of the Hanes Quadrangle, San Bernardino County, California. 1960, USGS Map MF-226.

39. Dibblee, T. W., Jr., Geologic Map of the Apple Valley Quadrangle, California. 1960, USGS-Map MF - 232.

40. Dibblee, T. W., Jr., Geologic Map of the Daggett Quadrangle, San Bernardino County, California. 1970, USGS Map I-592.

41. Dibblee, T. W., Jr., Geologic Map of the Old Woman Springs Quadrangle, San Bernardino, California. 1967, USGS Map I-518.

42. Dibblee, T. W., Jr., Geologic Map of the Lavic Quadrangle, San Bernardino County, California. 1966, USGS Map I-472.

43. Dibblee, T. W., Jr., Geologic Map of the Ord Mountains Quadrangle, San Bernardino, California. 1964, USGS Map I-427.

44. Dibblee, T. W., Jr., Geologic Map of the Cody Mountains Quadrangle, San Bernardino County, California. 1966, USGS Map I-467.

45. Dibblee, T.W., Jr. and A. M. Bassett, Geologic Map of the Newberry Quadrangle, San Bernardino County, California. 1966, USGS Map I-461.

46. Dunne, G. C., Geology and Structural Evolution of Old Dad Mountain, Mojave Desert, California. 1977, Geological Society of America Bulletin Vol. 88, No. 6, p.737-748.

47. Dunne, G. C., Geology of the Devil's Playground Area, Eastern Mojave Desert, California. 1972, PhD, Rice University.

48. Durrell, C., Barite Deposits Near Barstow, San Bernardino County, California. 1954, California Division of Mines and Geology Special Report 39.

49. Dutcher, L. C., Geologic and Hydrologic Features of Indian Wells Valley, California. 1973, California Division of Water Resources.

50. Engels, A., Gold Mines of Southern California. 1977, Argonaunt Enterprises, Denver, Colorado, 200p.

51. Evans, J. G., Structural Analysis and Movements of the San Andreas Fault Zone West Palmdale, Southern California. 1966, PhD University of California, Los Angeles.

52. Evans, J. R., Geology and Mineral Deposits of the Mescal Range Quadrangle, San Bernardino County, California. 1971, California Division of Mines and Geology - Map.

53. Evans, J. R., O. E. Bower and C. H. Gray, Jr., Carbonate Rock Resources of the Striped Mountain Area, San Bernardino County, California. 1975, California Division of Mines and Geology - Map.

54. Evenson, W. A., Geology of the Southern Kilbeck Hills and an Adjacent Portion of the Old Woman Mountains. 1973, Master's Thesis, University of Southern California, Los Angeles, 51p.

55. Fife, D. L., D. A. Rogers, G. W. Chase, et al, Geologic Hazards in Southwestern San Bernardino County, California. 1976, California Division of Mines and Geology, Special Publication No. 113.

56. Fuis, G., A Swarm of Earthquakes Near the Pisgah Fault in the Mojave Desert, California. 1974, American Geophysical Union, Vol. 56, No. 12, p.1149.

57. Gale, H. S., Geology of the Saline Deposits, Bristol Dry Lake, San Bernardino County, California. 1951, California Division of Mines and Geology, Special Report 13, and USGS.

58. Garfunkel, Z., A Model for the Young Structure of the Mojave Desert and its Relations with the Adjacent Regions. 1972, Geological Society of America Abstracts Vol. 4, No. 3, p.160.

59. Goldman, H. B., Sand and Gravel in California, An Inventory of Deposits, Southern California. 1968, California Division of Mines and Geology Bulletin 180-C.

60. Jones, J. A., Geology of the Northern Kilbeck Hills and One Adjacent Portion of the Old Woman Mountains. 1973, University of Southern California, 56p.

61. Greene, R. P., Metamorphosed McCoy Mountains Formation, Coxcomb Mountains, California. 1968, Master's Thesis, University of California at Santa Barbara.

62. Hagar, D., Geomorphology of Coyote Valley, San Bernardino County, California. 1967, PhD Thesis, University of Massachusetts.

63. Hall, D. K., Hydrothermal Alteration and Mineralization in the East Camp of the Turquoise District, San Bernardino County, California. 1972, Master's Thesis, University of Arizona.

64. Hamilton, W., Geologic Map of the Big Maria Mountains NE Quadrangle, Riverside County, California. 1964, USGS Map GQ-350.

65. Hawkins, H. G., Strike-Slip Displacement Along the Camp Rock - Emerson Fault, Central Mojave Desert, San Bernardino County, California. 1975, Geological Society of America, Vol. 7, No. 3, p.324.

66. Hawkins, H. G., Strike-Slip Displacement Along the Camp Rock - Emerson Fault, Near Twenty-nine Palms, California. 1975, Geological Society of America Abstract Programs, Vol. 7, No.3, p.374.

67. Hill, R. L., Recent Earthquakes Near Twenty-nine Palms, San Bernardino County, California. 1976, California Geology, Vol. 29, No. 6, p.134-135.

68. Keaton, J. R. and R. T. Keaton, Manix Fault Zone, San Bernardino County, California. 1977, California Geology, Vol. 30, No. 8.

69. Loe, W. S., The Great California Deserts. 1963, New York, Putman.

70. Leoltz, O. J., Geohydrologic Reconnaissance of the Imperial Valley, California. 1975, USGS.

71. Mabey, D. R., Gravity Survey of the Western Mojave Desert. 1960, USGS Professional Paper, 316-D.

72. Mabey, D. R., Principal Facts for Gravity Stations in the Western Mojave Desert, California. 1972, NTIS-PB2-06674.

73. McJunklin, R. D., Geology of the Sugarloaf Mountain Ridgeline, San Bernardino County, California. 1975, GSA Abstract Programs, Vol. 7, No. 3, p.345.

74. Meidav, T., and R. W. Rex, Geophysical Investigations for Geothermal Energy Sources, Imperial Valley, California. 1970, University of California, Riverside.

75. Metzger, D. G., and O. J. Leoltz, Geohydrology of the Needles Area, Arizona, California, and Nevada. 1973, USGS Professional Paper 486-J.

76. Molnar, J., Structure and Petrography of the Northern Shadow Mountains, San Bernardino County, California. 1973, Master's Thesis, University of Southern California.

77. Morton, D. M., Geologic Hazards in Southeastern San Bernardino County, California. 1976, California Division of Mines and Geology.

78. Morton, P. K., Geology and Mineral Resources of Imperial County, California. 1977, California Division of Mines and Geology.

79. Murdock, J. and R. W. Webb, Minerals of California. 1958, California Division of Mines and Geology Bulletin 173.

80. Norris, R. M., Geology of California. 1976, New York - Wiley.

81. Pemberton, H. E., The Crystal Habits and Forms of the Minerals of Searles Lake, San Bernardino County, California. 1975, Mineral Record, Vol. 6, No. 2, p.74-83.

82. Richmond, J. F., Geology of the San Bernardino Mountains North of Big Bear Lake, California. 1960, California Division of Mines and Geology, Special Report 65.

83. Rolstein, Y., J. Combs, S. Biehler, Gravity Investigation in the Southeastern Mojave Desert, California. 1976, Geological Society of America Bulletin, Vol. 87, No. 7.

84. Smith, G., Character and Distribution of Nonclastic Minerals in the Searles Lake Evaporite Deposit, California. 1964, USGS Bulletin 1181-P.

85. Smith, G. I., Geology and Volcanic Petrology of the Lava Mountains, San Bernardino County, California. 1964, Washington, Government Printing Office.

86. Stone, W. D., Geology of the Black Mountain Area, Apple Valley Quadrangle, California. 1964, Master's Thesis, University of California at Riverside.

87. Swolfs, H., Field Measurements of Tectonic Stress Variations in Southern California. 1977, Terra Tek Inc.

88. Tamura, A. Y., Origin, Nature and Significance of the Residual Mud Holes on Danby Dry Lake, California. 1969, Master's Thesis, University of Southern California.

89. Tarbet, L. A., Petroleum Potential of Imperial Valley, California. 1971, American Association of Petroleum Geologists Memoir, No. 15, p.384-391.

90. United States Geological Survey, Geologic Investigations in the Mojave Desert and Adjacent Region, California. 1960, Washington, Government Printing Office.

91. Weber, F. H., Jr., Geology and Mineral Deposits of the Ord Mountain District, San Bernardino County, California. 1963, California Division of Mines and Geology Special Report No. 77.

92. Wilson, R. C., Jr., The Structural Geology of the Shadow Mountains Area, San Bernardino County, California. 1966, Master's Thesis, Rice University.

93. Yelverton, C. A., Geology of the Southern Portion of the Old Dad Mountain Quadrangle, San Bernardino County, California. 1963, Master's Thesis, University of Southern California.

Table B-1. Matrix Showing Bibliography Cross-Referenced by Subdiscipline

PUBLICATION #	SEISMICITY	STRUCTURES/TECTONICS	GEOTHERMAL	MINERAL RESOURCES	GEOPHYSICS	LITHOLOGY	GENERAL
1	X	X					
2				X			X
3		X					
4							X
5			X				
6				X			
7			X				
8		X				X	X
9							X
10						X	X
11				X		X	X
12					X		
13					X		
14				X			
15				X			X
16	X						
17						X	X
18							X
19				X			
20				X			
21							X
22				X			X
23			X	X			X
24		X					X
25						X	X

Table B-1. Matrix Showing Bibliography Cross-Referenced by Subdiscipline (Con't.)

PUBLICATION #	SEISMICITY	STRUCTURES/TECTONICS	GEOTHERMAL	MINERAL RESOURCES	GEOPHYSICS	LITHOLOGY	GENERAL
26		X					
27						X	X
28			X				
29							X
30							X
31	X	X					
32		X					
33				X			X
34						X	X
35							X
36		X					
37		X					
38						X	X
39						X	X
40						X	X
41						X	X
42						X	X
43						X	X
44						X	X
45						X	X
46		X					X
47		X				X	X
48				X			
49							X
50				X			

Table B-1. Matrix Showing Bibliography Cross-Referenced by Subdiscipline

(Con't.)

PUBLICATION #	SEISMICITY	STRUCTURES/TECTONICS	GEOTHERMAL	MINERAL RESOURCES	GEOPHYSICS	LITHOLOGY	GENERAL
51		X					
52				X			X
53				X			X
54							X
55	X						X
56	X	X			X		
57						X	X
58		X					
59				X			
60							X
61						X	X
62		X					
63			X	X			
64						X	X
65		X					
66		X					
67	X	X			X		
68	X	X					
69							X
70							X
71					X		
72					X		
73						X	X
74			X		X		
75							X

Table B-1. Matrix Showing Bibliography Cross-Referenced by Subdiscipline

PUBLICATION #	SEISMICITY	STRUCTURES/TECTONICS	GEOTHERMAL	MINERAL RESOURCES	GEOPHYSICS	LITHOLOGY	GENERAL
76		X					X
77		X					X
78				X			X
79				X			
80							X
81		X		X			X
82						X	X
83					X		
84				X		X	
85		X					X
86						X	X
87		X			X		
88		X					X
89							X
90		X				X	X
91				X			X
92		X					X
93							X

APPENDIX C

ROSE DIAGRAMS

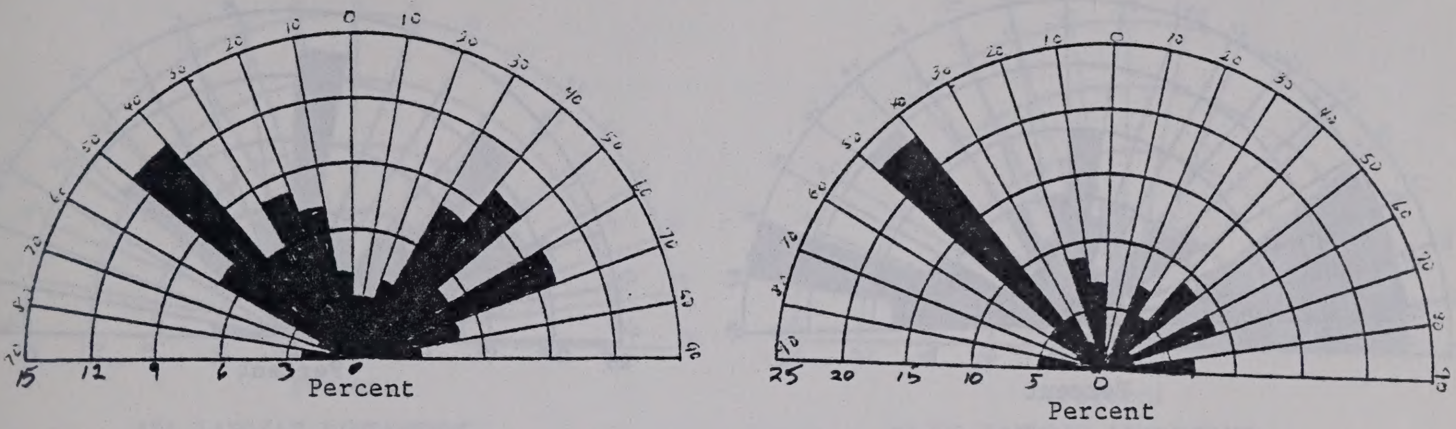

ALL LANDSAT LINEAMENTS

MAJOR LANDSAT LINEAMENTS

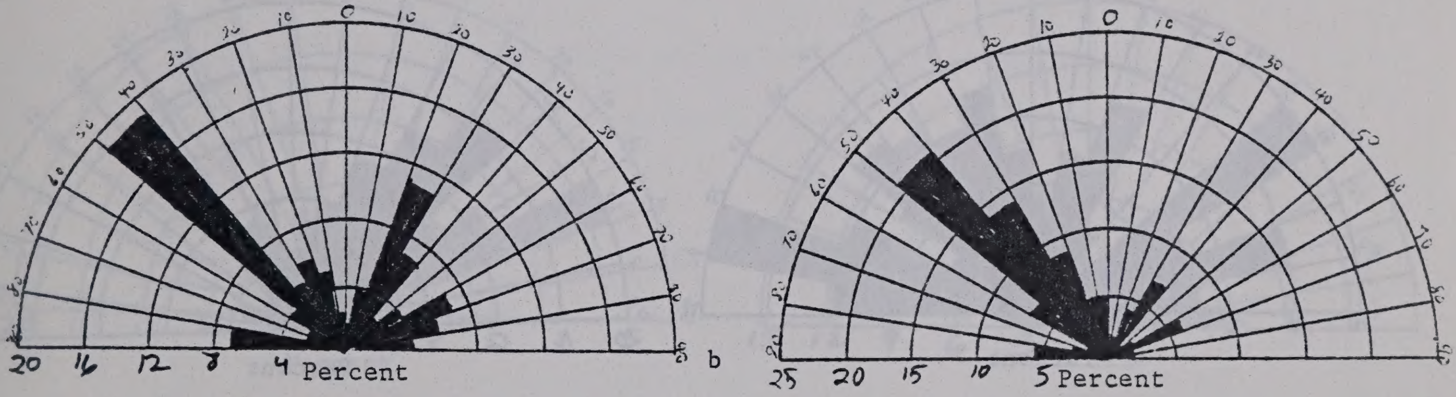

SKYLAB LINEAMENTS

LEVELS 1, 2, LINEAMENTS

(NOT PLOTTED)

HIGH ALTITUDE AERIAL PHOTO LINEAMENTS

Figure C-1. Rose Diagrams for Area 1 Showing Major Lineament Trends

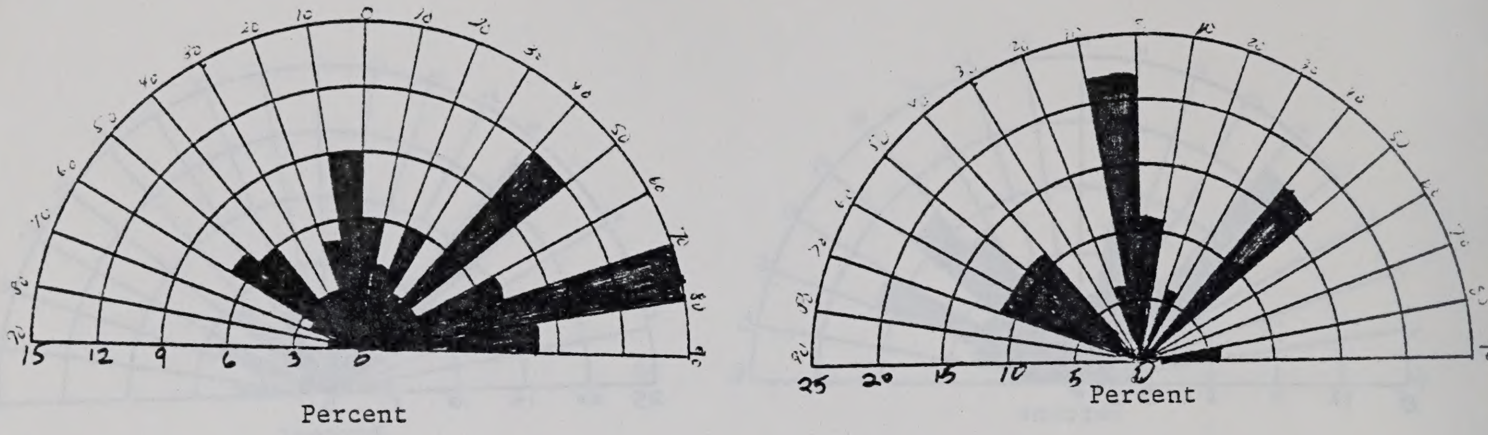

ALL LANDSAT LINEAMENTS

MAJOR LANDSAT LINEAMENTS

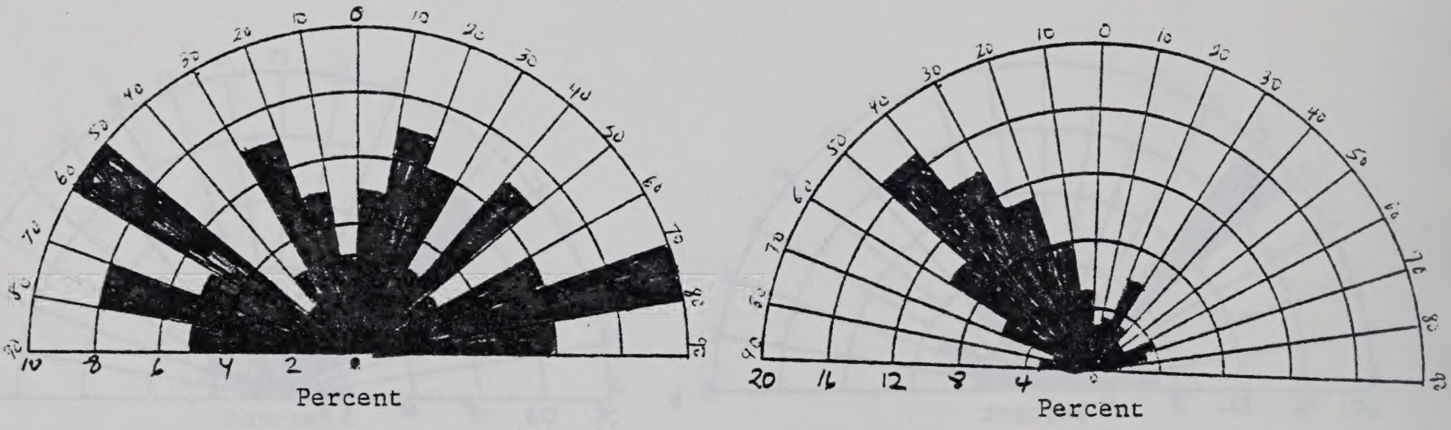

SKYLAB LINEAMENTS

LEVELS 1, 2, 3 LINEAMENTS

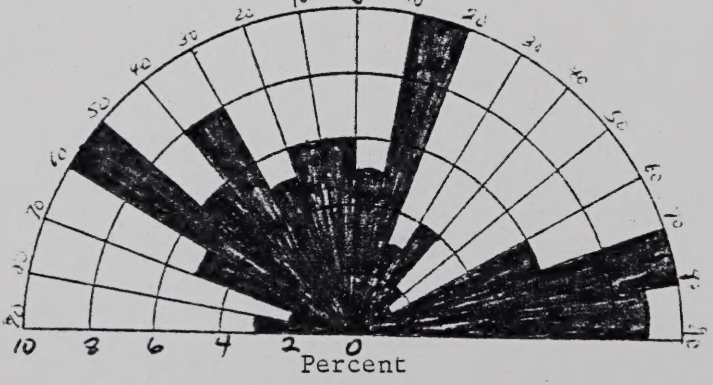

HIGH ALTITUDE AERIAL PHOTO LINEAMENTS

Figure C-2. Rose Diagrams for Area 2 Showing Major Lineament Trends

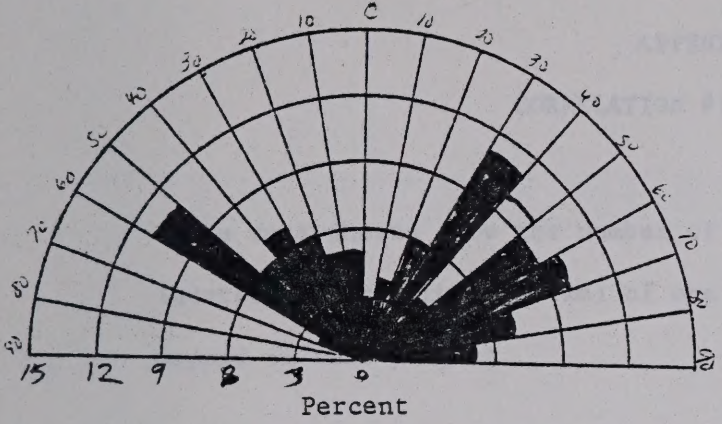

ALL LANDSAT LINEAMENTS

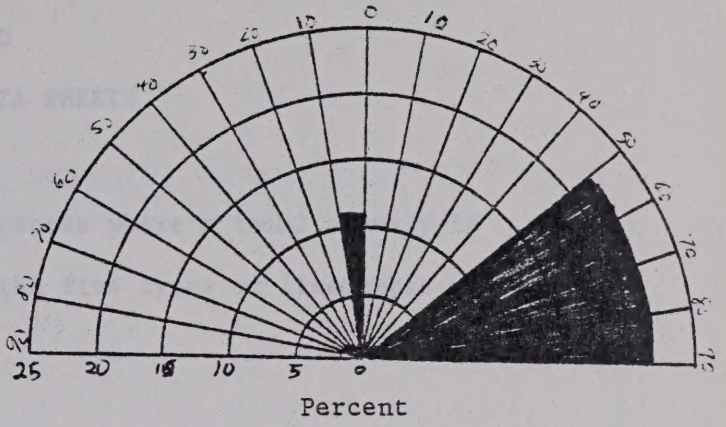

MAJOR LANDSAT LINEAMENTS

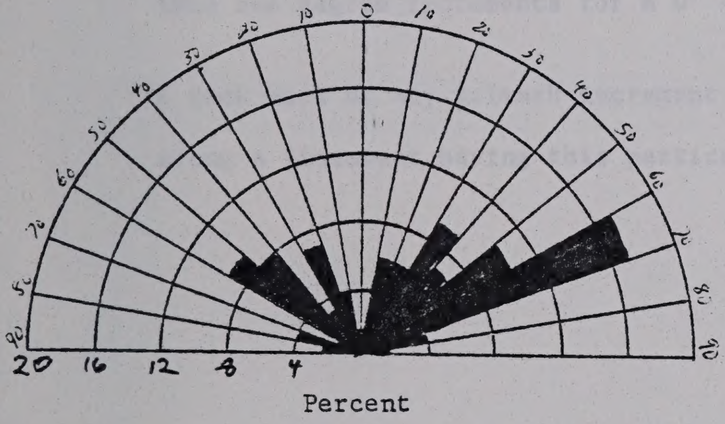

SKYLAB LINEAMENTS

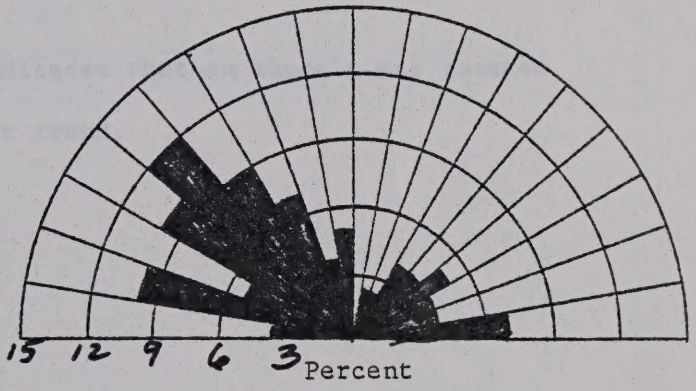

LEVELS 1, 2, 3 LINEAMENTS

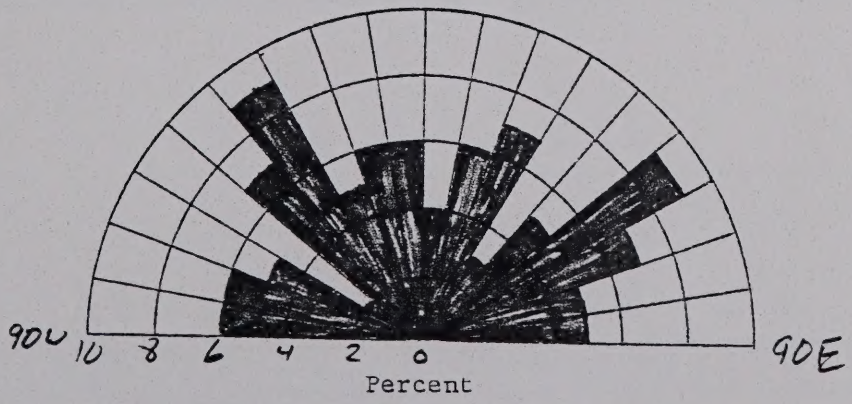

HIGH ALTITUDE AERIAL PHOTO LINEAMENTS

Figure C-3. Rose Diagrams for Area 3 Showing Major Lineament Trends

APPENDIX D

CORRELATION #1 DATA SHEETS

These data sheets show the number of instances where a tonal anomaly is located on (or within 0.6 km) of one of the five types of lineaments mapped in this project.

The data sheets show the 180 possible lineament azimuths proportioned into one degree increments for N 0° - 90°W and for N 0° - 90°E.

A tick mark by any azimuth increment indicates that an anomaly was located along a lineament having this particular trend.

Table D-1. Correlation of Landsat Lineaments (all) with Tonal Anomalies (Area 1)

NW	On	Within 0.6 km	NW	On	Within 0.6 km	NW NE	On	Within 0.6 km	NE	On	Within 0.6 km	NE	On	Within 0.6 km
0	~~1111~~ 11	11	37			74			21			58	1	
1	1	1	38			75			22			59		
2			39			76			23			60		
3			40			77			24			61	1	
4			41			78			25	1	11	62	~~1111~~	
5			42	1		79			26			63		
6			43			80			27			64	1	
7			44			81			28			65	1	1
8			45	111	~~1111~~	82			29			66		11
9			46	1	11	83			30	11	1	67	11	
10		1	47	1	11	84			31	1111	1	68	1	
11			48	~~1111~~ 11	1	85			32	11	111	69		
12			49			86			33			70	1	1
13	~~1111~~ 11	111	50			87			34			71		
14			51			88			35	1111		72		
15			52	1		89			36			73		1
16			53			90	~~1111~~ 111	~~1111~~	37			74		
17	1	1	54	11		1	111		38			75	11	11
18			55	1	1	2			39	1		76		
19	11	11	56			3			40		11	77	11	111
20			57			4			41			78		
21			58		1	5			42	11	11	79		
22	1		59			6			43			80		
23	1	1	60			7			44			81		
24	111	11	61	11	1	8			45	~~1111~~	1	82		
25	11	1	62			9			46	1	1	83	111	1
26			63			10			47			84		
27			64			11			48	1111	1111	85	1111	11
28			65			12			49			86		
29			66			13			50			87		
30			67			14			51			88		
31			68			15	1	1	52			89		
32			69			16			53					
33			70			17			54					
34	1		71			18			55	111				
35	111	11	72			19			56	1				
36			73			20			57					

Table D-2. Correlation of Landsat Major Lineaments with Tonal Anoamlies (Area 1)

NW	On	Within 0.6 km	NW	On	Within 0.6 km	NW NE	On	Within 0.6 km	NE	On	Within 0.6 km	NE	On	Within 0.6 km
0			37			74			21			58		
1	1	1	38			75			22			59		
2			39			76			23			60		
3			40			77			24			61		
4			41			78			25	1	11	62	111	
5			42	1	11	79			26			63		
6			43			80			27			64		
7			44			81			28			65	1	1
8			45	1111	1111	82			29			66		
9			46	1	11	83			30			67		
10			47			84			31			68		
11			48	~~1111~~ 111	~~1111~~	85			32			69		
12			49			86			33			70		
13			50			87			34			71		
14			51			88			35	11	11	72		
15			52			89			36			73		
16			53			90	~~1111~~ 1111	1111	37			74		
17	1	1	54			1			38			75	11	11
18			55			2			39			76		
19	1	1	56			3			40			77		
20			57			4			41			78		
21			58			5			42		1	79		
22	1	1	59			6			43			80		
23			60			7			44			81		
24			61			8			45			82		
25			62			9			46	1		83		
26			63			10			47			84		
27			64			11			48			85	1	~~1111~~
28			65			12			49			86		
29			66			13			50			87		
30			67			14			51			88		
31			68			15			52			89		
32			69			16			53					
33			70			17			54					
34	1		71			18			55	111	11			
35			72			19			56					
36			73			20			57					

Table D-3. Correlation of Skylab Lineaments with Tonal Anomalies (Area 1)

NW	On	Within 0.6 km	NW	On	Within 0.6 km	NW NE	On	Within 0.6 km	NE	On	Within 0.6 km	NE	On	Within 0.6 km
0	111		37			74			21	1	11	58	~~1111~~	1
1		1	38			75			22			59		
2			39			76	~~1111~~		23	1		60	1	
3			40	11	11	77			24			61		
4			41			78			25	1		62		
5			42	111		79			26			63		
6			43			80	11	1	27			64	1	
7			44			81			28	~~1111~~ 11		65	111	1
8		1	45	1111	1	82			29	1	11	66		
9			46		111	83			30	11		67		
10			47	1111		84			31			68	1	
11			48	1	1	85			32	1		69	11	1
12			49	1		86			33			70	1	
13			50			87			34	~~1111~~	11	71		
14	~~1111~~ 11		51			88	1111	1	35			72		
15			52	1	11	89			36			73		
16			53	1		90	11	1	37			74		
17	1	1	54	1	1	1			38			75		
18			55			2			39			76		
19	1		56			3			40			77		
20			57			4			41			78		
21			58			5			42	1		79	1	
22			59			6			43			80		
23			60			7			44			81		11
24			61			8			45			82		
25	111	111	62			9			46			83		
26			63			10			47			84		
27			64			11			48			85	11	
28			65			12			49			86		
29			66			13			50			87		
30			67			14			51			88		
31			68			15			52	1		89		
32			69			16			53					
33			70			17			54					
34			71			18			55					
35			72			19			56					
36			73			20	~~1111~~	~~1111~~ 1	57					

Table D-4. Correlation of Levels of Agreement Lineaments 1, 2, 4 with Tonal Anomalies (Area 1)

NW	On	Within 0.6 km	NW	On	Within 0.6 km	NW NE	On	Within 0.6 km	NE	On	Within 0.6 km	NE	On	Within 0.6 km
0			37	1	11	74			21		1	58	1	
1			38	111	11	75			22			59		
2	1		39			76			23	1		60	1	
3			40		~~1111~~	77			24			61		
4			41			78			25			62		
5			42			79			26			63		
6			43			80			27			64	1	
7			44	11		81			28			65		
8			45			82			29	111		66		
9			46		11	83			30		111	67		
10			47			84			31			68		
11			48			85			32	1		69		
12			49			86			33			70		
13			50	11		87			34			71		
14	~~1111~~ 111	1	51			88	1111	11	35	111	1	72		
15			52	1		89			36		1	73		
16	1	1	53	11		90			37			74		
17			54			1			38			75		
18			55			2			39			76		
19			56			3			40			77		
20			57			4			41			78		1
21			58			5			42			79		
22	1	111	59			6			43			80		
23			60			7			44			81		
24			61			8			45			82		
25			62			9			46			83		
26			63			10			47			84		
27			64			11			48			85		
28			65			12			49			86		
29			66			13			50			87		
30			67			14			51			88		
31			68			15			52			89		
32			69			16			53					
33	111		70			17			54	1	11			
34			71			18			55					
35			72			19			56					
36			73			20			57					

Table D-5. Correlation of Landsat Lineaments (all) with Tonal Anomalies (Area 2)

NW	On	Within 0.6 km	NW	On	Within 0.6 km	NW NE	On	Within 0.6 km	NE	On	Within 0.6 km	NE	On	Within 0.6 km
0	1111		37			74			21			58		
1	1		38			75			22	11		59		
2			39			76			23			60		
3			40	11	1	77			24			61		
4			41	1	~~1111~~ 1	78			25	111	1	62	1	
5			42			79			26	1	1	63		
6	1111	11	43	~~1111~~ 11	111	80			27			64		1
7			44			81			28		1	65		
8		11	45			82			29	~~1111~~		66		
9	1		46			83			30			67		
10			47			84	1		31			68		
11			48			85			32			69		
12			49	1		86			33			70	1	1
13		1	50			87			34			71		111
14		11	51	~~1111~~ 1	1	88			35			72	1	11
15			52			89			36			73		
16			53			90	11	11	37	11		74		
17			54			1			38	1	1	75		
18	11	11	55		111	2	1		39			76		
19			56			3		1	40	~~1111~~ 1	11	77		1
20		1	57	1	1	4			41	1	1	78		
21			58			5			42			79		
22	1	11	59			6		1	43			80		1
23			60	11		7			44			81		
24			61			8			45			82		
25			62			9			46			83		
26	1	1	63			10			47		111	84	1	1111
27			64			11			48	111	1111	85	11	1
28			65			12	1	1	49	1		86		
29			66			13			50			87		
30			67	1	111	14	1111	~~1111~~	51			88		1
31			68			15	1		52			89		
32			69			16			53					
33			70			17		1	54					
34			71	11	1111	18			55					
35			72			19			56					
36			73			20			57					

Table D-6. Correlation of Landsat Major Lineaments with Tonal Anomalies (Area 2)

NW	On	Within 0.6 km	NW	On	Within 0.6 km	NW NE	On	Within 0.6 km	NE	On	Within 0.6 km	NE	On	Within 0.6 km
0	111	11	37			74			21			58		
1			38			75			22			59		
2			39			76			23			60		
3			40			77			24			61		
4			41			78			25			62		
5			42			79			26			63		
6	11	~~1111~~	43	1111	~~1111~~	80			27			64		
7			44	1		81			28			65		
8			45			82			29	11	11	66		
9		1	46			83			30			67		
10			47			84			31			68		
11			48			85			32			69		
12			49	1	11	86			33			70		
13		1	50			87			34			71		
14			51	~~1111~~	1111	88			35			72		
15			52			89			36			73		
16			53			90			37			74		
17			54			1			38			75		
18			55			2			39			76		
19			56			3	1		40	1111	~~1111~~	77		
20			57			4			41			78		
21			58			5			42			79		
22			59			6			43			80		
23			60			7			44			81		
24			61			8			45			82		
25			62			9			46			83		
26			63			10			47			84		
27			64			11			48	11	111	85		
28			65			12			49			86		
29			66			13			50			87		
30			67	11	~~1111~~	14			51			88		
31			68			15			52			89		
32			69			16			53					
33			70			17			54					
34			71			18			55					
35			72			19			56					
36			73			20			57					

Table D-7. Correlation of Skylab Lineaments with Tonal Anomalies (Area 2)

NW	On	Within 0.6 km	NW	On	Within 0.6 km	NW NE	On	Within 0.6 km	NE	On	Within 0.6 km	NE	On	Within 0.6 km
0			37			74			21			58		
1			38			75	1		22			59		
2			39			76			23			60		
3			40			77		1	24			61		1
4			41			78			25	~~1111~~ 1		62		
5			42			79			26			63	1	1
6			43			80			27			64		
7			44			81			28			65		
8			45			82			29			66		
9			46			83			30			67		
10			47		1	84			31			68		
11			48			85			32			69		
12			49			86			33			70		
13			50	1	1	87		11	34			71		
14			51			88			35			72		
15			52			89			36			73		
16			53	11	11	90	1		37			74		
17			54			1			38			75		1
18			55	1		2			39		1	76		111
19		1	56			3		11	40	1111	111	77		
20		1	57			4			41			78		
21			58	11	11	5			42			79		
22			59			6			43			80		
23			60	11	1	7			44	1		81		
24			61			8			45			82		
25			62			9			46			83		1
26		11	63			10			47			84		
27			64			11			48			85		
28			65	1	1	12			49			86		
29			66			13			50			87		
30	1	11	67			14			51			88		
31			68			15	11	1111	52			89		
32			69			16			53					
33			70	1111		17			54					
34	11	111	71			18	~~1111~~ 11	~~1111~~ 1	55					
35			72		1	19			56					
36			73			20			57					

Table D-8. Correlation of Levels of Agreement Lineaments 1, 2, 3 with Tonal Anomalies (Area 2)

NW	On	Within 0.6 km	NW	On	Within 0.6 km	NW NE	On	Within 0.6 km	NE	On	Within 0.6 km	NE	On	Within 0.6 km
0			37			74			21		11	58		
1	1		38			75			22		1	59		
2			39			76			23	1		60		
3			40			77			24			61		
4			41			78			25			62		
5			42			79			26			63		
6			43		1	80			27			64		
7			44		111	81			28	1111		65		
8			45			82			29			66		
9			46			83			30			67		
10	1		47			84			31			68		
11			48	11	1	85			32	1		69		
12		1	49			86			33			70		
13			50			87			34			71		
14			51			88			35			72		
15			52			89			36			73		
16			53			90	11	11	37			74		
17			54			1			38			75		
18			55			2			39			76		
19			56			3			40			77		
20			57			4			41			78		
21			58	1		5			42			79		
22			59			6		11	43			80		
23		11	60	111	1	7			44			81		
24			61			8		1	45			82		
25		1	62			9			46			83		
26			63	11	11	10			47			84		
27			64			11			48			85		
28			65		1	12			49			86	11	1
29			66			13			50		1	87		
30		11	67			14			51			88		
31	1	111	68			15	11	11	52	1	11	89		
32			69			16			53					
33			70	1	111	17			54					
34		1	71			18			55					
35			72			19			56					
36			73			20			57					

Table D-9. Correlation of Aerial Lineaments with Tonal Anomalies (Area 2)

NW	On	Within 0.6 km	NW	On	Within 0.6 km	NW NE	On	Within 0.6 km	NE	On	Within 0.6 km	NE	On	Within 0.6 km
0	1		37			74			21			58		
1			38			75			22			59		
2	1		39			76			23			60		
3			40	11	1	77			24			61	1	11
4			41			78			25			62		
5			42	1	1	79			26	1	111	63	1	1
6			43			80			27			64		
7			44	1	111	81	1	1	28			65		
8	111	1	45			82			29			66		1
9		11	46			83			30	1	11	67		
10	11	111	47			84			31			68		
11			48			85			32			69		
12	1		49			86			33			70		1
13	11	~~1111~~	50	111	1111	87			34			71		
14			51	11	1111	88			35			72		
15			52	1		89			36			73		
16			53			90			37			74		
17			54			1	1		38			75	1	
18			55			2			39			76		
19			56			3			40			77	1111	1
20	1	11	57			4			41			78		
21			58			5			42			79		1
22	~~1111~~		59			6			43			80	1	1
23			60	~~1111~~ 1	1	7			44			81		
24			61	111	11	8			45			82		
25			62			9			46			83		11
26			63			10			47			84		
27			64	1	1	11	1	1	48			85		
28			65			12			49			86		
29			66			13	11	111	50			87	1111	11
30			67			14			51			88		
31			68			15			52			89		
32		11	69			16		11	53	11	1111			
33			70			17			54					
34			71			18			55					
35			72	1	1	19			56					
36			73			20			57					

Table D-10. Correlation of Landsat Lineaments (all) with Tonal Anomalies (Area 3)

NW	On	Within 0.6 km	NW	On	Within 0.6 km	NW NE	On	Within 0.6 km	NE	On	Within 0.6 km	NE	On	Within 0.6 km
0			37			74			21			58		
1			38			75			22			59	1	
2			39			76			23			60	111	
3	1	11	40	1		77			24			61		
4			41		1	78			25			62		
5	111		42			79			26	11	11	63	1111	
6			43			80			27			64		
7			44			81			28			65		
8			45	111	1111	82			29			66	11	1
9	111		46			83			30		1	67		
10		1	47			84			31			68		
11		1	48			85			32			69	1	
12			49			86			33	11		70	111	1
13	1		50			87			34		1	71		
14		1	51	1	1	88			35		1	72	1	
15			52		1	89			36	1	11	73	111	1
16	1		53	~~1111~~ 11	11	90			37	111	11	74		11
17			54		1111	1			38			75		
18			55	1	11	2			39	111	11	76	111	11
19	111	1111	56			3			40	~~1111~~	1111	77		
20	11		57			4			41			78		
21			58	1	111	5			42	1		79		
22			59			6	11		43			80		1
23		1	60			7			44			81		
24		11	61			8			45			82		
25			62	1	1	9			46			83		
26			63			10			47			84	1	11
27			64			11			48	1		85	~~1111~~ 11	1
28		11	65	1	11	12			49			86		
29			66			13	11	11	50			87		
30			67			14			51			88		
31		1	68			15			52		11	89		
32	1	111	69			16			53					
33			70			17			54					
34			71			18			55					
35			72			19	111		56	11				
36			73			20			57		11			

Table D-11. Correlation of Landsat Major Lineaments with Tonal Anomalies (Area 3)

NW	On	Within 0.6 km	NW	On	Within 0.6 km	NW NE	On	Within 0.6 km	NE	On	Within 0.6 km	NE	On	Within 0.6 km
0			37			74			21			58		
1			38			75			22			59		
2			39			76			23			60		
3			40			77			24			61		
4			41			78			25			62		
5			42			79			26			63		
6			43			80			27			64		
7			44			81			28			65		
8			45			82			29			66		
9			46			83			30			67		
10			47			84			31			68		
11			48			85			32			69	1	
12			49			86			33			70		
13			50			87			34			71		
14			51			88			35			72		
15			52			89			36			73		
16			53			90			37			74		
17			54			1			38			75		
18			55			2			39			76	1111	1
19			56			3			40			77		
20			57			4			41			78		
21			58			5			42			79		
22			59			6			43			80		
23			60			7			44			81		
24			61			8			45			82		
25			62			9			46			83		
26			63			10			47			84	1	11
27			64			11			48			85	~~1111~~ 11	~~1111~~ 1
28			65			12			49			86		
29			66			13			50		11	87		
30			67			14			51			88		
31			68			15			52			89		
32			69			16			53					
33			70			17			54					
34			71			18			55					
35			72			19			56					
36			73			20			57					

Table D-12. Correlation of Skylab Lineaments with Tonal Anoamlies (Area 3)

NW	On	Within 0.6 km	NW	On	Within 0.6 km	NW NE	On	Within 0.6 km	NE	On	Within 0.6 km	NE	On	Within 0.6 km
0			37			74	1111		21			58		
1			38			75	111	1	22			59		
2			39			76	1	11	23			60	1	111
3			40			77			24			61		
4			41			78			25			62	1	111
5			42			79			26			63	~~1111~~ ~~1111~~111	1
6			43			80			27			64		
7			44		111	81			28			65		1
8			45			82	11	1	29		1	66		11
9			46	11	1	83			30	1		67		
10			47		111	84			31			68		
11		11	48			85			32			69		
12			49	11		86			33			70		
13			50			87			34			71		
14			51			88			35			72		
15		1	52			89			36	11		73	11	11
16			53		111	90			37	11	111	74		
17			54			1			38	1	1	75		
18			55	1		2			39	1		76	1111	1
19			56			3			40		11	77		
20			57	11	1	4			41			78	1	
21	1	1	58			5			42	~~1111~~	1	79		
22	1	11	59	1	1	6			43			80	11	
23			60			7			44			81		
24	11	1	61			8			45	1	1	82	1	
25			62			9			46			83		
26			63			10			47	1		84		
27		11	64			11			48			85		
28			65			12			49			86	111	1
29			66			13	1	1	50			87		
30			67			14			51			88	111	1
31			68			15			52			89		
32			69			16			53		1111			
33			70	11		17			54					
34			71			18			55					
35			72			19			56					
36			73	11		20	1		57	1	1			

Table D-13. Correlation of Levels of Agreement Lineaments 1, 2, 3 with Tonal Anomalies (Area 3)

NW	On	Within 0.6 km	NW	On	Within 0.6 km	NW NE	On	Within 0.6 km	NE	On	Within 0.6 km	NE	On	Within 0.6 km
0			37			74	1	11	21			58		
1			38			75	11	111	22	1	1	59		11
2			39	1	1	76	1		23			60		
3	1		40	11		77			24			61		
4			41	11	1	78			25			62		
5			42			79			26			63	11	11
6			43		1	80			27			64	~~1111~~	
7			44	1	111	81	1		28			65	1	
8		1	45		1	82			29			66		
9			46			83		1	30			67	1	1
10	1		47		1	84			31			68		
11			48		11	85			32			69		
12			49			86			33			70		
13			50	111		87			34	1		71		
14			51			88			35			72		
15		1	52			89			36			73	~~1111~~	1
16			53		1	90		1	37			74	1	
17			54	1	1	1			38			75		
18			55	11		2			39	1	11	76		
19			56	1		3			40	1	1	77	1	
20			57	1		4			41			78		
21			58	1		5			42			79		
22		1	59	1	1	6			43			80	1	
23	11		60		1	7			44			81		
24	1		61			8			45	1	1	82		
25			62			9			46			83		
26			63			10			47			84		1
27	1		64			11			48			85		
28		1	65			12	1	111	49			86		1
29			66			13			50			87	1	1
30			67			14			51			88		
31			68	1		15			52			89		
32			69			16			53		1			
33	1		70			17	11		54		1			
34			71			18			55		11			
35		1	72			19			56					
36			73		1	20			57		1			

Table D-14. Correlation of Aerial Lineaments with Tonal Anomalies (Area 3)

NW	On	Within 0.6 km	NW	On	Within 0.6 km	NW NE	On	Within 0.6 km	NE	On	Within 0.6 km	NE	On	Within 0.6 km
0	1		37			74			21			58		111
1			38			75			22			59		
2			39	1		76			23			60		11
3			40			77			24			61		
4		1	41			78	11		25		1	62	1	11
5			42			79			26			63		
6	1	1	43	11		80		1	27			64		
7			44	11	1	81	111	11	28		1	65	111	
8	11	1	45			82			29			66		
9			46			83			30			67		
10			47			84			31			68		
11			48			85			32	11	11	69		
12			49			86	11	1	33	1		70		
13			50	11	1	87	11		34			71		
14			51			88			35			72		
15			52			89			36			73		
16		1	53			90	1111		37			74		
17			54			1			38			75	1111	
18		1	55	~~1111~~ 1	11	2			39			76		
19			56	1	1	3	1		40	1		77		
20	1	1	57			4			41			78	1	
21			58	1		5	1		42			79	1	
22			59			6			43		1	80		
23			60	11	11	7			44			81		
24			61			8			45			82		
25		11	62			9			46			83		
26			63			10			47			84		
27			64			11	1		48		1	85		
28			65	11		12			49			86		
29			66			13	1		50		1	87		
30			67		11	14			51			88		
31			68	11		15			52			89		
32			69			16			53	1111				
33			70			17			54					
34			71	11		18			55					
35			72			19			56					
36			73			20	1		57					

APPENDIX E

CORRELATION #2 DATA SHEETS

These data sheets show the results of the correlation between tonal anomalies and lineament intersection angles. A data sheet has been prepared for each of the five lineament types mapped in this project.

The data sheets are proportioned into 180 one-degree increments. A tick mark by the increments indicates the angle of the intersection for those lineaments having a spatial correlation with a tonal anomaly.

Table E-1. Data Sheets for Landsat Lineaments (all) Intersection Angles (Area 1) (where related to tonal anomalies).

DEG.	On	Within 0.6 km	DEG.	On	Within 0.6 km	DEG.	On	Within 0.6 km	DEG.	On	Within 0.6 km	DEG.	On	Within 0.6 km
0			37			74			111			148		1
1			38		1	75	11	1	112	1		149		
2			39	1		76			113			150	1	
3			40			77	11	1	114			151	1	
4			41			78		1	115			152		
5			42	1		79			116			153		
6			43			80			117		1	154		
7	1		44			81			118			155	1	1
8			45	1		82			119		1	156		
9			46			83		1	120	1	1	157		1
10			47		1	84		1	121			158		
11			48		1	85			122			159	1	
12		1	49			86	1	11	123			160		1
13		1	50			87		1	124			161		
14		1	51			88			125	1		162	1	
15			52	1		89		1	126		1	163		
16			53	1		90		11	127	1		164		
17			54			91	1		128			165		
18			55	1		92		1	129	1		166		
19			56	1		93			130	1		167		1
20			57			94		11	131			168		
21			58			95			132	11		169		
22			59			96	1		133			170		
23			60			97		1	134		1	171		
24			61		1	98			135	1	1	172		
25			62			99			136			173		
26			63			100		1	137		1	174		
27		1	64			101			138		1	175		
28			65			102	1	1	139			176	1	
29			66			103	1		140			177		
30			67			104		1	141	1		178		
31			68			105	1		142			179		
32			69			106			143			180		
33			70			107			144					
34			71			108			145	1				
35	1		72			109	1		146					
36			73			110	11	1	147					

Table E-2. Data Sheets for Landsat Major Lineaments Intersection Angles (Area 1) (where related to tonal anomalies).

DEG.	On	Within 0.6 km	DEG.	On	Within 0.6 km	DEG.	On	Within 0.6 km	DEG.	On	Within 0.6 km	DEG.	On	Within 0.6 km
0			37			74			111			148		
1			38			75			112			149		
2			39			76			113	1		150		
3			40		1	77			114			151		
4			41			78			115			152		
5			42		11	79			116			153		
6			43			80			117			154		
7			44			81			118			155		
8	1		45	1	1	82			119		1	156		
9			46			83			120	11		157		
10			47	1		84			121			158		
11			48			85			122			159		
12			49			86	1		123		1	160		
13			50			87			124	1		161		
14			51			88			125			162		
15			52			89			126			163		
16			53			90			127			164		
17			54			91			128			165		
18			55			92			129			166		
19			56	1		93			130			167		
20			57			94	1		131			168		
21			58			95			132			169		
22			59			96			133			170		
23		1	60	1		97			134			171		
24			61		1	98			135	1	1	172	1	
25			62			99			136			173		
26			63		1	100		1	137			174		
27			64			101		1	138		11	175		
28			65			102			139			176		
29			66			103			140			177		
30			67			104			141			178		
31			68			105			142			179		
32			69			106			143			180		
33			70			107			144					
34			71			108			145					
35			72			109			146					
36			73			110			147					

Table E-3. Data Sheets for Skylab Lineament Intersection Angles (Area 1) (where related to tonal anomalies)

DEG.	On	Within 0.6 km	DEG.	On	Within 0.6 km	DEG.	On	Within 0.6 km	DEG.	On	Within 0.6 km	DEG.	On	Within 0.6 km
0			37	1		74			111			148		
1			38			75			112			149		
2			39	1		76	1	1	113			150		
3			40			77			114			151		
4			41			78			115			152		
5			42			79			116	11		153		
6			43			80		11	117			154		
7	1		44			81			118	1		155		
8			45			82	11		119			156		
9			46			83	1	1	120			157		
10			47			84			121	1		158		
11			48			85			122			159		
12			49		1	86			123			160		
13			50	1		87			124			161		
14			51			88			125			162		
15			52			89		1	126			163		
16	1		53	1		90			127			164		1
17			54			91			128	1		165		
18			55			92			129			166		
19			56			93			130	1		167		
20			57			94			131			168		
21			58		1	95			132			169		
22			59			96			133			170		
23			60			97			134			171		
24			61			98	11		135			172		
25			62	1		99			136			173		
26			63			100		1	137			174		
27			64	1		101	1	1	138	1		175		
28			65		1	102			139			176		
29			66			103			140			177		
30	1		67			104		1	141	1		178		
31			68			105			142			179		
32			69	1		106	1		143			180		
33			70	1	1	107			144					
34		1	71			108	1		145					
35			72		11	109			146		1			
36			73			110	1		147					

Table E-4. Data Sheets for Levels of Agreement 1, 2, 4 Intersection Angles (Area 1) (where related to tonal anomalies)

DEG.	On	Within 0.6 km	DEG.	On	Within 0.6 km	DEG.	On	Within 0.6 km	DEG.	On	Within 0.6 km	DEG.	On	Within 0.6 km
0			37			74			111			148		
1			38			75			112			149		
2			39			76			113			150		
3			40			77			114			151		
4			41			78			115			152		
5			42			79			116			153		
6			43			80			117	1		154		
7			44			81			118			155		
8			45			82			119			156		
9			46			83			120			157		
10			47			84			121			158		
11			48			85			122			159		
12			49			86			123		1	160		
13			50			87			124			161		
14			51			88			125			162		
15			52			89			126			163		
16			53			90			127			164		
17			54			91			128			165		
18			55			92			129			166		
19			56			93			130			167		
20			57		1	94			131			168		
21			58			95			132			169		
22			59			96			133			170		
23			60			97			134			171		
24			61			98	1		135			172		
25			62			99			136			173		
26			63			100			137			174		
27			64			101			138			175		
28			65			102			139			176		
29			66			103			140			177		
30			67			104		1	141			178		
31			68		1	105			142			179		
32			69			106		1	143			180		
33			70		1	107			144					
34			71			108			145					
35			72			109			146					
36		1	73		1	110			147					

Table E-5. Data Sheets for Landsat Lineament (all) Intersection Angles (Area 2)
(where related to tonal anomalies)

DEG.	On	Within 0.6 km	DEG.	On	Within 0.6 km	DEG.	On	Within 0.6 km	DEG.	On	Within 0.6 km	DEG.	On	Within 0.6 km
0			37	1		74			111			148		
1			38	1		75			112	1		149		
2			39			76			113			150		
3			40	1		77			114		1	151		
4			41			78			115			152		
5			42		1	79	1		116			153		
6			43	1		80	1		117			154		
7			44			81		1	118			155		
8			45			82			119		1	156		
9			46			83			120			157		
10			47		11	84		11	121			158		
11			48	1		85			122			159		
12			49			86			123			160		
13			50			87		1	124			161		
14			51	1		88	1		125		1	162		
15			52	1		89	1		126			163		
16			53			90			127			164		
17			54			91	1		128			165	1	
18			55		11	92			129		1	166		
19			56			93		11	130		1	167		
20			57			94			131			168		
21			58		1	95		11	132	1	1	169		
22			59			96			133		11	170		
23	1		60			97			134			171		
24			61	1		98			135			172		
25			62			99			136			173		
26			63		1	100	1		137	11		174		
27			64			101	1		138	1		175		
28			65			102			139			176		
29			66		11	103			140	1		177		
30			67			104			141			178		
31			68			105			142	1		179		
32	1		69			106			143	1		180		
33			70			107	1		144	1				
34			71		1	108			145					
35			72			109		1	146					
36			73	1		110			147					

Table E-6. Data Sheets for Landsat Major Lineament Intersection Angles (Area 2) (where related to tonal anomalies)

DEG.	On	Within 0.6 km	DEG.	On	Within 0.6 km	DEG.	On	Within 0.6 km	DEG.	On	Within 0.6 km	DEG.	On	Within 0.6 km
0			37	1		74			111			148		
1			38			75			112			149		
2			39			76			113			150		
3			40			77			114			151		
4			41			78			115			152		
5			42			79			116			153		
6			43			80			117			154		
7			44			81			118			155		
8			45			82			119			156		
9			46		1	83			120			157		
10			47			84			121			158		
11			48			85			122			159		
12			49			86			123		1	160		
13			50			87			124			161		
14			51		1	88			125			162		
15			52			89			126			163		
16			53			90			127			164		
17			54			91			128			165		
18			55			92			129			166		
19			56			93			130			167		
20			57			94			131			168		
21			58			95			132			169		
22			59			96			133			170		
23			60			97			134			171		
24			61			98			135			172		
25			62			99			136			173		
26			63			100			137		1	174		
27			64			101			138			175		
28			65			102			139			176		
29			66			103			140			177		
30			67			104			141			178		
31			68			105			142			179		
32			69			106			143	1		180		
33			70			107			144					
34			71			108			145					
35			72			109			146					
36			73			110			147					

Table E-7. Data Sheets for Skylab Lineament Intersection Angles (Area 2) (where related to tonal anomalies)

DEG.	On	Within 0.6 km	DEG.	On	Within 0.6 km	DEG.	On	Within 0.6 km	DEG.	On	Within 0.6 km	DEG.	On	Within 0.6 km
0			37			74			111			148		
1			38			75			112			149		
2			39			76			113			150		
3			40			77			114			151		
4			41			78			115			152		
5			42			79			116			153		
6			43			80			117			154		
7			44			81			118			155		
8			45			82			119			156		
9			46			83		1	120			157		
10			47			84			121			158		
11			48			85			122			159		
12			49			86			123			160		
13			50			87			124			161		
14			51			88			125		1	162		
15			52			89			126			163		
16			53			90			127			164		
17			54			91			128			165		1
18			55			92	1		129			166		
19			56	1		93			130			167		
20			57			94			131			168		
21			58			95			132		1	169		
22			59			96			133			170		
23			60			97			134			171		
24			61			98			135			172		
25			62			99			136			173		
26			63			100			137			174		
27			64			101			138			175		
28			65			102			139			176		
29			66			103			140			177		
30			67			104			141			178		
31			68			105			142			179		
32			69			106			143			180		
33			70		1	107			144					
34			71		1	108			145					
35			72			109			146					
36			73	1		110		1	147					

Table E-8. Data Sheets for Levels of Agreement 1, 2, 3 Intersection Angles (Area 2)
(where related to tonal anomalies)

DEG.	On	Within 0.6 km	DEG.	On	Within 0.6 km	DEG.	On	Within 0.6 km	DEG.	On	Within 0.6 km	DEG.	On	Within 0.6 km
0			37			74	1		111			148		
1			38			75			112			149		
2			39			76			113			150		
3			40			77			114			151		
4			41			78			115			152		
5			42			79			116			153		
6			43			80			117			154		
7			44			81			118			155		
8			45			82			119			156		
9			46			83			120			157		
10			47			84			121			158		
11			48			85			122			159		
12			49			86			123			160		
13			50			87			124			161		
14			51			88			125			162		
15			52			89	1		126			163		
16		1	53			90			127			164		1
17			54			91	1	1	128			165		
18			55			92			129			166		
19			56			93			130			167		
20			57			94			131			168		
21			58			95			132			169		
22			59			96			133			170		
23			60			97			134			171		
24			61	1		98			135			172		
25			62			99			136			173		
26			63			100			137			174		
27			64			101			138			175		
28			65			102			139			176		
29			66			103			140			177		
30			67			104			141			178		
31			68			105			142			179		
32			69			106	1		143			180		
33			70			107			144					
34			71			108			145					
35			72			109			146					
36			73			110			147					

Table E-9. Data Sheets for Aerial Lineament Intersection Angles (Area 2)
(where related to tonal anomalies)

DEG.	On	Within 0.6 km	DEG.	On	Within 0.6 km	DEG.	On	Within 0.6 km	DEG.	On	Within 0.6 km	DEG.	On	Within 0.6 km
0			37			74		11	111			148	1	
1			38		1	75			112			149		11
2			39			76	1		113			150		1
3			40	1	1	77			114			151		
4			41			78			115			152		
5			42			79			116			153		
6			43		1	80			117			154		
7			44			81			118			155		
8			45			82		1	119		11	156		
9			46			83			120			157		
10			47	1		84			121			158		
11			48		1	85			122			159		
12			49			86		1	123	1		160		
13			50			87			124			161	1	
14	1		51			88			125			162		
15			52		1	89			126			163		
16			53		1	90			127		1	164		
17			54			91			128			165		
18			55			92			129			166	1	1
19			56			93		1	130			167		
20			57			94		1	131		1	168		
21			58			95			132		1	169		
22			59		1	96			133	1		170		
23			60			97			134			171		
24			61			98			135		1	172		
25			62			99			136			173		
26			63			100			137		11	174		
27			64			101			138		1	175		
28			65			102			139			176		
29			66			103			140	1	1	177		
30			67			104		1	141			178		
31		1	68			105			142	1		179		
32			69			106		1	143			180		
33			70			107			144		1			
34			71			108			145					
35			72			109			146					
36			73			110			147					

Table E-10. Data Sheets for Landsat Lineament (all) Intersection Angles (Area 3) (where related to tonal anomalies)

DEG.	On	Within 0.6 km	DEG.	On	Within 0.6 km	DEG.	On	Within 0.6 km	DEG.	On	Within 0.6 km	DEG.	On	Within 0.6 km
0			37	1		74			111			148		
1			38			75			112			149		
2			39			76		1	113			150		
3			40			77			114	1		151		
4			41			78			115			152		
5			42			79			116	1		153		
6			43		1	80			117			154		
7			44			81		1	118			155	1	
8			45		11	82		1	119			156		
9			46			83			120			157		
10			47			84			121		1	158		
11			48			85			122			159		
12			49			86			123	1		160		
13			50			87	11		124	1		161		
14			51			88			125			162		
15			52			89		1	126			163		
16			53		11	90			127			164		
17			54	11		91		1	128		1	165		
18			55	1		92			129			166		
19			56			93			130			167		
20			57			94		11	131			168		
21			58			95			132	1		169		
22		1	59	111	1	96		1	133			170		
23			60		1	97			134			171		
24			61		1	98			135			172		
25			62			99		1	136			173		
26			63			100		1	137		11	174		
27			64	1		101			138	1	1	175		
28			65			102			139		1	176		
29			66			103			140			177		
30			67		1	104			141			178		
31			68			105			142			179		
32			69			106			143	1		180		
33			70		11	107		1	144					
34			71			108			145					
35			72			109	1		146					
36			73		1	110			147					

Table E-11. Data Sheets for Skylab Lineament Intersection Angles (Area 3) (where related to tonal anomalies)

DEG.	On	Within 0.6 km	DEG.	On	Within 0.6 km	DEG.	On	Within 0.6 km	DEG.	On	Within 0.6 km	DEG.	On	Within 0.6 km
0			37	1		74			111			148		1
1			38			75			112			149		
2			39			76			113		1	150		
3			40			77			114			151		
4			41			78			115			152		
5			42	11		79			116		1	153		
6			43			80			117			154		
7			44			81		1	118		1	155		
8			45			82		1	119		11	156		
9			46	1		83		1	120		1	157		
10			47			84			121			158		
11			48			85			122			159		
12			49			86			123			160		
13			50			87			124			161	1	
14			51			88			125			162		
15			52	1		89			126			163		
16			53			90			127		1	164		1
17			54			91			128	1		165		
18			55			92			129			166		
19	1		56			93			130			167		
20			57			94			131			168		
21			58			95		1	132			169		
22			59			96			133			170		
23			60			97			134		1	171		
24			61		11	98			135			172		
25			62		1	99	1		136			173		
26			63			100			137			174		
27			64			101			138	1		175		
28			65			102			139			176		
29			66			103			140			177		
30			67		1	104			141			178		
31			68			105			142			179		
32		1	69			106			143			180		
33			70			107			144	1				
34			71			108			145					
35	1		72	1		109			146					
36	1		73			110			147					

Table E-12. Data Sheets for Levels of Agreement 1, 2, 3 Intersection Angles (Area 3) (where related to tonal anomalies)

DEG.	On	Within 0.6 km	DEG.	On	Within 0.6 km	DEG.	On	Within 0.6 km	DEG.	On	Within 0.6 km	DEG.	On	Within 0.6 km
0			37			74			111			148		1
1			38			75			112			149		
2			39			76			113			150		
3			40			77			114			151		
4			41			78			115			152		
5			42	1	1	79			116			153		
6			43			80			117	1		154		
7			44			81			118			155		
8			45			82			119			156		
9			46			83			120	1		157		
10			47			84			121	1		158		
11			48			85			122	1		159		
12			49			86			123			160	1	
13			50			87			124			161		
14			51			88			125			162		
15	1		52			89			126			163		
16	1		53			90			127			164		
17			54			91			128			165	1	
18			55			92			129			166		
19			56			93			130			167		
20	1		57			94			131			168		
21			58	1		95			132			169		
22			59			96			133			170		
23			60			97			134			171		
24			61	1		98			135			172		
25			62			99			136			173		
26			63		1	100			137		1	174		
27			64			101			138		11	175		
28			65			102			139			176		
29			66	1		103			140			177		
30			67			104			141			178		
31			68			105			142			179		
32			69			106			143			180		
33			70			107			144					
34			71			108			145					
35			72			109			146					
36			73			110			147					

Table E-13. Data Sheets for Aerial Lineament Intersection Angles (Area 3) (where related to tonal anomalies)

DEG.	On	Within 0.6 km	DEG.	On	Within 0.6 km	DEG.	On	Within 0.6 km	DEG.	On	Within 0.6 km	DEG.	On	Within 0.6 km
0			37			74			111			148		
1			38			75	1		112			149		11
2			39			76			113			150		11
3			40			77			114			151		1
4			41			78			115			152		
5			42			79			116			153	1	1
6			43			80			117			154	1	
7			44			81			118		1	155		
8			45			82			119			156		
9			46	1		83			120			157		
10			47	1		84			121			158		
11			48			85			122			159		
12			49			86			123			160		
13			50			87			124		11	161		
14			51			88			125			162		
15			52	1		89			126			163		
16			53			90			127			164		
17			54			91			128	1		165		
18			55	1		92			129			166		
19			56			93		1	130			167		
20			57			94			131			168		
21			58			95			132			169		
22			59			96			133			170		
23			60	1		97			134			171		
24			61	1	11	98			135	1	1	172		
25			62			99		1	136			173		
26			63			100			137			174		
27			64			101			138			175		
28			65	1		102			139			176		
29		1	66			103			140			177		
30			67			104			141		1	178		
31		1	68			105	1		142	1		179		
32			69			106			143			180		
33			70	1		107		1	144					
34			71			108	1		145					
35			72			109			146					
36			73		1	110			147					

APPENDIX F

CORRELATION #3 DATA SHEETS

These data sheets show the correlation between tonal anomalies and lineament sets, that is, where a tonal anomaly was located at the intersection of two lineaments.

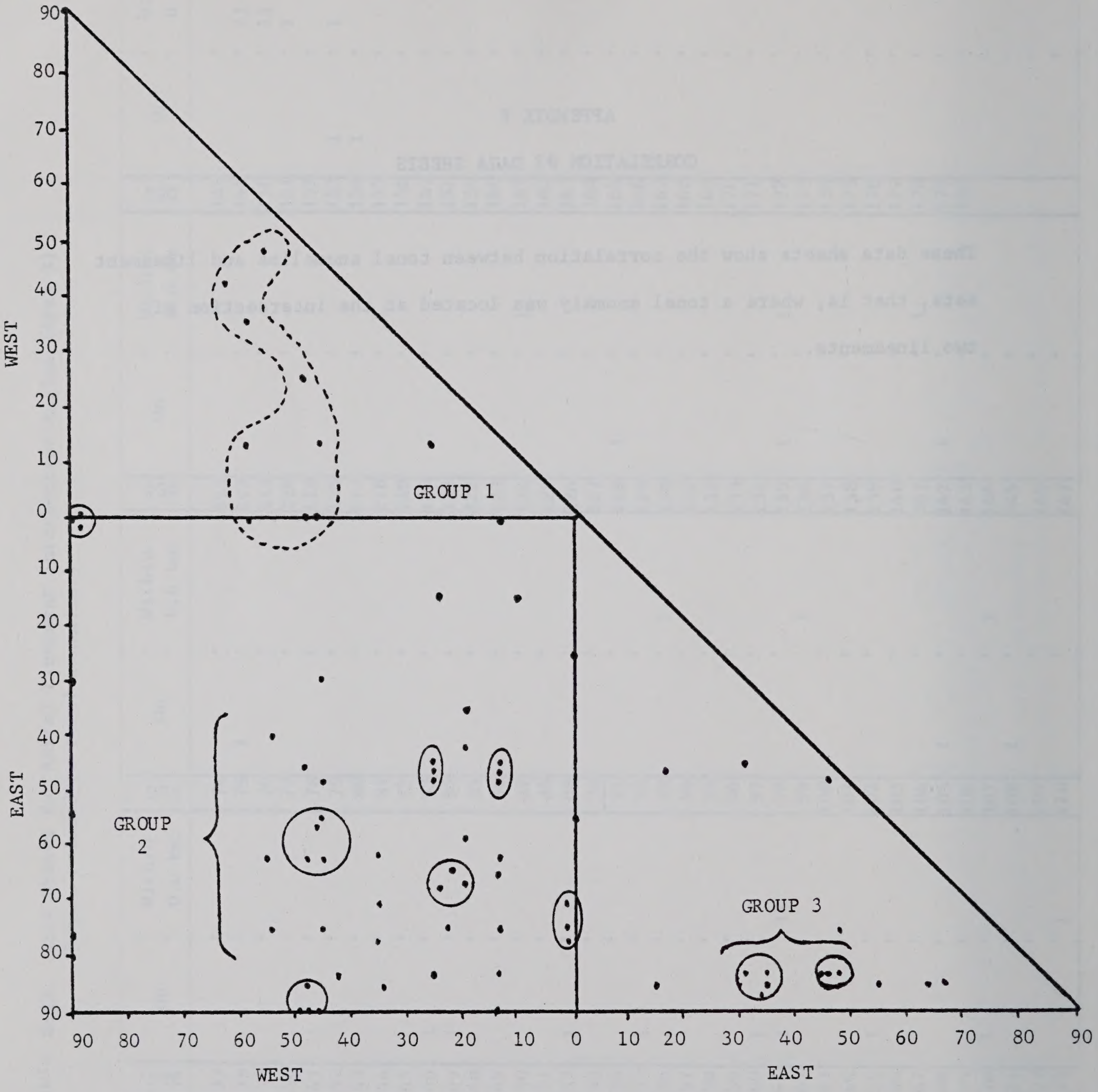

Figure F1. Matrix Showing Correlation of Tonal Anomalies with Landsat Lineament Intersection Sets (Area 1)

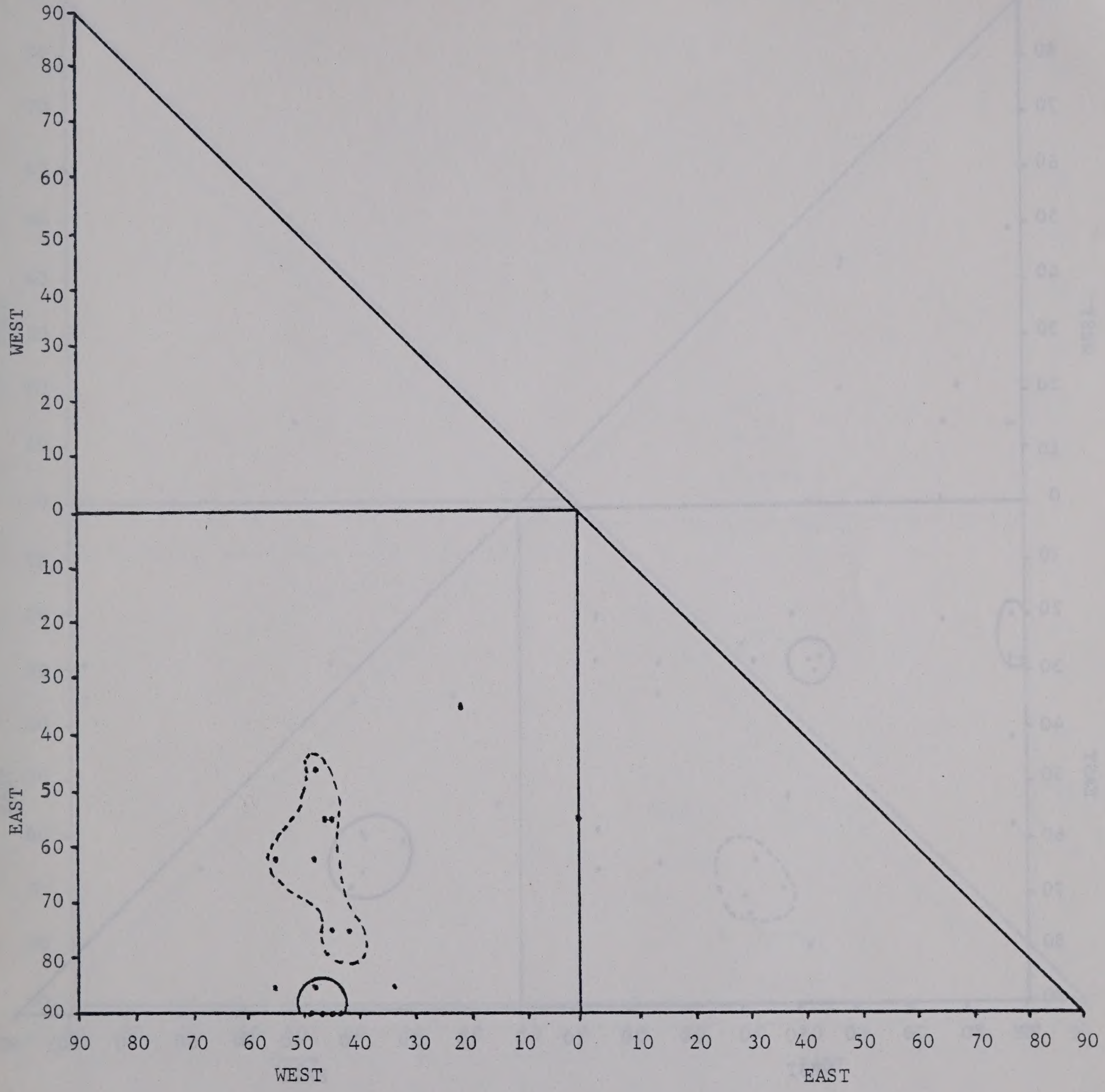

Figure F-2. Matrix Showing Correlation of Tonal Anomalies with Major Landsat Lineament Intersection Sets (Area 1)

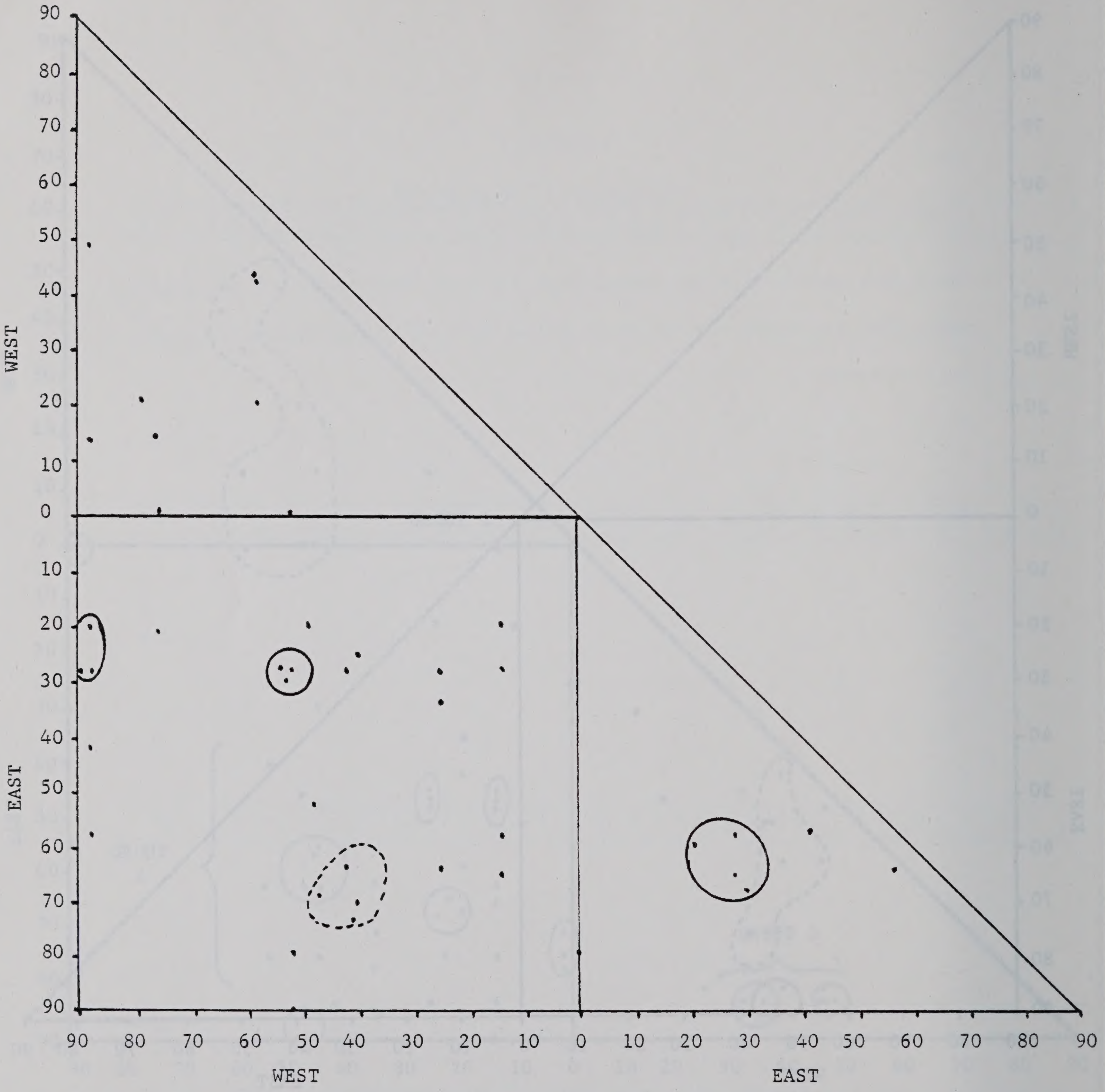

Figure F-3. Matrix Showing Correlation of Tonal Anomalies with Skylab Lineament Intersection Sets (Area 1)

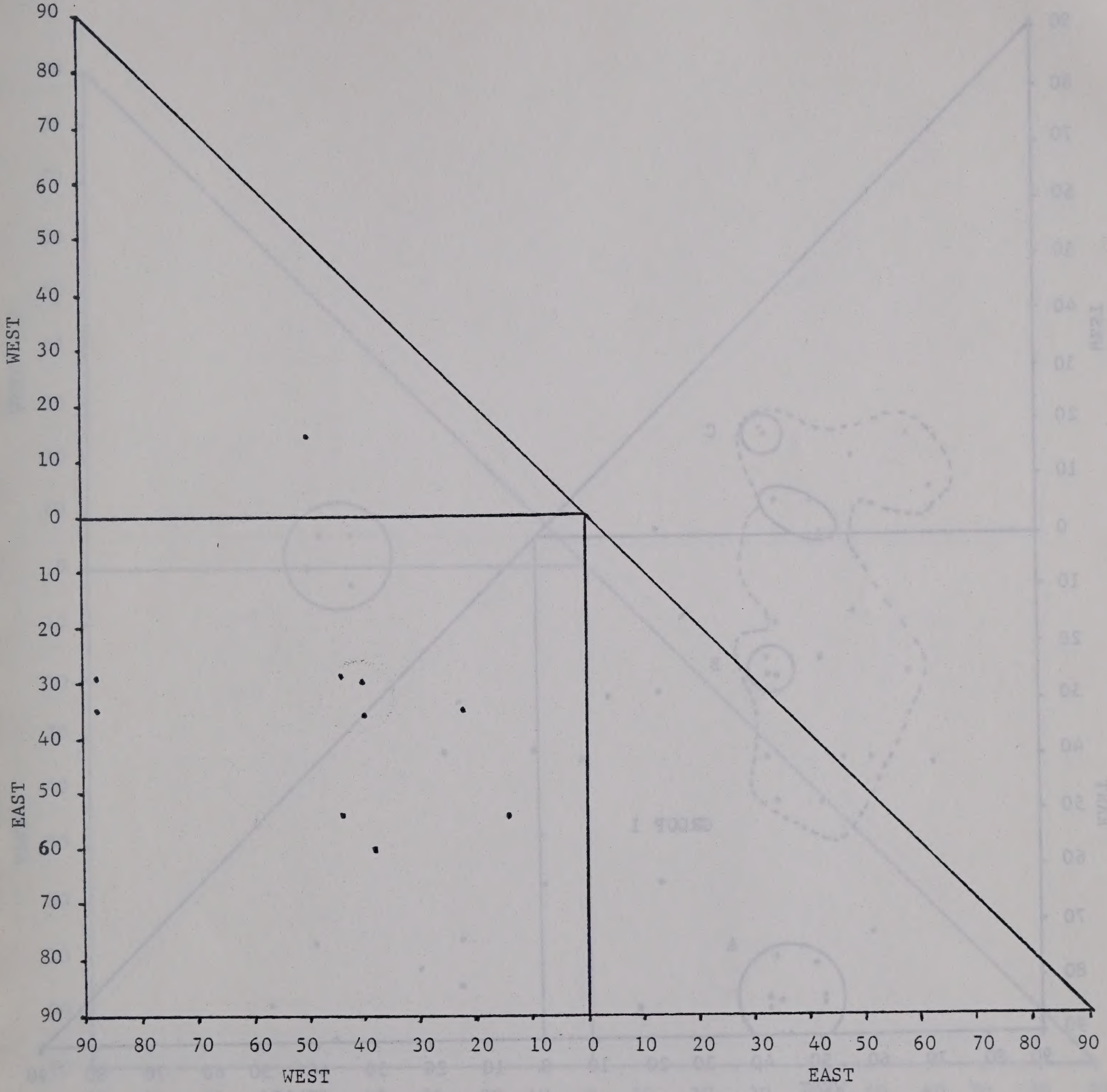

Figure F-4. Matrix Showing Correlation of Tonal Anomalies with Levels 1, 2, 4 Lineament Intersection Sets (Area 1)

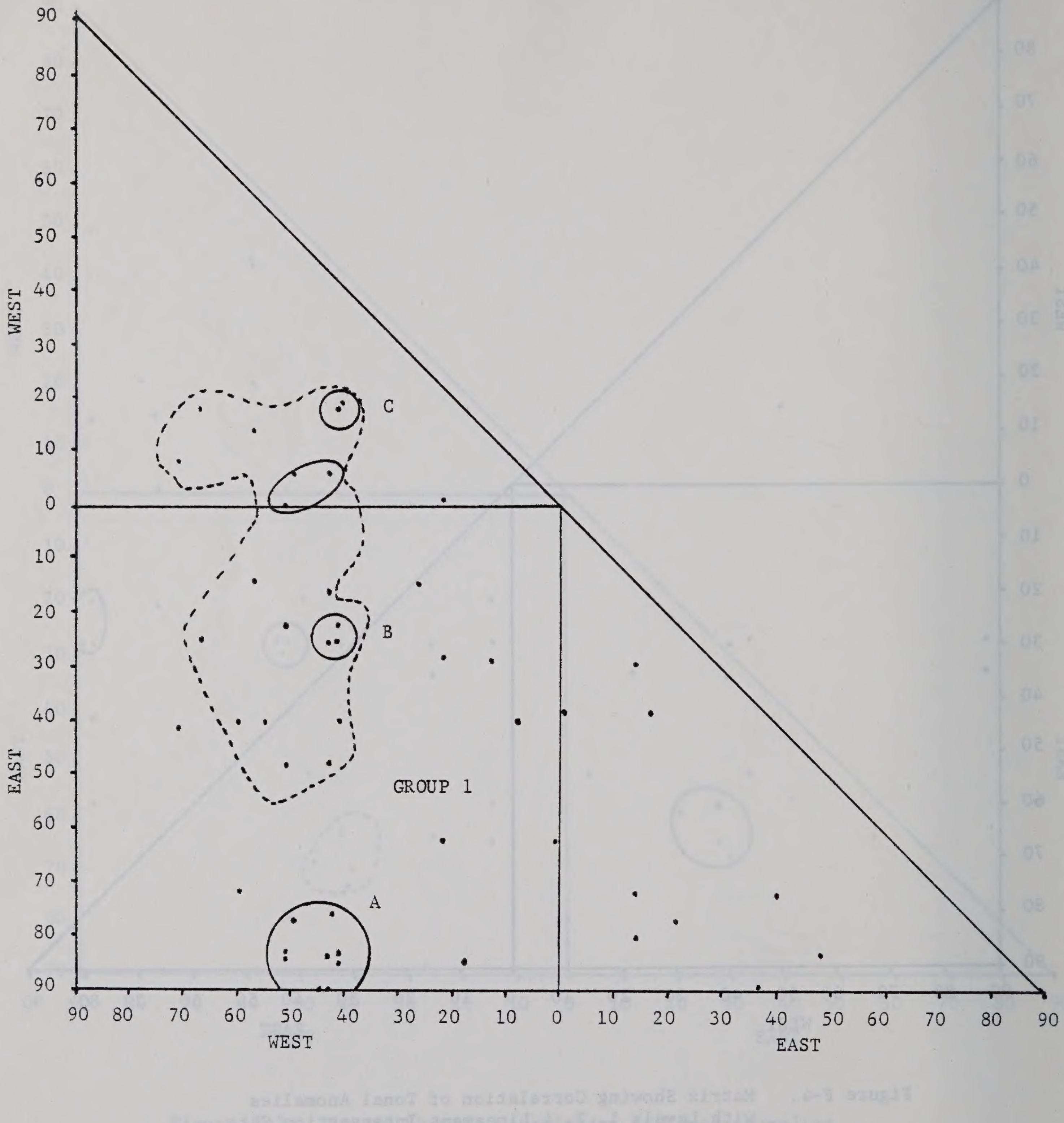

Figure F-5. Matrix Showing Correlation of Tonal Anomalies with Landsat Lineament Intersection Sets (Area 2)

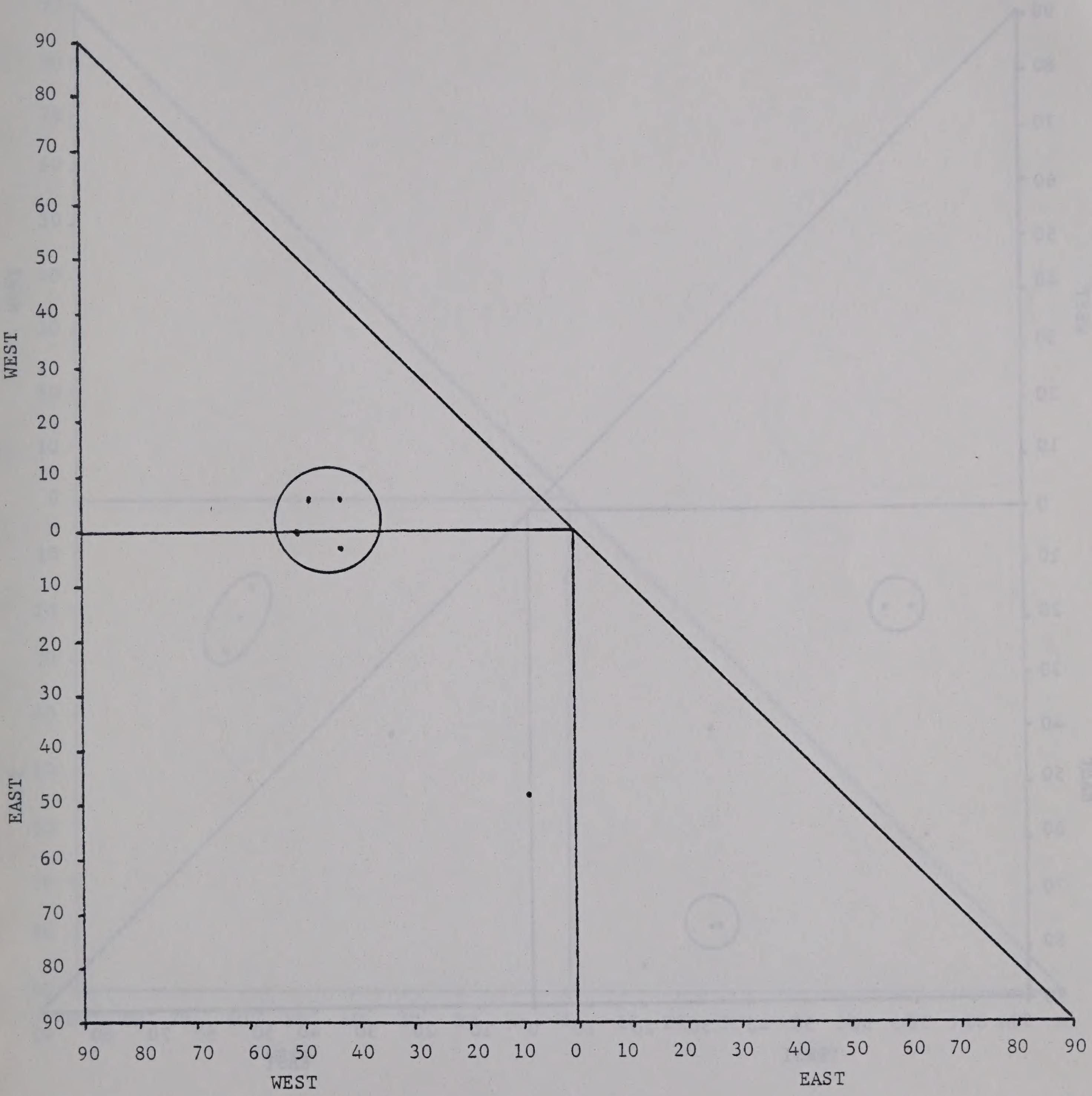

Figure F-6. Matrix Showing Correlation of Tonal Anomalies with Major Landsat Lineament Intersection Sets (Area 2)

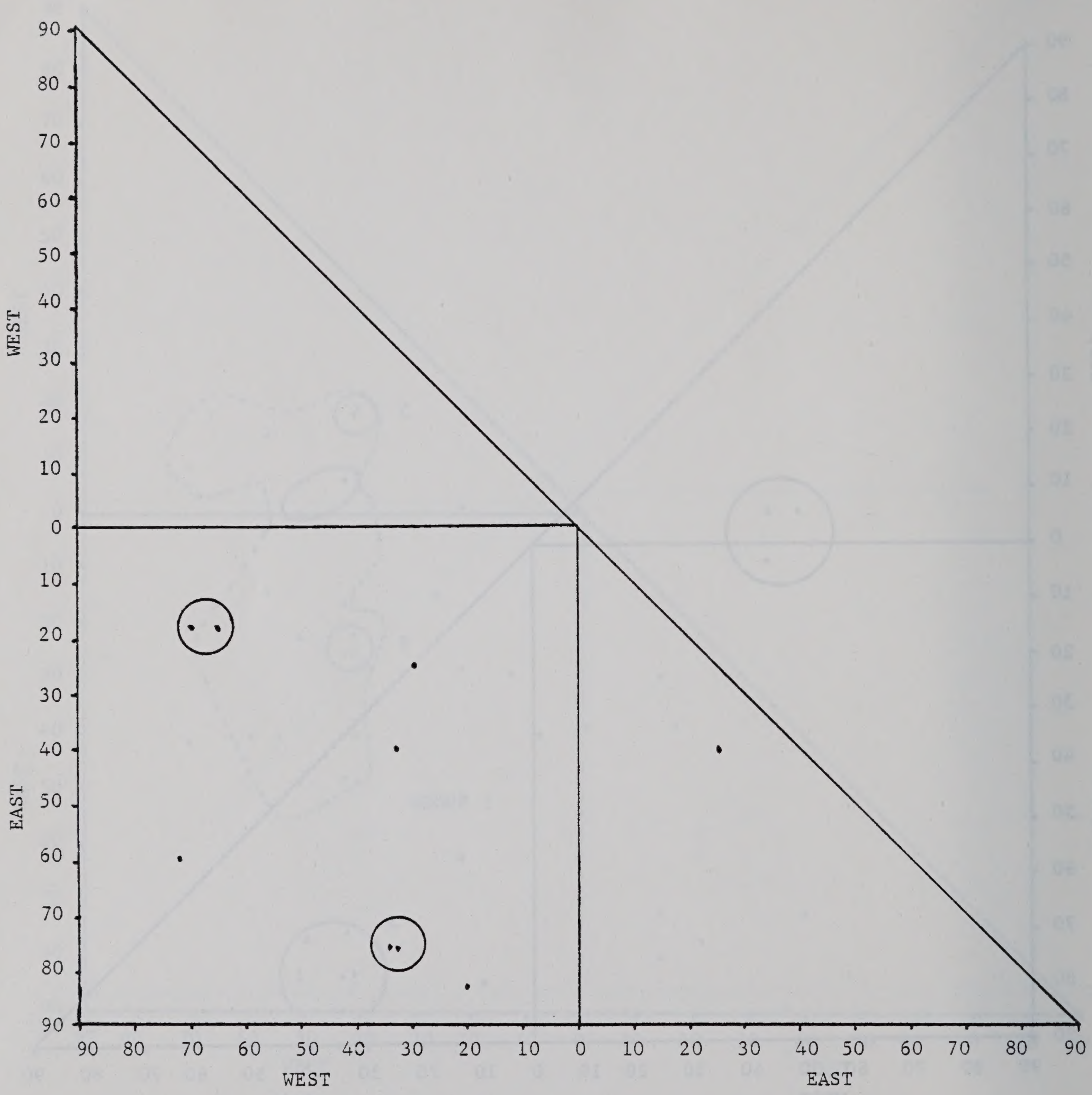

Figure F-7. Matrix Showing Correlation of Tonal Anomalies with Skylab Lineament Intersection Sets (Area 2)

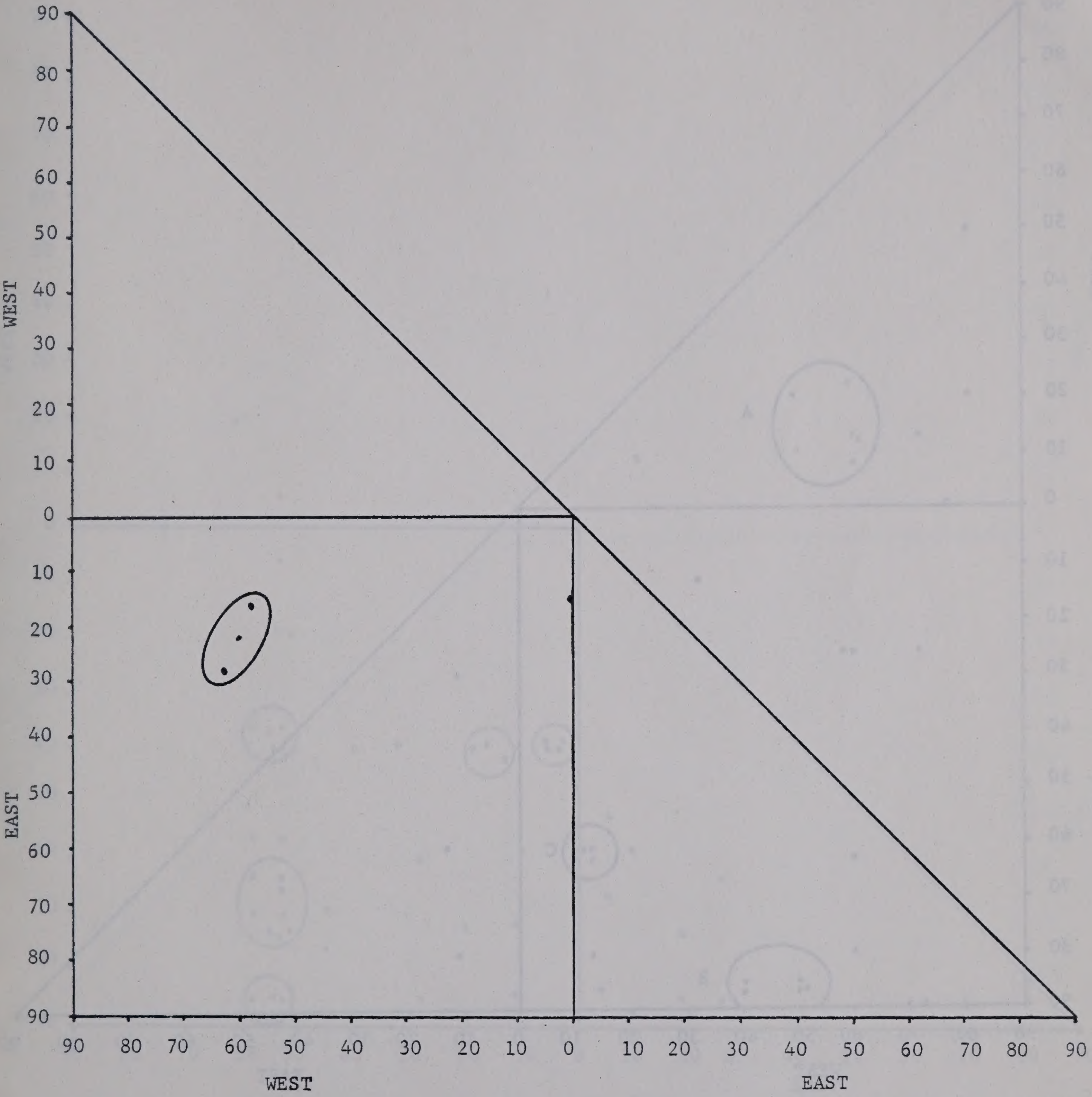

Figure F-8. Matrix Showing Correlation of Tonal Anomalies with Levels 1, 2, 3 Lineament Intersection Sets (Area 2)

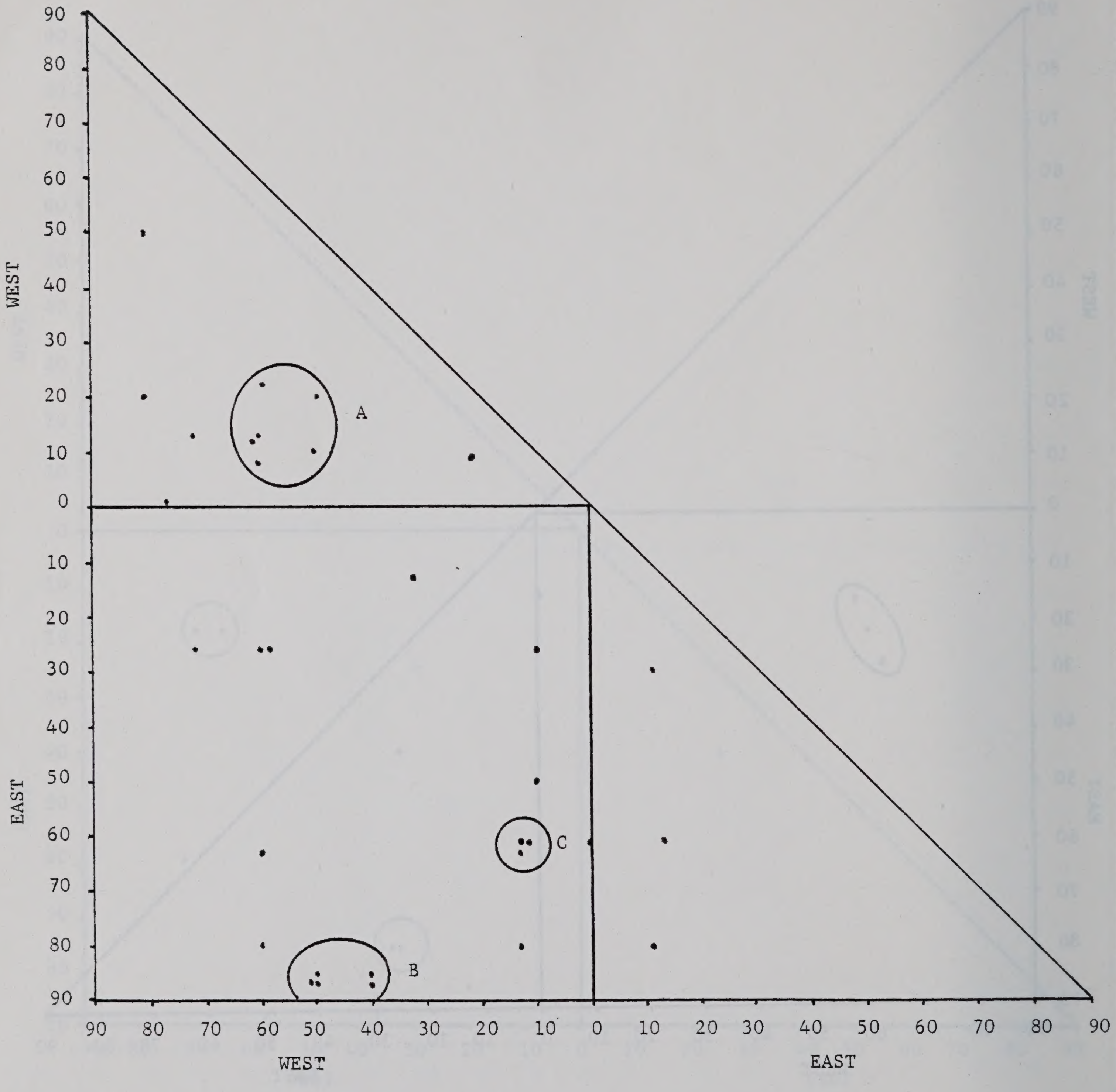

Figure F-9. Matrix Showing Correlation of Tonal Anomalies with Aerial Lineament Intersection Sets (Area 2)

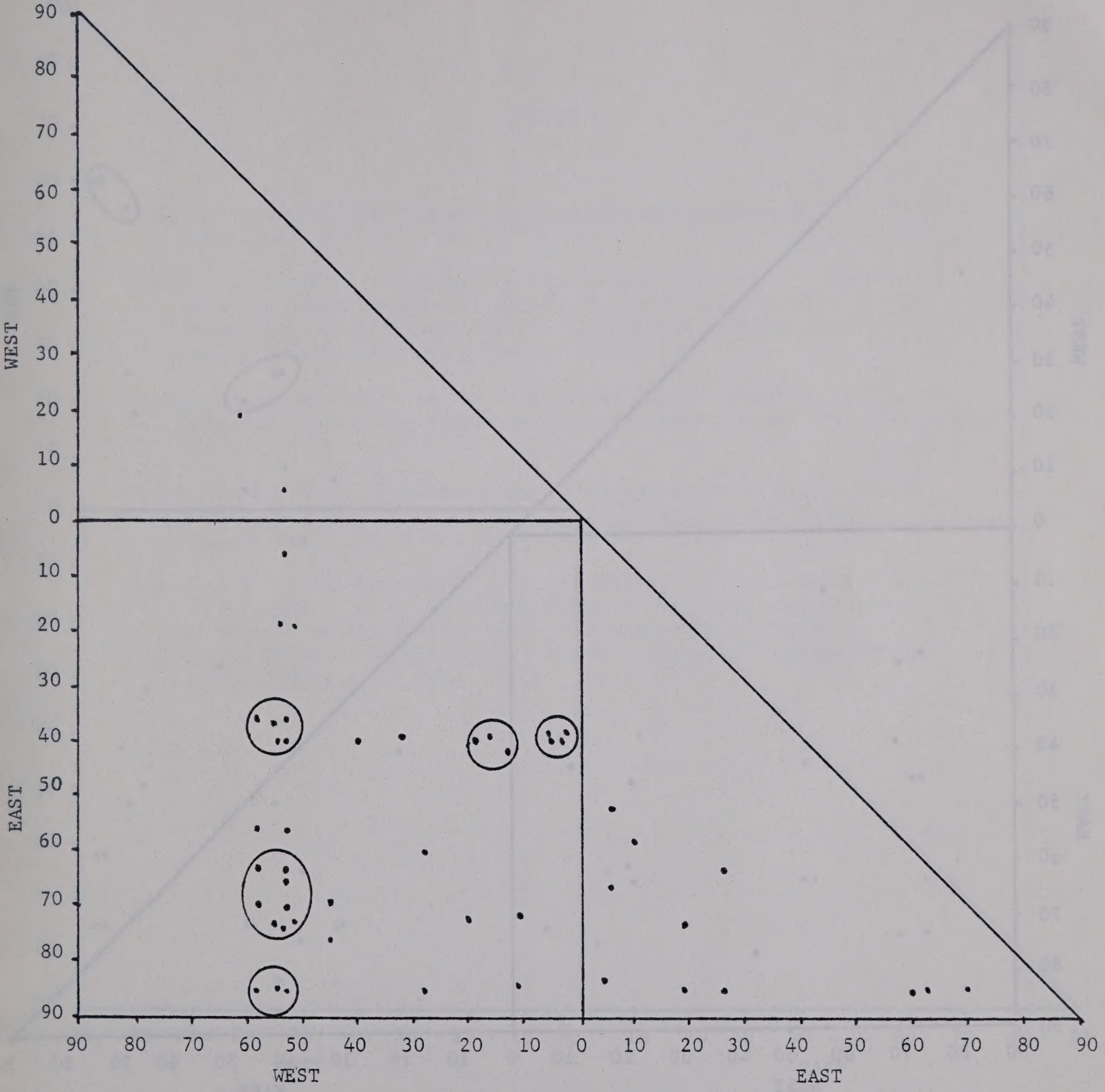

Figure F-10. Matrix Showing Correlation of Tonal Anomalies with Landsat Lineament Intersection Sets (Area 3)

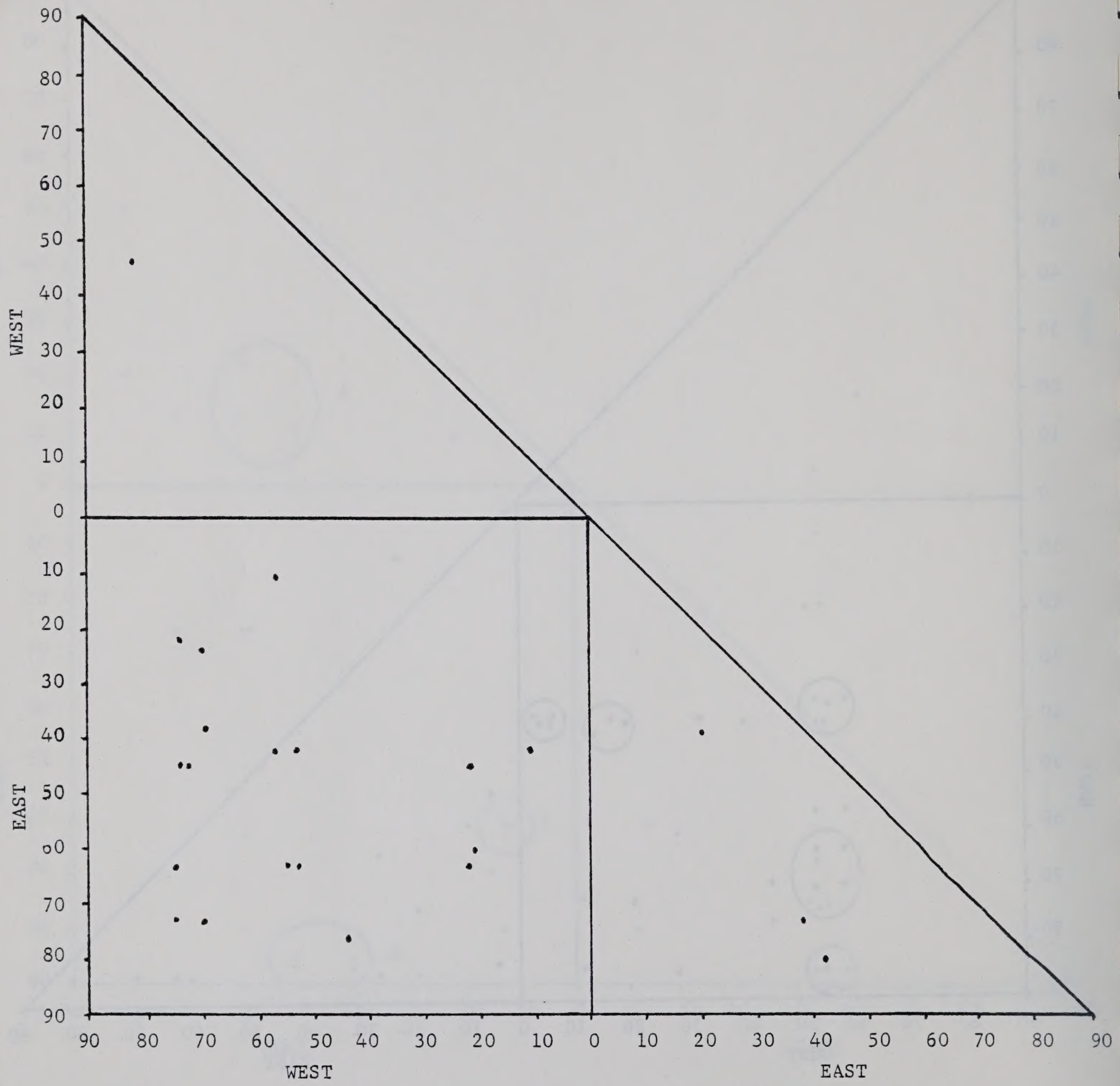

Figure F-11. Matrix Showing Correlation of Tonal Anomalies with Skylab Lineament Intersection Sets (Area 3)

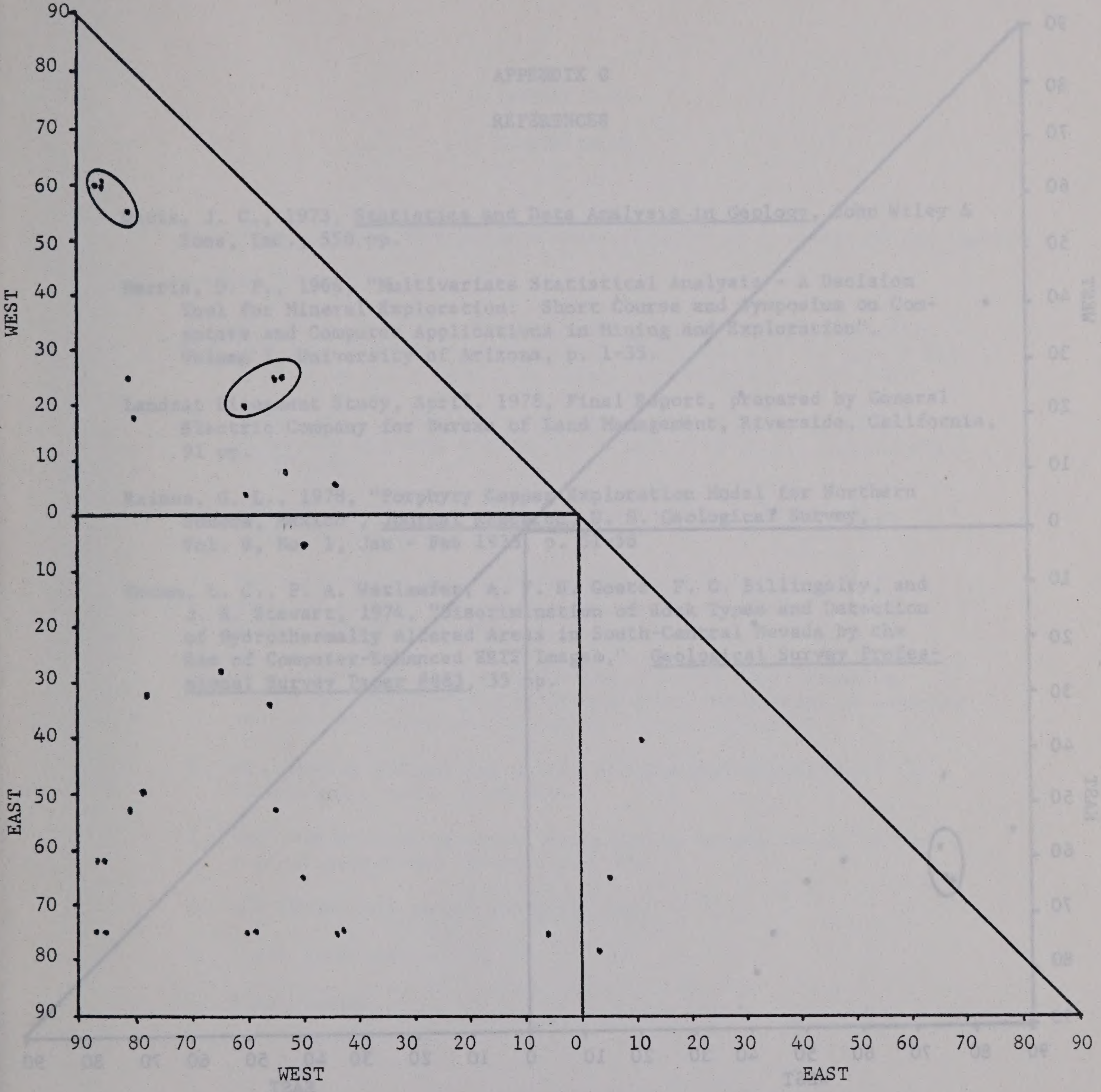

Figure F-12. Matrix Showing Correlation of Tonal Anomalies with Levels 1, 2, 3 Lineament Intersection Sets (Area 3)

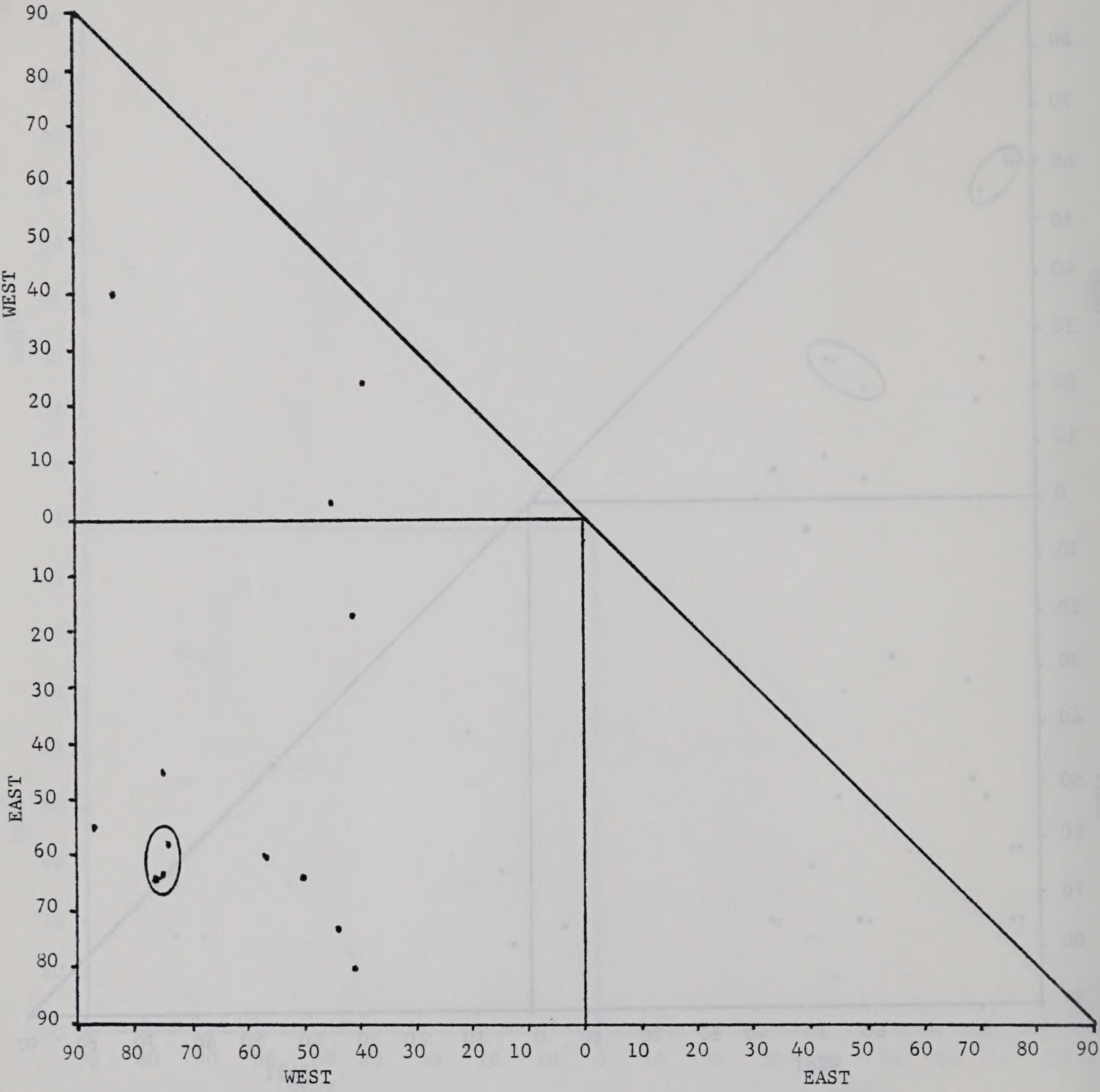

Figure F-13. Matrix Showing Correlation of Tonal Anomalies with Aerial Lineament Intersection Sets (Area 3)

APPENDIX G

REFERENCES

Davis, J. C., 1973, Statistics and Data Analysis in Geology, John Wiley & Sons, Inc., 550 pp.

Harris, D. P., 1966, "Multivariate Statistical Analysis - A Decision Tool for Mineral Exploration: Short Course and Symposium on Computers and Computer Applications in Mining and Exploration", Volume 1, University of Arizona, p. 1-35.

Landsat Lineament Study, April, 1978, Final Report, prepared by General Electric Company for Bureau of Land Management, Riverside, California, 91 pp.

Raines, G. L., 1978, "Porphyry Copper Exploration Model for Northern Sonora, Mexico", Journal Research, U. S. Geological Survey, Vol. 6, No. 1, Jan - Feb 1978, p. 51-58

Rowan, L. C., P. A. Wetlaufer, A. F. H. Goetz, F. C. Billingsley, and J. H. Stewart, 1974, "Discrimination of Rock Types and Detection of Hydrothermally Altered Areas in South-Central Nevada by the Use of Computer-Enhanced ERTS Images," Geological Survey Professional Survey Paper #883, 35 pp.

APPENDIX H

DELIVERABLES

The following products were prepared and delivered as a result of the Landsat Enhancement Project.

1. Digitally contrast enhanced, edge enhanced and geometrically corrected Landsat transparencies (one color and MSS band 5 and band 7) on 9 x 9 inch film (scale approximately 1:700,000).
2. Three types of digitally ratioed-stretched Landsat transparencies for each area on 9 x 9 inch film (scale approximately 1:700,000).
3. One set of prints of the above on 9 x 9 inch paper and at 1:100,000 scale.
4. One overlay for each area showing the relative potential for metallic mineral resources based on the statistical evaluation. Scale 1:100,000.
5. One overlay for each area showing inferred tonal anomalies (inferred hydrothermal alteration areas) as evident on enhanced ratioed-stretched Landsat images. Scale 1:100,000.
6. One overlay showing the levels of agreement (confidence) for lineaments. Scale 1:100,000.
7. One overlay showing areas identified as having potential for mineral resources. Scale 1:100,000.
8. All Skylab and aerial photos as used.
9. Draft final report.
10. Final Report.

BLM Library
Denver Federal Center
Bldg. 85, OC-521
P.O. Box 25047
Denver, CO 80225

BLM Library
Denver Federal Center
Bldg. 85, OC-521
P.O. Box 25047
Denver, CO 80225

GENERAL ELECTRIC

Space Division

Headquarters: Valley Forge, Pennsylvania ☐ Daytona Beach, Fla. ☐ Evendale, Ohio
☐ Huntsville, Ala. ☐ Bay St. Louis, Miss. ☐ Houston, Texas ☐ Sunnyvale, Calif.
☐ Beltsville, Md. ☐ Tacoma, Wash. ☐ Palmdale, Calif. ☐ Bedford, Mass.
☐ Washington, D.C. Area